ADVANCED FUNCTIONAL MATERIALS
www.afm-journal.de

Engineering Topographical Cues to Enhance Neural Regeneration in Spinal Cord Injury: Overcoming Challenges and Advancing Therapies

Wei Xu, Fenghui Wang, Joshua Stein, Siqiao Wang, Pengfei Jiang, Letao Yang, Liming Cheng,* and Ki-Bum Lee**

Spinal cord injury (SCI) poses significant challenges for regeneration due to a series of secondary injury mechanisms, including ischemia, oxidative stress, and neuroinflammation. These pathological processes lead to neuronal apoptosis and create a microenvironment that hinders neural regeneration. Recent advancements in tissue engineering have introduced biomaterials that feature precisely engineered micro- and nanoscale topographical cues, representing a novel class of therapeutic interventions. These biomimetic scaffolds are designed to modulate the mechanotransduction pathways of neural stem cells (NSCs), thereby enhancing neurogenesis and guiding neuronal differentiation. They also influence essential cellular processes such as adhesion, cytoskeletal alignment, morphological polarization, and gene regulation. This review systematically evaluates current strategies for optimizing topographical designs, emphasizing their role in promoting neurite outgrowth, axonal guidance, and synaptic reformation. The mechanisms are elucidated by which scaffold topographies regulate NSC fate decisions through mechanobiological signaling and interactions with the extracellular matrix. Additionally, critical barriers are analyzed for clinical translation, including the precision fabrication of tunable architectures, the scalability of novel materials, and strategies to mitigate glial scar formation. By synthesizing interdisciplinary insights from biomaterial science, neurobiology, and translational medicine, this work aims to provide a roadmap for developing next-generation topographical scaffolds that address the pressing clinical need for effective SCI repair.

1. Introduction

Spinal cord injury (SCI) typically results from physical traumatic events such as motor vehicle accidents, falls, or sports-related incidents.[1] Such physical trauma can further damage the spinal cord, initiating a cascade of pathological events, often referred to as secondary injury, within the central nervous system (CNS).[2,3] The first mechanical injury causes axons, which are lengthy nerve fibers necessary for transmitting information between neurons, to be damaged. This results in an instantaneous loss of communication between the brain and parts located below the lesion site. This primary axonal disruption affects various types of neurons, including motor neurons responsible for movement, sensory neurons responsible for sensation, and interneurons connecting different spinal cord neurons.[4] The initial injury is followed by various complex cellular responses, including inflammation and cell death, often resulting in widespread neuronal death.[5] Together, these devastating changes profoundly impair the neural circuitry of the spinal cord, causing a permanent loss of motor and sensory functions below the injury

W. Xu, S. Wang, L. Yang, L. Cheng
Division of Spine, Department of Orthopaedics, Shanghai Tongji Hospital
Tongji University School of Medicine
Key Laboratory of Spine and Spinal Cord Injury Repair and Regeneration
Ministry of Education
Tongji University
Shanghai 200092, China
E-mail: yangletao@tongji.edu.cn; chenglm@tongji.edu.cn

The ORCID identification number(s) for the author(s) of this article can be found under https://doi.org/10.1002/adfm.202508435

DOI: 10.1002/adfm.202508435

W. Xu, J. Stein, K.-B. Lee
Department of Chemistry and Chemical Biology
Rutgers University
Piscataway, NJ 08854, USA
E-mail: kblee@rutgers.edu

F. Wang, P. Jiang, L. Yang
Frontier Science Center for Stem Cell Research
School of Life Sciences and Technology
Tongji University
Shanghai 200092, China

site and significantly diminishing the affected individual's quality of life.[6]

Current treatments for SCI, such as surgical decompression, anti-inflammatory drugs, hyperbaric oxygen therapy, and modern rehabilitation, have often yielded limited functional recovery.[7–11] The compounded effects of primary mechanical trauma and subsequent secondary injury mechanisms result in extensive tissue damage characterized by widespread axonal severance, progressive neuronal death, and severe disruption of established neural circuits.[3,12] While surgical decompression aims to stabilize the spine and prevent further injury, it cannot reverse the initial damage.[13] Anti-inflammatory drugs can modulate the secondary injury response, but cannot fully prevent neuronal death or promote axonal regeneration.[14,15] Hyperbaric oxygen therapy, while potentially beneficial, has yet to demonstrate consistent efficacy in promoting long-term functional recovery.[16–19] Furthermore, rehabilitation, while essential for maximizing functional capacity, primarily focuses on compensatory strategies rather than reversing the underlying neuronal loss and circuit disruption.[20,21] In short, these limitations highlight the pressing need for innovative therapeutic approaches that can effectively target the fundamental pathological mechanisms of SCI and promote substantial neural regeneration.

To address these therapeutic limitations in SCI, neural tissue engineering has emerged as a promising approach, employing innovative biomaterial strategies and advanced engineering techniques to promote functional recovery after SCI.[22] Specifically, engineered scaffolds can modulate the physical, chemical, and biological microenvironments within the injury site, creating conditions conducive to neural repair and regeneration.[23–25] Among various design parameters, topographical features such as the sizes, shapes, and layout of extracellular matrix (ECM) have emerged as particularly influential elements that can significantly impact cellular behavior and tissue response.[26–28] Recent research has demonstrated a growing interest in understanding and optimizing specific topographical cues, as these structural elements can effectively regulate critical biological processes, including neural stem cell differentiation, inflammatory responses, axonal guidance, and synaptic reorganization.[29–31] These controlled modifications ultimately aim to enhance nerve regeneration and facilitate the reconstruction of functional neural circuits at SCI sites.

To this end, scientists have developed and investigated various topographical features—varying in size, shape, geometry, and spatial patterns, from both natural and synthetic ECM—to systematically elucidate their influence on neural regeneration and circuit reconstruction, offering promising advances in therapeutic strategies for SCI[32–34] (**Figure 1**). The efficacy of these topographical designs has been rigorously evaluated through both in vitro studies, which allow for precise control and detailed mechanistic investigations, and in vivo models that better represent the complex pathophysiological environment of SCI.[35–39] Nevertheless, topographical features do not act in isolation; rather, they function within a broader matrix context that includes material composition, biodegradability, and biomechanical characteristics. While this review emphasizes the role of topography in modulating neural responses, we also acknowledge that scaffold mechanical properties (e.g., stiffness, tensile strength) and degradation kinetics may influence cell–material interactions and regenerative outcomes, particularly in relation to neurite extension and glial scar modulation.[36,40–42]

Despite substantial progress in topography-based design, several critical challenges continue to impede successful neural regeneration at the injury site. These obstacles include persistent severe inflammation, an inhospitable microenvironment for neural stem cell survival and differentiation, and the formation of inhibitory glial scars that create both physical and chemical barriers to axonal regrowth.[43–47] Thus, a careful and systematic approach coordinating structural, mechanical, and biological factors to these complex, interrelated challenges is *essential* when developing effective engineering strategies to restore structure and function for the damaged spinal cord.

This comprehensive review examines the emerging role of topographical cues in tissue engineering strategies for treating spinal cord injury (SCI). We begin by analyzing the complex pathological cascade following SCI, with particular attention to both acute and chronic phases of injury progression. Subsequently, we provide an in-depth exploration of innovative biomaterial approaches that utilize specific topographical features to modulate the behavior and function of diverse cell populations involved in SCI pathology, including neurons, astrocytes, oligodendrocytes, and infiltrating immune cells. This systematic analysis of cell-topology interactions provides a fundamental framework for designing scaffold architectures that can effectively promote regeneration and functional recovery in injured spinal tissue. Finally, we critically evaluate promising future directions in this rapidly evolving field, highlighting both the opportunities and challenges in translating topography-based biomaterial therapies from preclinical models to clinical applications. Throughout this review, we intend to focus on non-conventional approaches and identify key parameters that may accelerate the development of more effective therapeutic interventions for SCI patients.

2. Understanding the Pathophysiology of Spinal Cord Injury and Its Impact on Neural Regeneration

Spinal cord injury (SCI) typically triggers extensive cellular death and compromises the integrity of the blood-spinal cord barrier (BSCB), a specialized vascular structure that usually maintains CNS homeostasis. This barrier disruption leads to the uncontrolled infiltration of peripheral immune cells into the normally immune-privileged spinal cord tissue, initiating a complex inflammatory cascade that can exacerbate tissue damage.[48–51] This initial trauma initiates a complex secondary injury cascade characterized by a temporally and spatially coordinated series of pathological events. These events include acute inflammation, excessive production of reactive oxygen species and free radicals, and orchestrated responses from multiple cell populations at and around the lesion site. The resulting pathophysiological changes display distinct temporal phases and spatial patterns fundamental to understanding SCI progression and recovery (**Figure 2**). There is currently no universally accepted standard for the clinical staging of spinal cord injury (SCI), but it is generally divided into acute, subacute, intermediate, and chronic phases.[4,52] In our previous work, we employed single-cell sequencing to

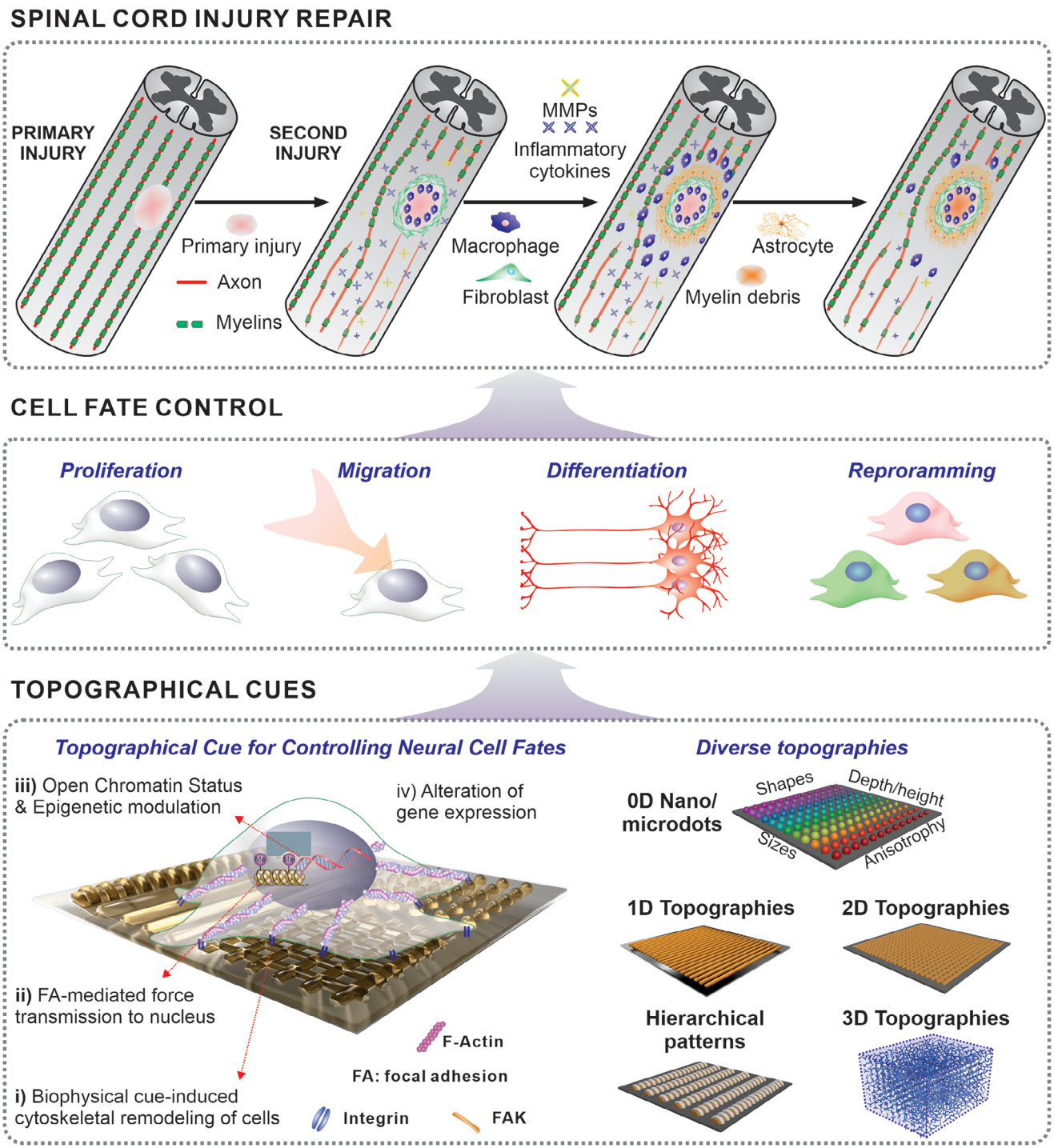

Figure 1. Schematic diagram of spinal cord injury-inspired engineering of topographical cues for neural regeneration.

analyze the temporal molecular pathology of SCI and proposed a three-phase model that reflects dynamic changes in cellular and molecular responses over time. Phase I (0–3 days post-injury) is characterized by a rapid decline in neuronal function, accompanied by robust activation of astrocytes, oligodendrocyte progenitor cells, and microglia, as well as vascular disruption and neutrophil infiltration. This phase represents the onset of neuronal shock and acute inflammation, highlighting a critical window for early intervention to mitigate secondary damage. Phase II (3–14 days post-injury) marks a transitional period, during which partial recovery occurs across multiple cell types, including neurons. Key features include glial scar formation, endothelial remodeling, and sustained immune cell infiltration, events that may be amenable to therapies aimed at enhancing regeneration.

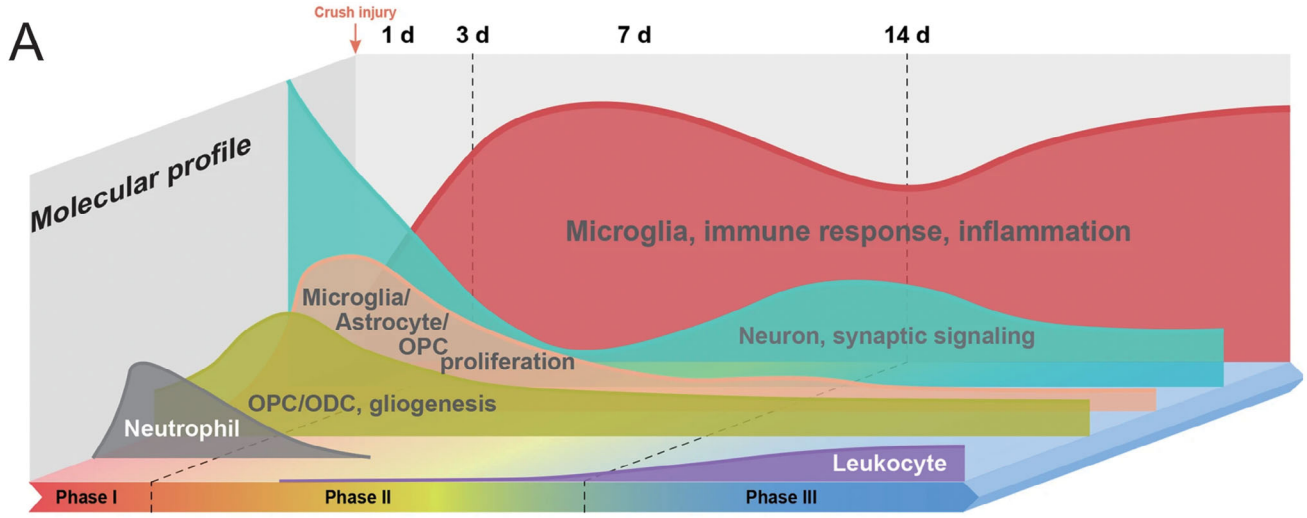

B

Cell population	Cells/ section	Prolif. 4m (%)	Turnover (cells)	Net addition intact (cells)	Fold increase injured		Net addition injured (cells)		Phenotype of new cells (cells)		Contribution to new cells (%)		Contribution to new astrocytes (%)		Contribution to new oligodendrocytes (%)	
					2 w	4 m	2 w	4 m	2 w	4 m	2 w	4 m	2 w	4 m	2 w	4 m
Ependymal cells	46 ± 2.3	14	6.4	0	5.5	4.6	210	160	Astrocytes 210 / Oligodendrocytes 0	Astrocytes 160 / Oligodendrocytes 1.9	25	39	30	53	0	3.2
Astrocytes	480±22	2.2	10	0	2.0	1.3	480	140	Astrocytes 480	Astrocytes 140	58	34	70	47	0	0
Oligodendrocyte progenitors	140±30	180	140	Progenitors 0 / Oligodendrocytes 160	2.0	1.8	140	110	Progenitors 70 / Oligodendrocytes 70	Progenitors 57 / Oligodendrocytes 57	17	27	0	0	100	97

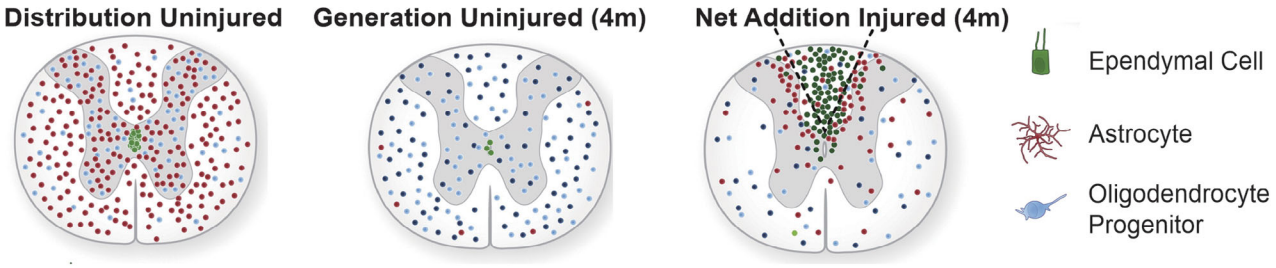

Figure 2. Illustration of the pathological changes and neurogenesis following spinal cord injury (SCI). After SCI, neural stem cells, astrocytes, and oligodendrocytes activate in response to inflammatory factors, undergoing temporally regulated changes with varied outcomes. A) Cellular and molecular pathology evolve over time and space post-SCI. Adapted with permission.[5] Copyright 2022, Nature Publishing Group. B) Ependymal cells, astrocytes, and oligodendrocyte progenitors proliferate, contributing to new glial cells. Tracking their proliferation and distribution highlights their distinct roles in tissue repair and spinal cord regeneration. Adapted with permission.[81] Copyright 2010, Cell Press.

Phase III (beyond 14 days) involves a second wave of microglial activation, progressive loss of neuronal and glial populations, and persistent inflammation, signaling a shift toward chronic degeneration in the absence of targeted therapeutic strategies[5] (**Table 1**). Throughout these stages, the expression profiles of specific biomarkers are closely linked to clinical outcomes. Favorable recovery is associated with reduced levels of pro-inflammatory cytokines (IL-6, IL-8, MCP-1), structural damage markers (GFAP, S100β, Tau), and matrix metalloproteinases (MMPs).[53] In contrast, elevated levels of neurotrophic factors (BDNF, GDNF, NGF, NT-3, NT-4/5) and myelin-associated proteins such as MBP correlate with enhanced regenerative capacity and improved functional recovery.[54] These observations underscore the therapeutic potential of early modulation of inflammation and sustained neurotrophic support to promote long-term recovery following SCI.

Within this complex microenvironment, specific cell populations—including reactive astrocytes, activated microglia, infiltrating immune cells, and surviving neurons—interact dynamically to influence the injury outcome.[55–58] Hence, a comprehensive understanding of these temporal and spatial dynamics is essential for designing and implementing effective topographical features in biomaterial scaffolds to strategically facilitate SCI repair. This understanding must encompass the intricate relationship between neural regenerative processes and the behavior of diverse immune cell subsets.

Table 1. Spinal cord injury phases and key pathological events.

Data source and key events	Time post-SCI and injury phases				
	0 – 2 h	2 h – 2 d	2 d – 2 w	2 w – 6 M	≥ 6 M
Anjum et al. 2020[4]	immediate	early acute	subacute	intermediate	chronic
Bennett et al. 2024[52]	immediate	acute	acute	intermediate	chronic
Single-cell resolution Study[5]	0 – 4 h (Phase I)	4 h – 3 d (Phase I)	3 d – 2 w (Phase II)	2 – 7 w (Phase III)	
	immediate	early acute	a) late acute b) early subacute	a) late subacute b) intermediate	
Key Events		spinal shock	a) initiation of astroglia scar b) BSB repair c) Resolution of edema	lesion stabilization	

In the following sections, we will examine the roles of various cell types, particularly neural and immune cells involved in spinal cord injury and regeneration (**Table 2**), and discuss how specific topographical features can modulate the behavior of these cells to enhance the design and efficacy of biomaterial-based therapies.

2.1. Cellular Dynamics in Neural Repair: Interactions Among Stem Cells, Astrocytes, and Oligodendrocytes

NSCs, astrocytes, and oligodendrocytes are crucial for nerve regeneration and neural circuit reconstruction post-spinal cord injury. In the postnatal and adult stages, specific populations of neural stem cells (NSCs) persist in designated neurogenic niches. In adult mammals, neurogenesis primarily occurs in the subependymal zone of the lateral ventricle wall and the subgranular zone of the hippocampus.[82,83] Studies have demonstrated that the adult spinal cord contains distinct populations of neural stem and progenitor cells, specifically neural progenitor cells (NPCs) and endogenous NSCs (eNSCs), which reside within the specialized ependymal region surrounding the central canal. This region is characterized by unique topographical features and highly organized cellular niches that maintain stem cell quiescence and regulate their proliferative and differentiation capacities under physiological conditions.[66,84,85] The architectural organization of this specialized microenvironment, including its distinct extracellular matrix (ECM) composition and 3D spatial arrangements, provides critical biophysical and biochemical cues that help maintain the stem cell population's regenerative potential. Following SCI, these cells become activated, migrate to the injury site, and differentiate primarily into astrocytes and oligodendrocytes.[66,81,85,86] The adult spinal cord ependyma acts as a latent stem cell niche that, upon activation, contributes to glial scar formation.[85] Thus, modifying the neural stem cell niche is crucial for guiding endogenous neural stem cell differentiation and regulating the development of glial scars.

At the same time, astrocytes serve as the predominant supportive cells in the nervous system, supplying metabolites essential for maintaining neuronal homeostasis.[87] After SCI, astrocytes become activated and transition into a diverse population of reactive astrocytes.[88] Transcriptome analysis identifies two key subtypes: neurotoxic subtype A1, due to NF-κB activation, and neuroprotective subtype A2, driven by STAT3 activation.[5,62–64,89] Microglial interactions significantly influence the differentiation and development of specific astrocyte phenotypes. Activated microglia release TNFα, IL-1α, and C1q, which drive astrocytes to polarize into the A1 subtype.[64,89,90] A1 astrocytes lose their supportive roles in promoting neuronal survival, outgrowth, synaptogenesis, and phagocytosis and instead contribute to the death of neurons and oligodendrocytes.[62] Consequently, controlling microglial activation and astrocyte polarization is essential for minimizing glial scar formation, preserving neuronal homeostasis, and promoting tissue repair after injury.

In addition to NPCs and eNSCs, endogenous oligodendrocyte precursor cells (OPCs) play a crucial role in spinal cord repair.[91] These cells, residing throughout the white matter and central canal, are activated in response to SCI and migrate to the lesion site. Upon activation, OPCs proliferate and differentiate into new oligodendrocytes, which are responsible for myelinating axons in the central nervous system.[59,60] Interestingly, after SCI, OPCs can also differentiate into Schwann cells, the myelinating cells of the peripheral nervous system, contributing to a unique regenerative response.[59,92,93] This process is regulated by a complex interplay of signaling pathways, including PDGF, FGF, and Notch, and is influenced by various growth factors and cytokines present in the injured microenvironment.[94–98] While OPCs contribute to remyelination and functional recovery, they also affect the formation of the astrocytic scar, secreting factors that can modulate astrocyte activity.[99] Furthermore, the generation of new oligodendrocytes often depends on a pro-inflammatory response to degrade myelin debris, highlighting the complex interplay between inflammation and remyelination.[61] This suggests that remyelination repair following injury is not only dependent on oligodendrocyte precursor cell (OPC) activation and differentiation but also closely related to inflammatory regulation. Therefore, designing topographical cues to recruit oligodendrocyte precursor cells (OPCs), regulate their proliferation and differentiation, and modulate the inflammatory response represents a promising strategy for remyelination-driven spinal cord regeneration.

Table 2. Essential neural and immune-related cell populations in spinal cord injury.

Cell category	Cell type	Source	Function	Key markers	Key cytokines released	Supplementary
Neural-related Cells	Neurons	Spinal cord	Signal transmission; regulate local microenvironment	NeuN, β-III Tubulin (TUJ1)	BDNF, NGF, NT-3	Undergo apoptosis post-injury; release neurotrophic factors that modulate glial activity and synaptic repair.[5,14,15,57]
	Oligodendrocyte Progenitor Cells (OPCs)	Spinal cord	Remyelination; axonal support	Olig2, NG2, PDGFR-α	IL-1β, TGF-β (low levels), FGF2	Activated early post-SCI; may influence microglial phenotype and remyelination.[59–61]
	Astrocytes	Spinal cord (gray and white matter)	Structural support; blood-brain barrier; glial scar	GFAP, S100β	IL-6, TNF-α, CXCL10, MCP-1 (CCL2), TGF-β	Reactive astrocytes can amplify or suppress inflammation depending on context (A1 neurotoxic vs A2 supportive).[62–64]
	Neural Stem Cells (NSCs)	Spinal cord (central canal, ventricular zone)	Multipotent regeneration	Nestin, Sox2, DCX	IL-6, LIF, CNTF	Endogenous NSCs show limited spontaneous differentiation post-injury; potential target for enhancing regeneration.[65–67]
Immune-related Cells	Microglia	Spinal cord (resident macrophages)	Immune surveillance; phagocytosis; cytokine signaling	Iba-1, CD11b, CX3CR1	IL-1β, TNF-α, IL-6, IL-10, TGF-β, CCL2, CXCL10	Phenotypic shift from M1 (pro-inflammatory) to M2 (anti-inflammatory/regenerative) is a therapeutic target.[68–70]
	Neutrophils	Blood, recruited to injury site	Acute inflammation; debris clearance	Ly6G, CD11b	IL-1β, IL-6, TNF-α, MMP-9, ROS	First immune cells to arrive post-injury; can exacerbate BBB breakdown and secondary injury.[43,55,71]
	Macrophages	Blood, recruited to injury site	Phagocytosis; immune modulation; tissue repair	CD68, F4/80, CD11b	M1: IL-1β, IL-6, TNF-α, iNOSM2: IL-10, TGF-β, Arginase-1	Macrophage polarization (M1/M2) influences lesion resolution and regenerative signaling.[72–75]
	T cells	Blood, recruited to injury site	Immune modulation; cytokine production	CD3, CD4, CD8	Th1: IFN-γ, TNF-αTh2: IL-4, IL-5, IL-10Th17: IL-17Treg: IL-10, TGF-β	Infiltrate subacutely; balance between effector and regulatory T cells shapes immune outcomes.[76–78]
	B cells	Blood, recruited to injury site	Antibody production; immune regulation	CD19, CD20, CD79a, IgM	IL-6, IL-10, GM-CSF	May contribute to chronic inflammation and autoimmunity in SCI; interacts with T cells and microglia.[79,80]

2.2. The Role of Immune Cells in Spinal Cord Injury: Balancing Inflammation and Repair

Immune responses are critical in influencing the outcome of spinal cord injury (SCI). In the local microenvironment, microglial activation leads to alterations in cellular morphology and protein expression. This activation enhances microglial phagocytic capacity, facilitating the removal of cellular debris, but often promotes a pro-inflammatory phenotype, which contributes to secondary injury progression following SCI.[68,69,100] Microglia, similar to astrocytes, have phenotype-specific functions. M1 microglia release neurotoxic cytokines and chemokines, promoting inflammation and neuronal damage. Conversely, the M2 phenotype exhibits anti-inflammatory properties and promotes tissue repair.[70] However, additional microglial subtypes are likely present in the injured spinal site. Our previous study identified eight distinct microglial subpopulations in SCI mice mode by single-cell RNA seq, each exhibiting specific traits.[5] The phenotypic shift of microglia is dynamic and shaped by multiple factors within the damaged niches. For instance, Advanced Oxidation Protein Products (AOPPs) activate the MAPK-NF-κB signaling pathway in microglia, leading to neuroinflammation.[101] Conversely, inhibiting the HMGB1-RAGE axis diminishes the pro-inflammatory polarization of these microglia, resulting in a neuroprotective effect after spinal cord injury.[102] The morphological alterations and associated signaling pathway activation have thus become potential therapeutic targets for modulating local microenvironmental cues after SCI. Furthermore, disruption of the blood-spinal cord barrier (BSCB) enables the infiltration of hematogenous immune cells, including neutrophils, monocyte-derived macrophages, and lymphocytes, into the lesion site. These cells actively influence the post-injury microenvironment.[43]

For example, monocyte-derived macrophages (MDMs) inhibit immune cell-mediated neuronal damage in the injury site.[72] Hematogenous macrophages exhibit a more pronounced capacity to induce neuronal damage compared to activated astrocytes.[72] These macrophages infiltrate the lesion site following microglial activation and contribute to the exacerbation of axonal degeneration.[103] Like microglia and astrocytes, MDMs are functionally heterogeneous, comprising two primary phenotypes: M1 and M2. M1 macrophages are pro-inflammatory, contributing to neurotoxicity and hindering neuronal regeneration, whereas M2 macrophages exert anti-inflammatory effects, promoting axonal growth and functional recovery.[73]

In the early stages of SCI, M1 macrophages are detected early and sustain elevated levels, while M2 macrophages are transiently elevated and return to pre-injury levels within a week.[73,104] Studies have indicated that increased intracellular iron ions and myelin debris could promote a harmful M1 phenotype.[105,106] Conversely, cytokines like MGF-E8 and IL-4 induce M2 polarization through the SOCS/STAT pathway, reducing inflammation and preventing neuronal apoptosis.[107,108] Because of the immune cell-to-neuron crosstalk, regulating MDM subpopulations by designing novel biomaterials with the desired topographical cues is crucial to managing the post-injury microenvironment.[109] Neutrophils are another key mediator of secondary injury processes following SCI, predominantly contributing to detrimental effects. They release a variety of pro-inflammatory mediators, such as reactive oxygen species (ROS), lysosomal enzymes, proteases (e.g., elastase and matrix metalloproteinase-9 (MMP-9)), and myeloperoxidase (MPO).[55,110] Additionally, neutrophils produce neutrophil extracellular traps (NETs), exacerbating the injury by intensifying neuroinflammation and further compromising the integrity of the blood-spinal cord barrier (BSCB).[71]

Adaptive immunity, primarily mediated by T and B lymphocytes, plays a complex role in spinal cord injury (SCI) repair, often hindering functional recovery. CD8+ cytotoxic T cells are prominent in the post-injury immune response. These cells release perforin, a cytolytic protein that compromises the integrity of the blood-spinal cord barrier (BSCB). This increased BSCB permeability facilitates the infiltration of inflammatory cells and cytokines into the lesion site, further exacerbating inflammation and impeding neurological recovery.[111] The adult dorsal spinal cord T-cell infiltration also contributes to neuropathic pain.[76,77,112,113] SCI models with T and B cell deficiencies exhibit improved neurological recovery.[78,79] However, T cells activated by myelin basic protein (MBP) can support CNS repair. An increase in Th2 cells facilitates the transformation of both Th1 into Th2 and M1 into M2 cells, correspondingly improving the local environment and supporting SCI recovery.[114] *Consequently*, mitigating neutrophil infiltration and modulating adaptive immune responses represent crucial therapeutic strategies for regulating the post-injury microenvironment. These approaches hold significant promise for influencing microenvironmental cues and promoting functional recovery following spinal cord injury (SCI).

2.3. Neural-Immune Interplay: Implications for Recovery and Chronic Pain Management

The interplay between NSCs and the local microenvironment is crucial throughout the process of spinal cord injury (SCI) repair. A hostile inflammatory microenvironment can indirectly induce neuronal apoptosis and is a major contributor to the development of chronic pain following SCI. Specifically, interactions between microglia and neurons play a key role in mediating chronic pain after SCI. For example, the release of prostaglandin E2 (PGE2) from microglia is regulated by phosphorylated extracellular signal-regulated kinase 1/2 (pERK1/2), while the PGE2 receptor, E-prostanoid 2 (EP2), is expressed in neurons. Blockade of the neuronal EP2 receptor has been shown to attenuate the hyperexcitability of dorsal horn neurons, suggesting a potential therapeutic target for chronic pain management.[8]

Microglia play multifaceted roles in functional recovery, tissue homeostasis, and the efficacy of rehabilitation following SCI. They exert a beneficial influence on recovery by modulating the transcriptional programming, functional phenotype, and intercellular communication among various non-neuronal cell types. Furthermore, microglia are integral to glial scar formation, interacting with reactive astrocytes. This interaction is mediated, in part, by fibronectin, which acts as a primary ligand for the β1 integrin receptor (β1R) on microglia, thereby amplifying microglial-mediated neuroinflammation.[115–117]

In short, neural regeneration and microenvironmental remodeling represent significant challenges in treating spinal cord

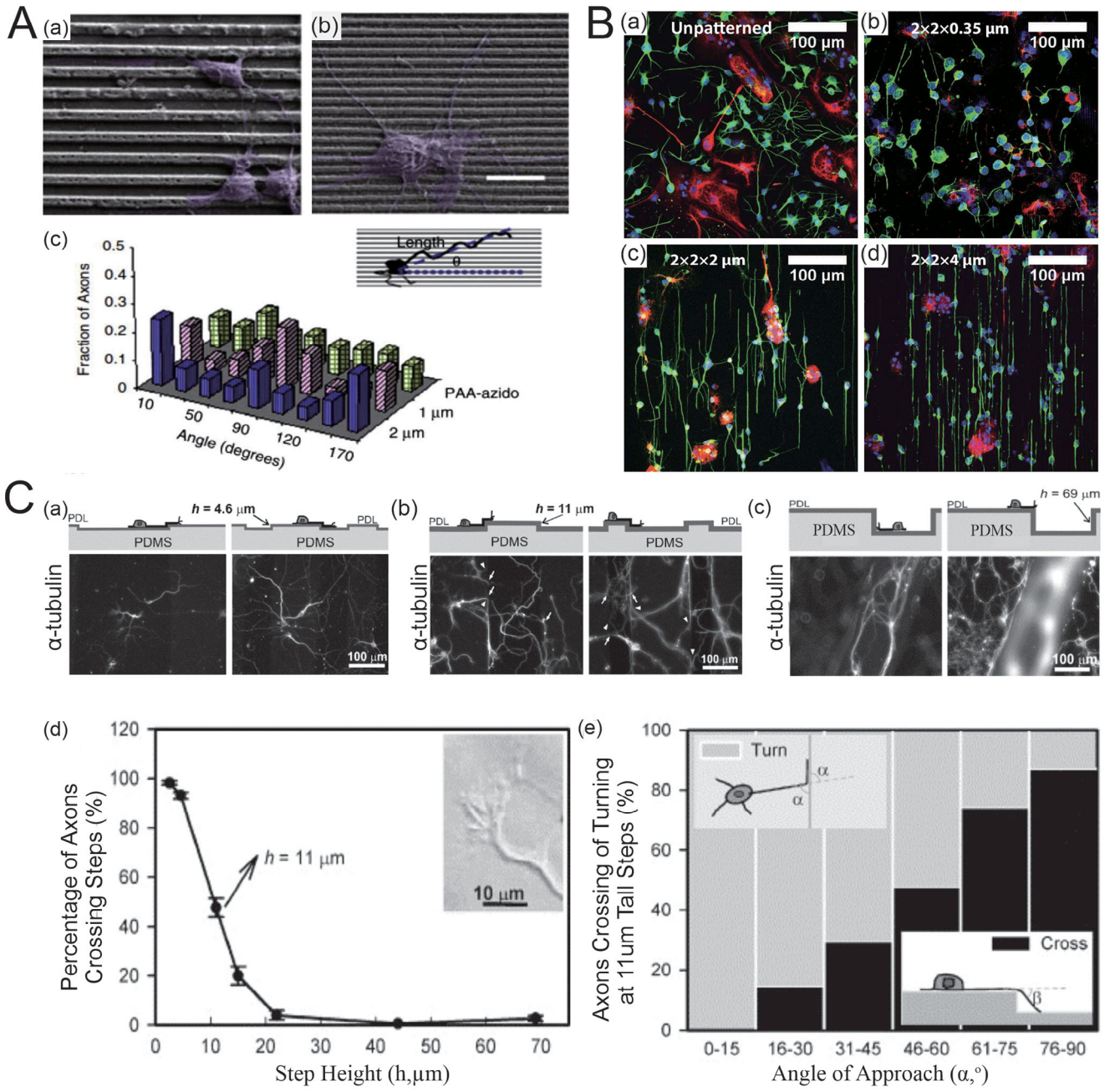

Figure 3. Effect of groove depth and width on neurite outgrowth. A) SEM images depict hippocampal cells cultured on substrates with 2 μm-wide, 800 nm-deep grooves Aa) and 1 μm-wide, 400 nm-deep grooves Ab), with axonal angle distributions shown for the latter (Ac). Adapted with permission.[127] Copyright 2017, Elsevier. B) Neuronal differentiation of hippocampal mNPCs after two weeks on unpatterned PDMS Ba) and PDMS gratings of 2 × 2 dimensions with depths of 0.35 μm Bb), 2 μm Bc), and 4 μm Bd) is quantified. TUJ1 Be) and GFAP Bf) positivity percentages reveal substrate-dependent differentiation. Adapte with permission.[152] Copyright 2014, IPC Science and Technology Press. C) Cross-sectional schematics and a-tubulin immunofluorescence illustrate neurons on PDL-coated PDMS grooves with depths of 4.6 μm Ca), 11 μm Cb), and 69 μm Cc).Graphs show axonal crossing efficiency over steps (Cd) and dependency on approach angle (Ce). Reproduced with permission.[133] Copyright 2005, Academic Press.

injury (SCI). These complex processes are profoundly influenced by local microenvironmental cues, which play a critical role in directing cellular behavior and tissue organization. Consequently, understanding and harnessing the modulatory effects of these cues has emerged as a central focus of research aimed at promoting functional recovery after SCI.

3. The Effect of Topographical Cues on SCI Repair

Numerous cell types implicated in SCI pathogenesis exhibit a spectrum of phenotypes, ranging from pro-inflammatory to anti-inflammatory states. This phenotypic plasticity is observed in astrocytes, which can adopt A1 or A2 polarization states, and

is also characteristic of microglia and macrophages, which exhibit M1 or M2 polarization. T cells enhance ligand recognition through topographically constrained contacts with antigen-presenting cells (APCs),[118] and their functional polarization is specifically regulated by membrane curvature at the immunological synapse.[119] Similarly, B cells utilize dynamic plasma membrane topographies, such as ridge-like structures, to modulate the 3D spatial distribution and mobility of IgM-BCR clusters, thereby influencing receptor localization and transport.[120] These findings highlight the potential of utilizing surface topography to precisely regulate immune cell responses, presenting a promising strategy for modulating immunity after spinal cord injury (SCI). Similarly, neurons exhibit distinct structural polarity, characterized by axons and dendrites that extend in a directional manner to form functional neural circuits. However, aberrant guidance of these neuronal processes compromises the efficiency of neural circuit formation, thereby significantly hindering regeneration and functional recovery after SCI. Contact guidance, a phenomenon whereby the surface topography of a material directs cell orientation and movement, plays a crucial role in governing neuronal polarity and regeneration. Originally introduced by Weiss in his seminal studies on the directed growth of nerve fibers,[121] this concept continues to play a central role in guiding the design and development of biomaterials for facilitating neural repair. Contact guidance cues can be provided through both planar structures and 3D scaffolds. Current research indicates that anisotropic and isotropic topographies differentially influence cell polarization, thereby modulating cell fate. Generally, anisotropic topographies are characterized by continuous features, such as grooves and ridges, whereas isotropic topographies are defined by discontinuous features, including pillars, nanowires, and even nanoscale surface roughness.[122,123] Our review primarily focuses on the influence of these topographical cues on neural regeneration and microenvironmental regulation following SCI.

3.1. Directional Guidance: The Influence of Anisotropic Structures on Cell Behavior

Among planar anisotropic topographies, groove-ridge and fiber-filament patterns represent the most thoroughly studied geometrical configurations. The spinal cord, characterized by its highly organized architecture of aligned conductive tracts, represents an ideal target for neural tissue engineering approaches employing these topographies. Numerous studies have investigated the responses of NSCs, primary neurons, and glial cells to aligned fiber structures. Given the distinct cellular responses elicited by groove-ridge versus fiber-filament patterns, these will be discussed separately. Groove-ridge patterns present continuous anisotropic features within a planar topography, with experimental parameters typically focusing on variations in groove and ridge depth and width to optimize cellular responses.

3.1.1. Groove Depth

Groove depth significantly influences the alignment of neural-related cells. Research on four types of submicron-grooved polystyrene films (800/400, 800/100, 400/400, and 400/100) revealed that all these films could facilitate the alignment of the Schwann cell and re-organization of the cytoskeleton in a groove depth-dependent manner.[124] Coumarin polyester membranes with depths ranging from 15 to 20 nm have been shown to enhance the alignment of nervous system cells by 42% to 49%.[117,125,126] Another study showed that neurites of differentiated human embryonic stem cells aligned along a 350-nanometer grooved patterned substrate.[127] Moreover, NSCs were aligned and elongated along the grating axis on silicon micropatterns (linear or circular anisotropic, 2 or 10 μm wide, 4 μm deep).[128] As groove dimensions increase from several micrometers to dozens of micrometers, embryonic hippocampal neurons typically grow in parallel alignment with the grooves.[129]

The depth of the groove regulates neurite length. When groove depth ranges from ≈0.2 to 4 micrometers, neurite length increases with depth, although no effect is observed for features smaller than 200 nanometers.[130–132] Interestingly, groove depth also influences neurite growth direction. For instance, when embryonic mouse cortical neurons were cultured on microgroove ridges with depths ranging from 2.5 to 69 μm, axons crossed shallow grooves (2.5 or 4.6 μm) but turned when encountering deeper grooves (22 or 69 μm).[133] At intermediate depths of 11 μm, approximately half of the axons successfully traversed the steps, while the remaining axons altered their trajectories. This behavior depended highly on the angle at which the axons approached the step edges. Axons approaching from a perpendicular angle were more likely to traverse the steps, while those approaching more parallel to the groove turned to align with it.[134] Interestingly, Kwang et al. observed a similar turning behavior in their study on T cell motility. Using ramp-like microstructures with a height of 5 μm and varying slopes to mimic tissue alterations caused by inflammation or trauma, they found that T cells exhibited directed turning behavior mediated by lamellipodia and myosin light chain kinase (MLCK).[135] These findings indicate that we can customize topographical cues to control alignment, growth, and direction during neural regeneration.

3.1.2. Groove and Ridge Width

The spacing between anisotropic topographical cues represents another crucial parameter in guiding neurite orientation. Both ridge width and the width of the groove base provide distinct topographical signals that influence cellular behavior. Notably, groove width has been shown to affect cell polarity. For instance, studies have demonstrated that embryonic hippocampal neurons adjust their polarity in response to the underlying topographical features, specifically the dimensions of the groove width (**Figure 3**). When the spacing between grooves significantly exceeds the cell size, unipolar and bipolar cells often develop into multipolar cells.[136] Additionally, groove width influences neurite alignment and distribution. Researchers designed grooves with a depth of 200 nm and found that increasing the groove and platform width from 500 to 750 nm reduced the alignment rate of PC12 neurites from 90% to 75%.[137] For grooves with a depth of 300 nm and groove widths ranging from 100 to 400 nm, along with platform widths from 100 to 1600 nm, neurons preferred growing on the ridge edges and platforms rather than within the grooves.

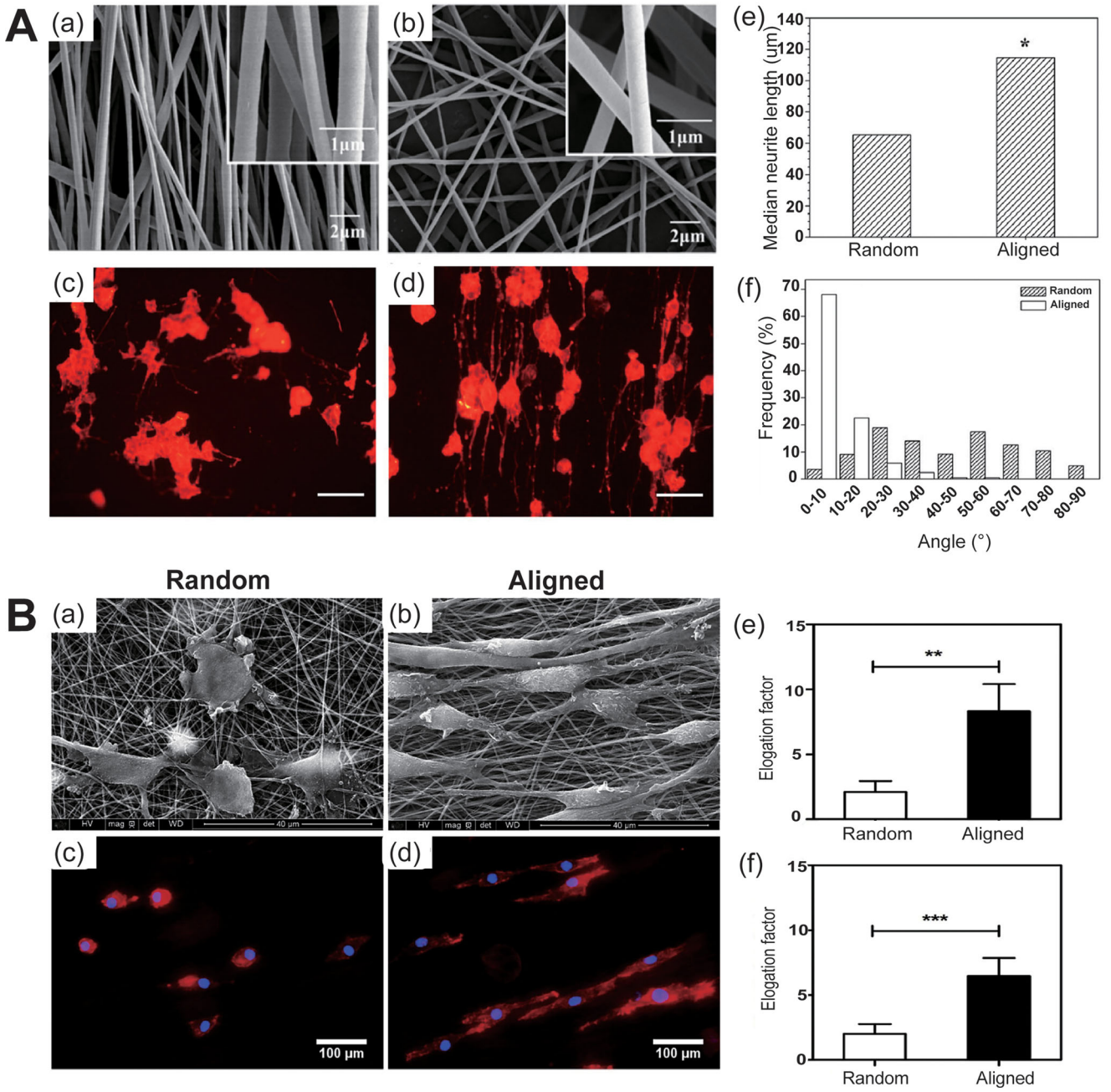

Figure 4. Effects of fiber arrangement on cell behavior. A) SEM images display electrospun aligned Aa) and random Ab) PLLA fibers, with fluorescence images of PC12 cells cultured on random Ac) and aligned Ad) PPy-PLLA fibers. Neurite median length Ae) and distribution Af) highlight alignment-induced growth differences. Scale bars: 100 μm. Adapted with permission.[158] Copyright 2016, American Chemical Society. B) SEM and rhodamine-phalloidin staining reveals macrophage morphology differences on random Ba) and aligned Bb) nanofiber membranes. Quantitative analysis of elongation Be,Bf) indicates greater elongation on aligned substrates. Adapted with permission.[159] Copyright 2019, Elsevier.

Additionally, 100 nm patterns were less effective at guiding neurite alignment compared to larger widths.[138] When groove depths reach 2–3 μm, PC12 cells cultured on 5 and 10 μm features exhibit oriented neurites.

While cells are too large to fit within the grooves physically, their neurites preferentially grow along the groove patterns. This growth demonstrates increased straightness and alignment, particularly when interacting with smaller topographical features.[139] However, studies on surfaces with grooves deeper than cell height and comparable to cell diameter found that PC12 cells exhibit oriented neurites on substrates featuring a depth of 11 μm and wall spacings ranging from 20 to 60 μm. The most substantial orientation was observed in the thinner grooves.[134] Bedeuer et al. cultured hNSCs on 25 μm deep PDMS grooves and observed distinct cell responses with increasing groove width. They found fewer neurites extended and aligned tightly along

the microchannels when the width was less than the cell body diameter. When the width exceeded the cell body diameter, cells exhibited multiple evenly distributed neurites. The study highlighted that neurites preferentially aligned along the edges of microchannels at narrower widths, emphasizing that channel dimensions are critical for neurite growth and stem cell advancement.[140] Interestingly, groove-ridge width is crucial for neural cell differentiation. Adult NSCs cultured in silicon grooves of 10 and 2 μm widths showed a preference for neuronal over astrocyte differentiation, especially at 2 μm.[128] Smaller grooves enhanced neuronal differentiation compared to flat substrates, with nanopatterns showing more pronounced effects.[141] hESCs cultured on 350 nm wide polyurethane acrylate grooves differentiated into neurons but not glial cells, and cells on 250 nm wide, spaced, and high grooves expressed more mature neuronal markers like MAP2.[142]

To further analyze whether groove-ridge continuous topographical cues affect macrophage and neutrophil morphology and polarization, Liu et al. used deep etching methods to create grooves of various widths on titanium surfaces and co-cultured them with BMDMs. The findings revealed that these groove-ridge continuous topographical cues induced macrophage elongation, peaking at groove widths of 400–500 nanometers, promoting the polarization of the anti-inflammatory, pro-healing macrophage phenotypes. Notably, macrophages cultured on 5 μm grooves secreted significantly higher levels of the anti-inflammatory cytokine IL-10, highlighting the potential of surface topography to modulate macrophage function and improve the post-spinal cord injury microenvironment. Another study employed Reversal Nanoimprint Lithography (NIL) techniques to construct parallel gratings with a width: height: period ratio of 1:1:2, ranging from 250 nanometers to 2 micrometers, for co-culture with macrophages. Macrophages showed maximum adhesion and elongation on 500-nanometer gratings, with the most significant TNF-α secretion. As the grating scale increased, both adhesion and secretion effects diminished.[143] When engineered zinc substrates with groove-ridge structures of approximately 15 micrometers in width and 200 nanometers in height were co-cultured with THP-1-derived macrophages, the results indicated a reduction in macrophage inflammatory polarization in vitro, thereby improving biocompatibility and tissue integration.[74] Zheng combined gold nanorods with PCL films and utilized near-infrared radiation to create dynamic groove-ridge topographical cues ranging from 5 to 30 micrometers. The study found that films with groove widths of 10 and 20 micrometers more effectively induced macrophage elongation and phenotypic changes compared to those with 5 and 30-micrometer grooves. These films also upregulated the expression of arginase 1 and IL-10, which corresponded to an anti-inflammatory response.[144]

Anisotropic topographical structures significantly impact cell shape and neutrophil migration. The development of advanced topographical structures has the potential to act as physical cues, modulating neutrophil behavior and reducing inflammation at the injury site. However, the precise influence of topographical cues on neutrophil morphology and motility remains poorly understood, necessitating further investigation.[145,146] Early studies demonstrated that neutrophils exhibit contact guidance on grooved surfaces (2 μm wide and 2 μm deep) and on jagged nano-patterns on glass and acrylic substrates.[147,148] Sung et al. utilized a flexible UV-curable polymer to create rectangular grooves with a width and depth of 0.8 μm, finding that these microgrooves induced stronger neutrophil polarization during migration. In addition, the study revealed an enhanced positive correlation between aspect ratio and speed in micro-scale topography research.[149]

Groove space width directly affects T-cell spreading and activation. Brittany et al. engineered parallel nanoridges, ≈600 nm high and 200 nm wide, with spacings of 1, 1.8, 3, and 5 μm to investigate T-cell responses. Compared to flat surfaces, nanoridges reduced the maximum spreading area of T cells, with 3 and 5 μm spacings promoting greater spreading than narrower spacings or flat surfaces. These structures enhanced actin and ZAP-70 accumulation at the immune synapse and altered actin and microtubule dynamics, coordinating T-cell signaling.[150] Additionally, the nanostructures induced calcium oscillations and reorganized B-cell receptor clusters, modulating B-cell signaling. These results highlight the critical role of nanotopography in immune cell activation.[151]

These findings indicate that immune-related cell morphological changes and cytokine secretion are susceptible to groove-ridge continuous topographical cues, with potential optimal parameters for regulation. As observed in the previous examples, the spacing of anisotropic linear geometrical cues significantly impacts not only the morphology and polarization of macrophages but also the alignment of neurites. Cells and their extensions tend to align with wide and shallow grooves but bridge across narrow and deep grooves, a phenomenon known as "cell bridging." Additionally, NSCs in narrower grooves exhibit a greater tendency for neuronal differentiation. Nanometer-scale grooves promote macrophage M1 polarization and pro-inflammatory cytokine secretion, while micrometer-scale grooves are more likely to enhance M2 polarization and anti-inflammatory cytokine secretion. However, more precise parameter ranges for these effects are currently lacking. Understanding the influences of vertical contact guidance, differentiation fate, and inflammation regulation is crucial for designing topographical cues in spinal cord injury repair materials.

3.1.3. Optimizing Fiber Orientation: Enhancing Neurite Growth and Alignment

The alignment of fibers and filaments plays a crucial role in guiding the orientation and differentiation of neural cells. Specifically, the influence of anisotropic fiber orientation on neuronal differentiation has been demonstrated in studies employing parallel or randomly oriented submicron-diameter polycaprolactone (PCL) fibers with diameters of 260, 480, and 930 nm (**Figure 4**). They observed that NSCs cultured on aligned fibers demonstrated higher expression of the neuronal differentiation marker Tuj1 following retinoic acid (RA)-induced differentiation compared to those grown on random fibers or un-patterned surfaces.[153] Similarly, another study found that when dorsal root ganglion (DRG) explants were cultured on poly(L-lactic acid) nanofibers with varying degrees of alignment (highly, moderately, and randomly aligned), the neurites initially sprouted radially on aligned fibers but then oriented themselves along the fiber axis upon

contact, leading to significantly longer neurites compared to those on randomly or moderately aligned fibers.[154] ESC differentiation on 250 nm diameter random and oriented PCL fibers showed that oriented nanofiber substrates enhanced differentiation into both neurons and oligodendrocytes while limiting the formation of astrocytes.[155] Shah reported that NSCs grown on randomly oriented 200–300 nm PCL fibers coated with graphene oxide (GO) exhibited selective differentiation into oligodendrocytes, with the effect varying according to GO concentration.[156] Rat NSCs cultured on randomly oriented electrospinning fibers in a medium supporting mixed lineage differentiation into neurons, astrocytes, and oligodendrocytes showed a threefold enhancement in oligodendrocyte differentiation on 283 nm diameter fibers compared to the tissue culture polystyrene (TCPS) control. Cells on 749 nm diameter fibers demonstrated the highest neuronal differentiation, as indicated by marker expression, with scanning electron microscopy confirming these differences in cell morphology. However, cells grown on larger diameter fibers (1452 nm) had lower viability.[157]

Moreover, studies have shown that fiber alignment affects macrophage polarization. Aligned nanofibers alter macrophage morphology and increase the activation of the anti-inflammatory phenotype, whereas random nanofibers induce a pro-inflammatory phenotype.[75,159] In contrast, studies using parallel and randomly oriented PLLA nanofibers (250 nm) and microfibers (1250 nm) found that cerebellar stem cells showed increased differentiation into the neural lineage (cell number and neurite length) on nanofibers, regardless of fiber orientation. These findings suggest that neuronal differentiation may be influenced by fiber diameter independent of alignment, while alignment primarily affects neurite outgrowth and cell morphology.[160] Discrepancies between studies might be attributed to variations in cell source and culture conditions. Nevertheless, these observations underscore that fiber alignment is not the sole determinant in fiber-based scaffold design, necessitating further investigation to elucidate the underlying mechanisms governing these cellular responses.

3.1.4. Fiber and Filament Diameters

Fiber and filament diameters are critical factors in directing cell migration and neurite outgrowth. Studies have demonstrated that larger fiber diameters, such as 10 µm, can induce precursor cells to migrate from neurospheres in a chain-like pattern.[161] Similarly, experiments using poly(L-lactic acid) (PLLA) fibers with diameters ranging from 300 to 1300 nm revealed that larger diameters not only promoted longer and more directed neurite outgrowth but also increased Schwann cell (SC) migration distances.[162] Similarly, this phenomenon was observed in Schwann cells cultured on chitosan fibers with diameters of 15 µm.[163] When the diameter of PVC hollow fibers decreased from supracellular (100 to 500 µm) to cellular (30 µm) and to subcellular (5 µm), there was a corresponding decrease in Schwann cell migration and neurite outgrowth.[164] Although PLLA microfibers with a diameter of 375 µm effectively directed neurite extension and Schwann cell migration, they significantly promoted neurite growth when combined with laminin (LN).[165] Wen and Tresco proposed that there might be an optimal filament diameter range for cell culture, where filaments neither too large nor too small relative to the size of the growth cone would not exhibit distinguishable energy differences in various growth directions.[164,166]

Fiber and filament diameters also regulate cell differentiation (**Figure 5**). For instance, electrospun micro- and nanoscale PLLA fibers can orient NSC somas and neurites, while nanoscale fibers enhance NSC differentiation on microscale fibers, which have average diameters of 250 nm and 1.25 µm, regardless of their orientation.[160] In contrast to 2D substrates, 3D polyphenylsulfone (PPS) nanofibers significantly improve NSC adhesion and growth. GFAP and β-III tubulin fluorescence staining revealed that over 85% of axons were aligned at a specific angle, demonstrating that aligned nanofibers effectively promoted extensive parallel axonal growth.[140] To investigate the relationship between fiber diameter and cell behavior, polyethersulfone (PES) fibers were uniformly coated with laminin. This approach revealed differentiation differences among cells cultured on fibers with varying diameters, highlighting the influence of fiber size on cellular responses. Cells cultured on fibers with larger diameters of 749 and 1452 nm showed differentiation into neurons; however, cells on 238 nm fibers tended to differentiate into oligodendrocytes.[157,167,168] This preferential differentiation of oligodendrocytes may be related to the fiber size, which is morphologically similar to axon diameter.[123] However, an earlier study indicated that randomly electrospinning PCL fibers measuring 750 nm in diameter also promoted NSCs to preferentially differentiate into oligodendrocytes.[169] These findings highlight the importance of optimizing fiber diameters to guide cell migration and differentiation, offering valuable insights for applications in tissue engineering and regenerative medicine. Notably, it suggests that fiber alignment is not the only parameter influencing macrophage phenotype; the diameter of the fibers also plays a role in regulating macrophage activation. Studies have shown that compared to electrospinning poly (L-lactic acid) (PLLA) fibers with a diameter of approximately 1.5 micrometers, fibers with a diameter of ≈600 nanometers elicit the least inflammatory response in macrophage culture systems.[170]

3.2. Isotropic Patterns: Their Role in Cellular Differentiation and Neurite Orientation

Isotropic topographical cues, such as nano- or micron-scale pillars, holes, and nano-rough surfaces, are characterized by their diverse, discontinuous morphologies and provide guidance at specific, discrete locations. The size and spacing of these features are critical parameters that influence the effectiveness of isotropic topographical cues in guiding cellular behavior.[171,172]

3.2.1. Alignment and Differentiation

Current research suggests that discontinuous isotropic topographical structures impact differentiation toward glial rather than neuronal lineages. Researchers have designed micropatterned polymer membranes with pore sizes ranging from 3

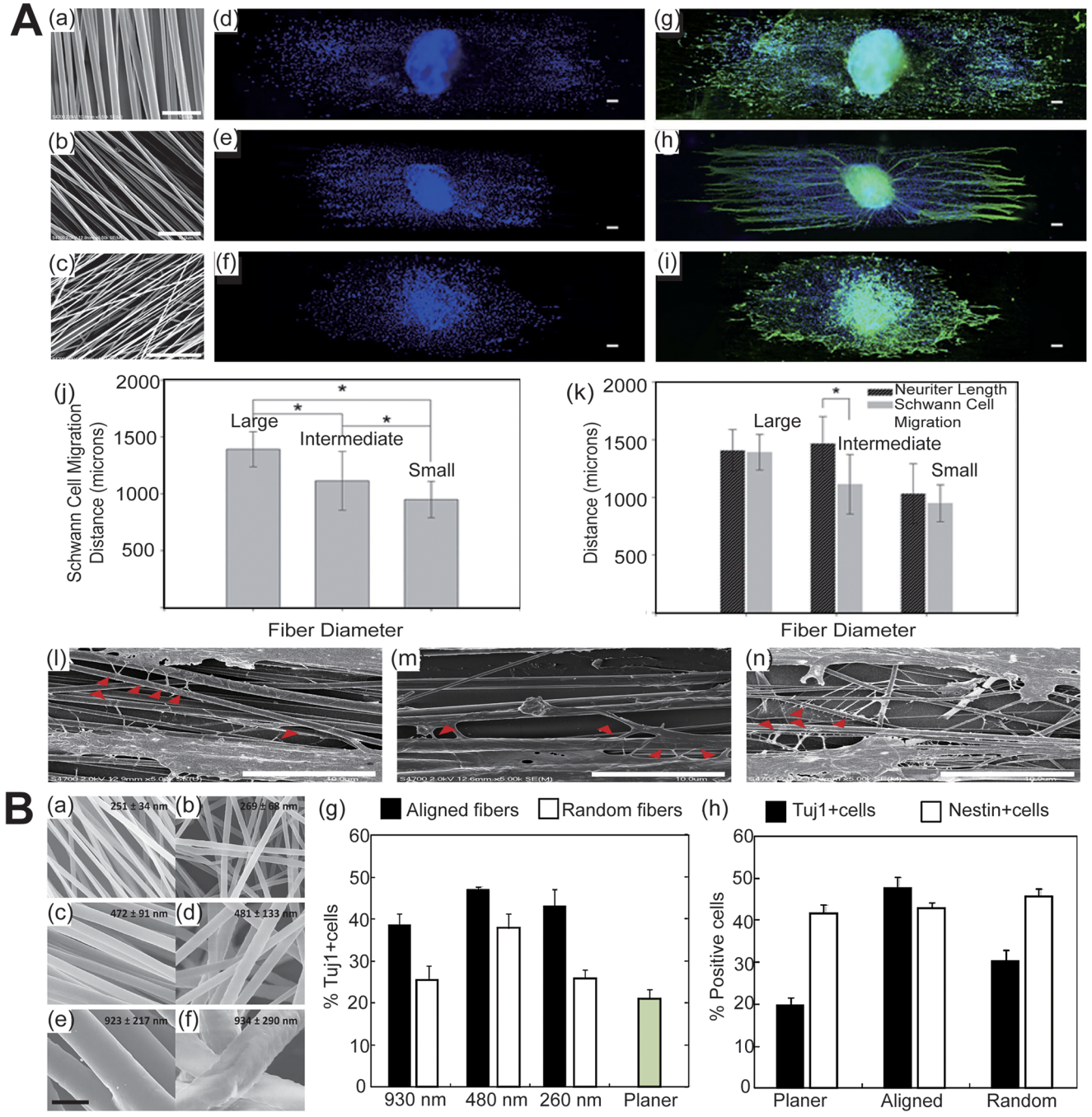

Figure 5. Fiber and filament diameters regulate cell differentiation. A) SEM images illustrate aligned fibers with diameters of 1325 ± 383 Aa), 759 ± 179 Ab), and 293 ± 65 nm Ac). Schwann cell migration, shown in DAPI-stained images Ad–f), was highest on larger fibers and lowest on finer fibers Aj). Neurofilament/DAPI images of DRG cells after 5 days Ag–i) indicate neurite alignment along fibers, with intermediate-diameter fibers promoting the greatest neurite outgrowth Ak). SEM images Al–n) display neurite extensions and filopodia (red arrows) on each fiber condition, demonstrating orientation-dependent growth. Reproduced with permission.[162] Copyright 2010, Elsevier. B) Adult NSCs (ANSCs) exhibit distinct behaviors on planar TCPS and fiber substrates. SEM images of aligned and random electrospun PCL fiber meshes with varying diameters, fabricated from 12 wt% PCL with R18 Ba-b), 12 wt% PCL Bc-d), and 14 wt% PCL Be-f). Quantification Bg-h) confirms higher Tuj1+ neuron percentages on aligned 480 nm fibers. Adapted with permission.[153] Copyright 2010, IPC Science and Technology Press.

to 15 μm to study the differentiation of NSCs and found that membranes featuring pore sizes of 3 and 5 μm obstruct NSC differentiation, with the highest inhibition observed at 3 μm.[173] In another study, researchers developed linear, circular, and dot micro-patterns of different micron scales and co-cultured them with adult NSCs. Unlike the high alignment of cells on continuous anisotropic topographies, cells on isotropic dot micro-patterns showed no preferential direction or alignment and had reduced differentiation capacity into neuronal lineages, indicating that cell polarity can impact the outcome of differentiation, a trend more pronounced with smaller feature sizes.[128] A similar conclusion was drawn from another study. hESCs were cultured on both continuous anisotropic grating patterns and discontinuous isotropic micro-scale structures. The micro-scale features included arrays of pillars (1 μm diameter, 1 μm height) with a spacing of 6.5 μm, and arrays of holes (2 μm diameter, 2 μm depth) with a spacing of 12 μm. Discontinuous isotropic pillar and hole structures promoted hESC differentiation into glial cells rather than neurons. Quantitative PCR showed varying levels of expression between oligodendrocyte- and astrocyte-specific genes when comparing the two discontinuous patterns. This indicated that hESCs differentiated more into oligodendrocytes on pillar structures and into astrocytes on hole structures.[142]

3.2.2. Neurite Orientation

Previous studies have demonstrated that neurites accurately respond to disrupted guidance cues (**Figure 6**). Cells on isotropic features smaller than 5 μm exhibit small, rounded morphologies with poorly organized cytoskeletons.[174] When PC12 cells were cultured on nano-pillars and nano-holes, they exhibited shorter and fewer neurites compared to those grown on smooth substrates, indicating that specific nano-patterns restrict cell morphology and growth.[175] When hippocampal neurons were seeded on 1 μm high pillars with diameters of 0.5 or 2 μm, neurites typically spanned the shortest path across pillars, aligning predominantly at 0 or 90°. Larger pillars demonstrated the greatest degree of alignment with minimal spacing. As pillar spacing increased, alignment fidelity diminished, and at 4.5 μm spacing, neurite distribution resembled that observed on flat surfaces.[176] When pillar diameter and edge-to-edge spacing increased (ranging from 10 to 100 and 10 to 200 μm, respectively), neurites aligned and connected linearly between adjacent pillars, primarily growing in one direction with occasional perpendicular branching. As the diameter was enlarged, neurites wrapped over existing pillars, especially when spacing exceeded to 40 μm. A spacing of 200 μm encouraged random growth and wrapping, whereas flat surfaces led to non-directional growth. As feature size and spacing increased, neurite growth transitioned from alignment to wrapping and eventually to randomness.[172]

3.3. Randomness and Design: How Surface Roughness Affects Cellular Responses

Stochastic topographies can be described as complex, random surface textures, with roughness being the primary experimental parameter. Substrates with specific ranges of statistical roughness parameters can regulate polarity, neurite length, and the survival and differentiation of neural cells.[177,178]

3.3.1. Roughness

Surfaces with less than 1 μm height differences are generally classified as nano-structured or nano-rough. Research has demonstrated that such surfaces significantly impact cell morphology, adhesion, proliferation, and differentiation, highlighting their potential to influence cellular behavior.[174] Roughness is typically quantified by the average feature size (Arithmetic Average Roughness, Ra). One study discovered that nano-textured titanium nitride films with Ra values ranging from 1.3 to 5.6 nm diminished the attachment of primary hippocampal neurons compared to PDL-coated glass.[179] Another study demonstrated that nano-textured silicon (Ra values: 18–204 nm) exerted an unimodal influence on the adhesion and viability of primary embryonic cortical neurons. The optimal neuronal response was observed with a Ra of 64 nm; higher and lower roughness values diminished this response.[180] Furthermore, local nano-roughness and surface energy variations similar in scale to growth cones enhanced PC12 cell outgrowth and neuronal differentiation patterns even without NGF.[181] By using monodisperse silica colloids to mimic receptor cluster-level topographies, it was observed that when Rq was 16–32 nm, telencephalic NSCs spontaneously differentiated into neurons.[177] Interestingly, on nanoporous titanium dioxide (TiO2) surfaces with pore sizes between 200 and 500 nm, rat NSCs exhibited a stronger tendency to differentiate into astrocytes rather than neurons.[182] The differentiation of telencephalic NSCs into astrocytes could only be induced in the presence of astrocyte differentiation inducers by adjusting random nano-roughness.[183] Furthermore, hippocampal neurons demonstrated improved survival and functionality on surfaces with nano-rough textures.[184] A novel nanotopography-based reverse uptake (NanoRU) delivery system was developed to influence neural stem cell (NSC) differentiation by facilitating the targeted delivery of siRNA into cells. By using optimal uptake parameters of 100 nm, they suppressed SOX9 to differentiate NSCs into neurons selectively.[185]

Surface roughness can also modulate macrophage polarization. Some studies also indicate that surface roughness can simultaneously induce both anti- and pro-inflammatory activation.[186–188] The narrow roughness range (Ra = 0.51–1.36 μm) enhanced anti-inflammatory polarization, while roughness outside this range upregulated both pro- and anti-inflammatory markers.[189] Anodizing titanium to create 30-nanometer pores promotes M2 polarization, while 100-nanometer pores favor M1 polarization.[190] Similarly, nanopores (35 nanometers in diameter and 3 micrometers deep) created on Ti50Zr alloy through anodization reduce macrophage metabolic activity and pro-inflammatory cytokines.[191,192] Conversely, Li et al. found that micron-scale roughness on tricalcium phosphate upregulated iNOS and IL-1β in RAW264.7 cells, whereas submicron-scale roughness promotes an anti-inflammatory phenotype.[193] These discrepancies may be attributable to variations in cell lines and culture conditions, highlighting the need for further investigation

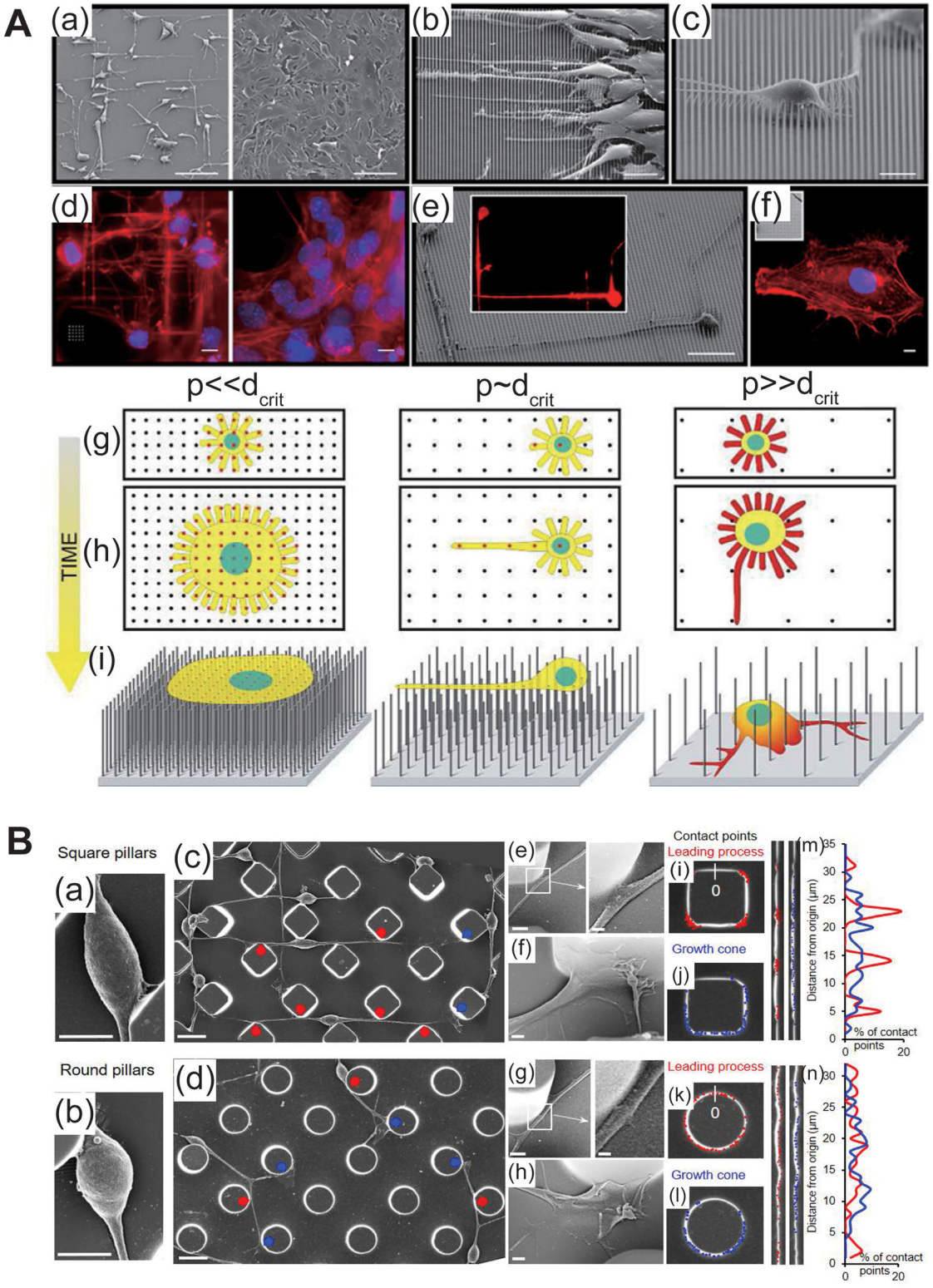

Figure 6. Neurites accurately respond to micro- and nano-topographical disrupted guidance cues. A) Polarization of C3H10T1/2 cells on nanopillar (NP) arrays. SEM images show cells align with NP grids (l = 10 μm, r = 100 nm, p = 2 μm) after 1 day, contrasting with polished silicon wafers Aa). Actin (red) and nuclei (blue) staining after 2 days highlights differences in polarization and spreading Ad). Schematic models suggest NP density and spacing affect adhesion and alignment relative to critical spacing (d_{crit}). Adapted with permission.[171] Copyright 2012, American Chemical Society. B) Micro-pillar shape influences interneuron morphology and migration. Square pillars promote elongated processes, while round pillars induce branching and frequent growth cone divisions Ba–d), with quantification across 60 cells Bm-n). Contact point distributions vary by pillar shape. Adapted with permission.[319] Copyright 2019, IPC Science and Technology Press.

into the relationship between surface roughness and macrophage response (**Figure 7**).

3.3.2. Patterned Topographical Cues

Patterned topographical cues play a role in regulating neural regeneration, primarily influenced by image features and sizes. Using etching techniques, square micro-nano structures of poly L-lysine (PLL) with a size of 10^4 μm^2 were synthesized and co-cultured with NSCs, resulting in increased cell adhesion and the formation of axon-like projections with high levels of β-tubulin III expression.[194] Additionally, micro-nano structures with linear, circular, and dot patterns on silicon surfaces were found to promote NSC proliferation and preferentially induce differentiation into mature neurons compared to flat surfaces.[128] In another study by Buzanska, controlling the micro-nano topography of fibronectin and PLL substrates effectively regulated stem cell neural differentiation. Interconnected square micro-nano patterns significantly enhanced stem cell adhesion and promoted neurite outgrowth post-differentiation.[195] Interestingly, when these square topographical cues are arranged through stacking or orthogonal methods to form axial pores with micron-scale 3D geometries, they significantly induce macrophages to produce more pro-inflammatory cytokines, such as TNF-α and IL-12/23.[196]

Generally, stochastic and patterned topographical cues not only affect the adhesion, proliferation, survival, and differentiation of neural-related cells but also the activation of immune cells, underscoring the critical role of specific feature sizes and roughness parameters in neural tissue engineering and regenerative medicine. Given the vast complexity of unconventional topographical cue combinations, there is an urgent need for high-throughput methods to screen diverse topographies for their effects on neural and inflammatory cell behaviors. To address this, we recently developed a combinatorial biophysical cue array comprising thousands to millions of unique topographies—including anisotropic, isotropic, and hierarchical designs—with feature sizes ranging from tens of nanometers to microns. This advanced array system enables us to systematically investigate the interactions between substrate topographies and cell fate regulation (**Figure 8**).

Through a systematic comparison of studies, we found that anisotropic topographies, such as aligned fibers or grooves, effectively guide neural cell alignment, axonal regeneration, and directional growth by mimicking the native spinal cord architecture. In contrast, isotropic topographies like pillars, holes, and nano-rough surfaces influence neural stem cell fate and neurite behavior through non-aligned cues. While progress has been made in understanding the role of topological structures in spinal cord injury, key areas remain underexplored, including systematic screening, fabrication, intelligent responsiveness, and dynamic integration of topographies. Several underutilized cues could enhance therapeutic efficacy, such as multiscale hierarchical structures combining micro- and nano-topographies, 3D scaffolds with anisotropic gradients, and stimuli-responsive surfaces that adapt to the dynamic healing process. Furthermore, the role of curvature, geometric complexity, and topography-mediated immune modulation, particularly in axonal growth and immune response, is still poorly understood. Ultimately, investigating the relationship between topography and substrate rigidity may offer new insights into mechanotopographical control, thereby enhancing the potential for translational applications in SCI treatment. To provide a consolidated view of these parameters, we have summarized representative examples of material types, surface structures, and mechanical properties and their respective effects on neural regeneration in **Table 3**.

4. Mechanotransduction Pathways: How Topographical Cues Influence Cell Fate

The mechanisms by which neural stem cells (NSCs) and immune cells interpret topographical cues, both in vitro and in vivo, are not yet fully elucidated. It has been suggested that adherent cells can sense local micro- and nanoscale topographical features. This process is mediated by integrins, which facilitate cell adhesion to the extracellular matrix (ECM) and activate intracellular signaling pathways involving tyrosine kinases and phosphatases. These interactions enhance cell-ECM signal transduction, triggering biochemical reactions that ultimately regulate cell fate,[205] as shown in (**Figure 9**).

Integrins are cell surface receptors that attach to specific ECM motifs, allowing cells to sense and respond to the physical and topographical features of their extracellular surroundings.[206] Activation and clustering of integrins lead to the formation of focal complexes, which evolve into focal adhesions (FAs). FAs are multi-protein structures that connect integrins to actin filaments within the cytoskeleton. The recruitment of actin-binding FA proteins, such as paxillin and talin, promotes the development of actin stress fibers and facilitates force transduction through the actin-myosin network, resulting in alterations in cytoskeletal tension.[207] FAs offer mechanical and physical connections for cell contraction structures, directly influencing cytoskeletal organization, structure, and cell shape.[208] Additionally, FAs interact with signaling proteins to trigger downstream biochemical pathways, such as phosphorylation and G protein activation (e.g., Rho-mediated pathways and ROCK). These interactions lead to long-term alterations in transcriptional regulation, cell adhesion, proliferation, and differentiation.[209]

Studies have shown that the β1 integrin subunit is crucial in NSC migration and differentiation. Specific topographical cues can achieve selective protein deposition, influencing cell adhesion and subsequent biological behaviors through β1 integrin.[210–212] For instance, distinct protein adsorption on hydrogen-terminated ultra-crystalline nanodiamond films (H-UNCD) with an average grain size of 5 nm triggers the spontaneous differentiation of NSCs. This behavior can be markedly inhibited using a β1 integrin inhibitor, while an increase in phosphorylation of FAK and Erk1/2 is observed in NSCs. Treatment with the MEK inhibitor U0126 reduces the activation of the Erk1/2 pathway, suggesting that fibronectin adsorbed on the nanodiamond surface binds to β1 integrin. This binding activates integrin signaling pathways, leading to FAK tyrosine phosphorylation and subsequent activation of the MEK/Erk signaling pathway.[210] Enhanced differentiation of human NSCs (hNSCs) on a hierarchically patterned surface model with nanopore-patterned microgroove structures appears to be

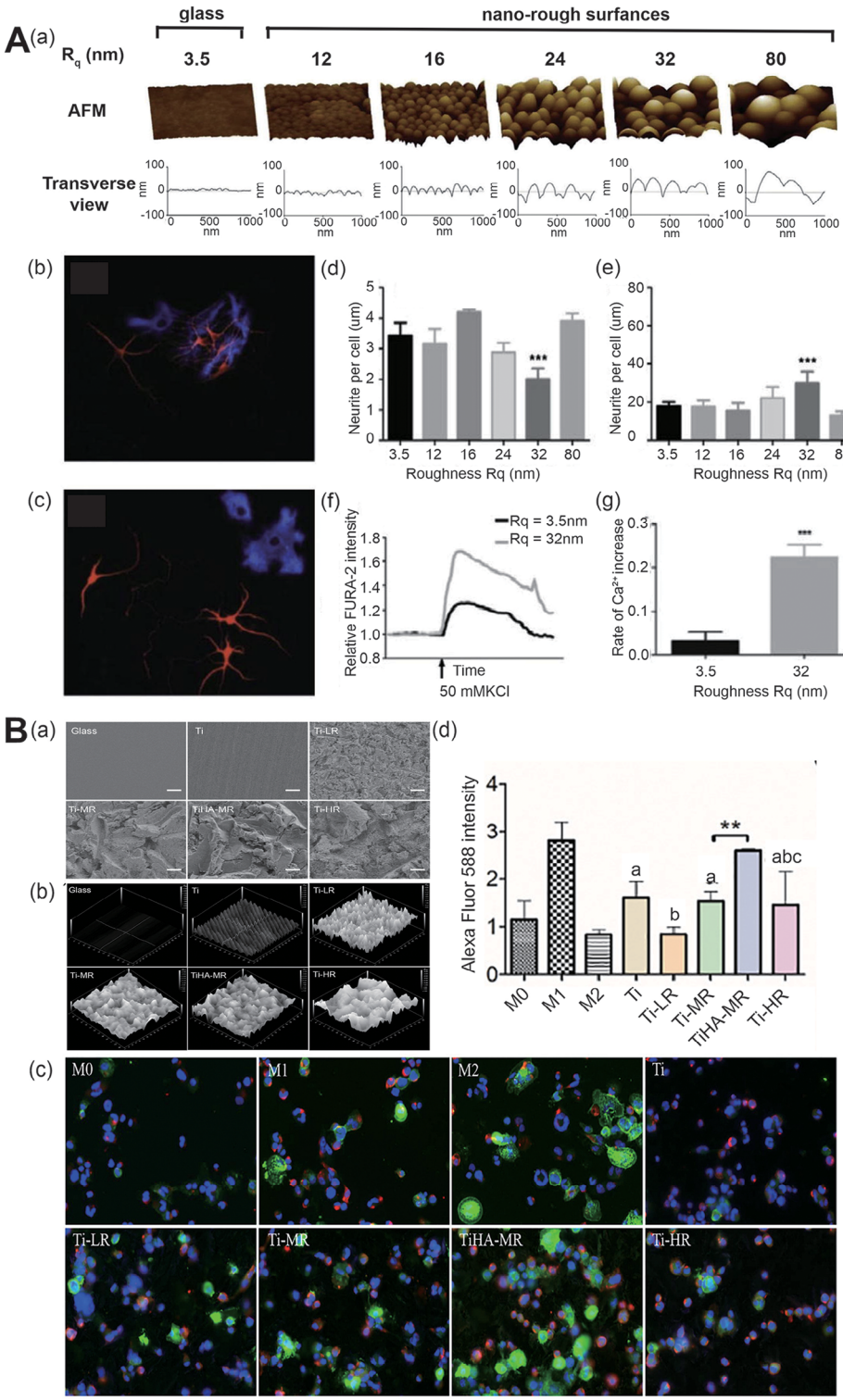

Figure 7. Nanorough substrates in the regulation of cell morphology and function. A) Influence of nanorough substrates on PC-12 cell morphology and neuronal function: Aa) AFM characterization of SNP-modified substrates with varying roughness (Rq). Ab) Neuron-astrocyte interactions on smooth and Rq = 32 nm substrates, visualized by GFAP (blue) and MAP-2 (red) staining, with quantification in short-term (5 days, Ad) and long-term (6 weeks, Ae) cultures. Af,g) FURA-2 calcium imaging reveals intracellular calcium changes and depolarization rates upon KCl stimulation, highlighting functional differences between smooth and nanorough substrates. Adapted with permission.[127] Copyright 2014, National Academy of Sciences. B) Modulation of immune response by titanium surfaces: Ba,b) SEM and surface scanner analysis of glass and titanium substrates. Bc,d) Immunostaining of THP-1 cells cultured on titanium shows differential expression of M1 (CCR7, red) and M2 (CD36, green) markers, quantified using ImageJ and GraphPad Prism. Adapted with permission.[189] Copyright 2019, Elsevier.

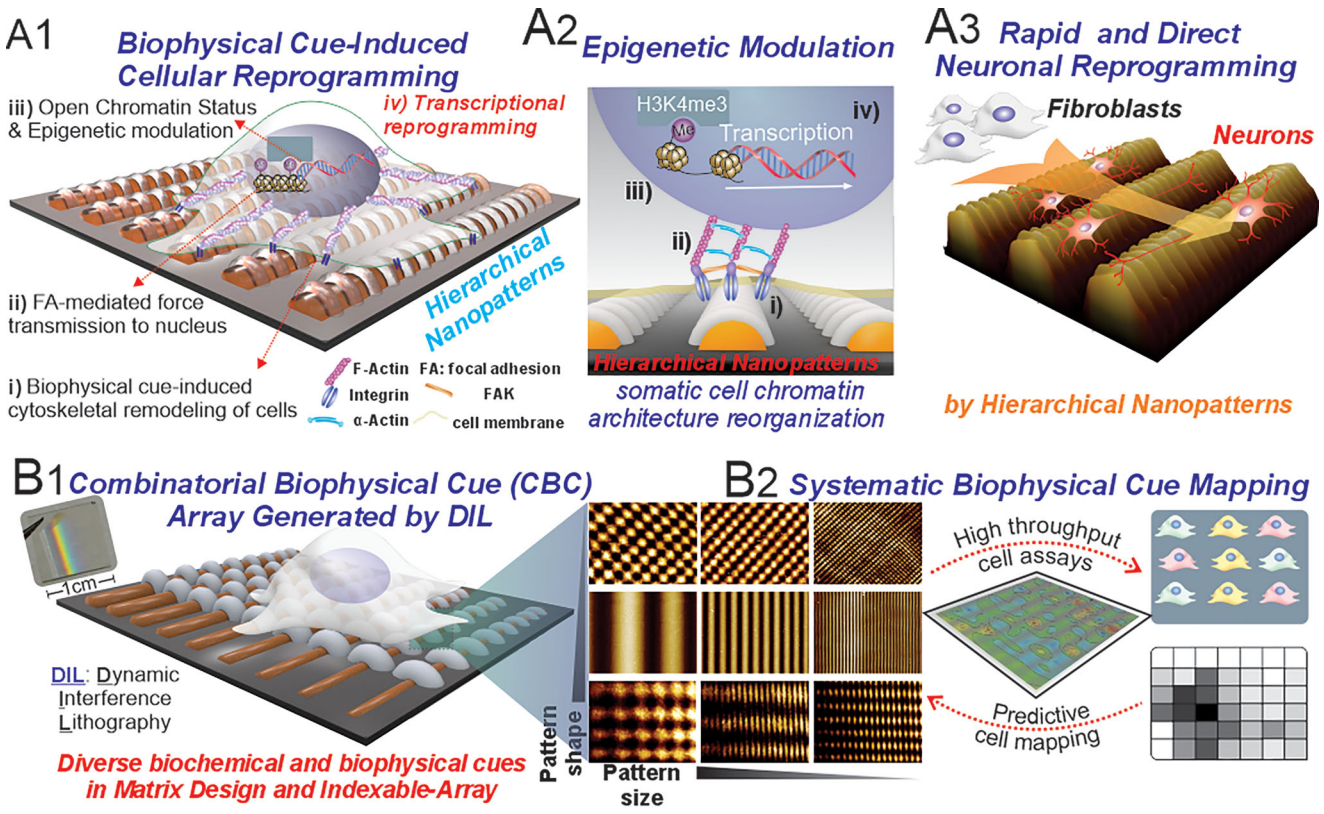

Figure 8. Hierarchical topographical cues for modulating neuronal reprogramming. a) Biophysical cue screening using combinatorial nanoarrays composed of both anisotropic, isotropic, and hierarchical topographical cues. Effects of topographies on neuronal reprogramming through epigenetic mechanisms were studied as a proof-of-concept. b) The synthesis of a combinatorial biophysical cue (CBC) array through dynamic interference lithography (DIL). c) Hierarchical nanopattern-mediated epigenetic modifications induce neuronal reprogramming, as revealed by the CBC array and on the scale-up of hierarchical patterns. Adapted with permission.[245] Copyright 2022, American Chemical Society.

associated with integrin binding, F-actin reorganization, and FAs assembly.[183]

To further investigate the role of β1 integrin in regulating NSC fate, researchers developed a hierarchically patterned substrate (HPS) platform. This platform combines microgroove patterns with nanopore clusters to create a multi-scale HPS. Compared to 2D-patterned substrates, NSCs grown on HPS exhibit highly aligned, elongated morphologies and increased differentiation into both neurons and astrocytes. Treatment with ROCK inhibitor Y27632 showed similar effects, with both treatments reducing adhesion mediated by N-cadherin. These findings highlight the crucial role of β1 integrin-mediated assembly and ROCK-mediated signaling pathway activation in promoting FA formation and FAK pathway activation, thereby enhancing hNSC differentiation on specific hierarchical topographical models.[213] Similar conclusions were drawn by Czeisler.[161] In vitro, electrospinning studies indicate that hierarchical patterns might enhance hNSC differentiation through mechanotransduction mechanisms.

To explore the mechanisms by which specific topographical cues induce selective differentiation of NSCs into neurogenic lineages, Qi examined the percentage of neurons, astrocytes, and oligodendrocytes differentiated under treatment with Erk1/2 pathway inhibitors. They found that the percentage of neuronal differentiation changed significantly, indicating that topographical cues contribute to neuronal preferential differentiation.[128] This selective differentiation is linked to focal adhesion kinase (FAK) and mediated through the fibronectin-β1 integrin

Table 3. Effects of material types, surface structures, and mechanical/physicochemical properties on neural regeneration.

Category	Design/Feature	Effect on neural regeneration
Material type	Natural polymers (e.g., collagen, chitosan, gelatin)	Biocompatible; promotes cell adhesion, ECM mimicry; modulates immune responses (e.g., promotes M2 macrophage polarization).[71,72,141]
	Synthetic polymers (e.g., PLGA, PCL, PEG)	Tunable mechanical and degradation properties; long-term support.[197,198]
	Composite materials (natural + synthetic)	Balance of bioactivity, mechanical strength, and tunability.[199,200]
	Immunomodulatory biomaterials	Modulate inflammatory microenvironment and support axonal regeneration.[71,201]
Topographical Cues	Grooves, ridges, aligned fibers	Guide axonal alignment and elongation; support directional neurite outgrowth.[124,137,150]
	Random fibers or isotropic topographies	Less effective in directional guidance; may hinder axon guidance.[139,172]
	Hierarchical micro/nanostructures	Mimic ECM complexity; enhance migration, extension, and regeneration.[124,192]
	3D architectures	More biomimetic; support circuit reconstruction and deeper cell infiltration.[197,202,203]
	Surface biofunctionalization (e.g., RGD, IKVAV)	Promote adhesion, differentiation, and glial cell integration.[137]
Mechanical Properties	Elastic modulus (soft, 0.1–1 kPa)	Mimics neural tissue; enhances axonal growth and neuronal differentiation.[198]
	High stiffness (>10 kPa)	Promotes glial scarring and inhibits axonal growth.[198]
	Tensile strength	Supports large-gap repair and mechanical integration.[202,204]
	Crosslinking density	Influences scaffold degradation and cell migration.[198]
Physicochemical	Degradation kinetics	Affects scaffold persistence and immune response; balanced degradation supports repair.[198,199]
	Electrically conductive materials (e.g., graphene, polypyrrole)	Facilitate electrical signaling; promote neurite growth and synapse formation.[150,153]

interaction along with the FAK/MAPK/Erk signaling pathways.[210] Lim et al. co-cultured NSCs with submicron-diameter polycaprolactone (PCL) fibers ranging from 260 to 930 nm while simultaneously applying various biochemical cues. Their findings revealed that different differentiation lineages of NSCs exhibited distinct responses to parallel fiber topographical cues. This differential response was found to be mediated through the Wnt/β-catenin signaling pathway.[153] These findings indicate that gene expression changes can be influenced by substrate topography through cytoskeletal elongation. The synergistic effect of stem cell shape control and biochemical cues plays a crucial role in determining cell fate.

In addition to affecting integrin activation and intercellular communication, topographical cues may also modulate stem cell function by activating mechanosensitive ion channels or altering the proportion of nuclear YAP/TAZ. Magnetic nanobubbles (MNBs), composed of magnetic nanoparticles, were used to induce intracellular hydrostatic pressure and cytoskeletal alterations in NSCs through membrane volume oscillation. This process activated the Piezo1-Ca^{2+} mechanotransduction channel, triggering the BMP2/Smad pathway and leading to the differentiation of NSCs.[214] Yang developed a topographical gradient of polydimethylsiloxane (PDMS) based on a high-throughput screening (HTS) method to study its effect on the destiny regulation of bone marrow mesenchymal stem cells (BMSCs) toward neuronal differentiation. The results showed that specific substrate parameters significantly enhanced neurogenesis, with BMSCs on these substrates exhibiting lower nuclear YAP/TAZ percentages and weaker cellular contractility. These findings suggest that the promotion of neurogenesis is mediated by alterations in cellular tension and the YAP/TAZ pathway.[215] While the precise role of this pathway in regulating NSC differentiation into neurons remains unclear, cytoskeletal dynamics are believed to play a crucial role in guiding NSC fate determination.

In contrast to β1 subtype, β2 integrin plays a key role in regulating the inflammatory microenvironment. Zheng constructed biocompatible Mg-Al layered double hydroxide (LDH) nanosheet arrays on titanium surfaces with sizes ranging from 75 nm to 0.85 µm and investigated their regulatory effects on macrophages. They found that nanosheet array structures promoted M2 macrophage polarization by activating the PI3K-AKT-mTOR signaling pathway, characterized by high gene expression of integrin β2 and FAK, thereby suppressing inflammatory responses.[216] Different aspect ratios of nanostructures can generate micro-nano forces to finely tune the conformation of integrin β2, precisely regulating inflammatory responses. To investigate the impact of varying structural parameters on integrin $\alpha X\beta 2$ conformational compression and inactivation, three nanostructured surfaces with low aspect ratios were created. It was found that low-aspect-ratio micro-nano structures, such as nanorods and nanospheres, effectively inhibited the extension and activation of integrin β2 conformation. This inhibition led to reduced focal adhesion activity, downstream PI3K-Akt signaling, and decreased NF-κB signaling and macrophage inflammatory responses.[217] Existing studies have confirmed that mesh and linear micro-nano structures regulate inflammatory cell phenotypes, while low-aspect-ratio micro-nano structures regulate inflammatory responses. This regulatory effect is related to integrin activation, PI3K-AKT-mTOR, and Src-ROCK signaling pathways.[218] However, the exact mechanism for regulating these micro-nano structures requires further investigation.

5. Synthesis of Topographical Substrate for Enhanced SCI Repair

Given the highly oriented and well-organized structure of spinal cord tissue, effective neural regeneration and circuit reconstruction require materials specifically designed with carefully engineered topographical cues to optimize injury repair.

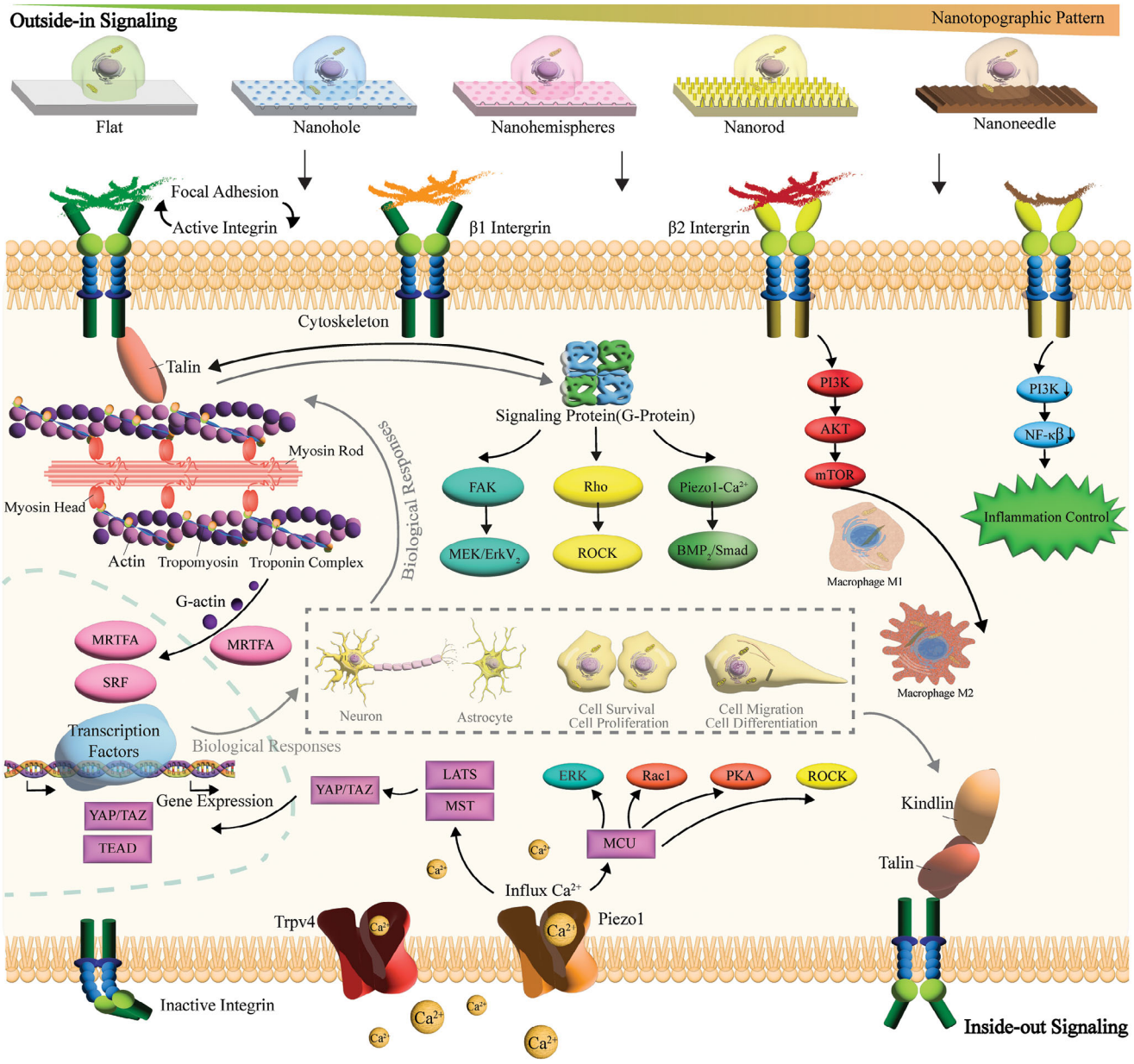

Figure 9. Mechanistic insights on topographical cues enhance neural regeneration following spinal cord injury. Topographical cues regulate cellular behavior through integrin signaling. β1-integrin activation triggers FAK/MAPK/Erk and Rho/ROCK pathways, promoting cytoskeletal remodeling, cell survival, and NSC differentiation into neurons and astrocytes. Mechanosensitive ion channels, such as Piezo1, and nuclear YAP/TAZ dynamics further support NSC differentiation. Additionally, β2-integrin-mediated PI3K-AKT-mTOR signaling modulates inflammation by promoting M2 macrophage polarization and reducing inflammatory responses. These mechanisms provide a foundation for designing topographical scaffolds to enhance spinal cord injury (SCI) repair.

5.1. Preserving Structure: The Role of Freeze-Drying in Scaffold Fabrication

Freeze-drying provides an effective method for preparing porous scaffolds by rapidly dehydrating materials to preserve their original 3D structure.[219] The ice-freezing method is commonly used to create porous scaffolds for tissue engineering, particularly in spinal cord regeneration. A material solution is frozen, forming ice crystals that create a temporary template.[220,221] The ice is then removed through freeze-drying, leaving behind a porous structure with aligned pores that guide axonal growth, making it ideal for neural tissue applications.[222] By controlling the freezing rate during ice crystal formation, the pore size of the scaffold can be adjusted, with a faster rate leading to narrower ice crystals and smaller pores.[223] Additionally, directional freeze-drying can create 3D scaffolds with uniform porosity and highly aligned structures.[197] For example, freeze-dried collagen/chitosan scaffolds have been demonstrated to

increase the density of BDA-labeled axons, suggesting enhanced axonal growth.[224] Li utilized freeze-drying to simulate the corticospinal tract and construct freeze-dried collagen/silk fibroin scaffolds. Although these scaffolds had some repair effects, they exhibited larger lesion areas and more disorganized structures compared to 3D-printed scaffolds, with fewer GAP43+ cells, suggesting that the uncontrollable topographical cues of freeze-dried scaffolds may lead to differential cellular responses and varying repair outcomes.[225] While porosity can be controlled through freezing rates, achieving consistently aligned topographical cues is challenging with freeze-drying. Furthermore, the cytotoxicity of crosslinking agents remains a challenge in their application.

5.2. Nanofiber Engineering: Tailoring Topographical Features for Neural Applications

As previously mentioned, nanofiber matrices can replicate the topographical features of the natural extracellular matrix and affect cellular behavior through both long-range and short-range biochemical signals. The alignment and diameter of the fibers dictate the topographical features and the corresponding effectiveness of spinal cord injury repair.[204,226] Electrospinning is a widely employed technique for fabricating oriented morphologies in nanofiber mats or tubes. Its precision in controlling fiber diameter, alignment, and signal encapsulation makes it a highly versatile approach for various scaffold applications. Creating a nervous tract-inspired multi-nanoyarn model system using nanotopography holds significant potential for advancing research on neural differentiation and transcriptional regulation, offering a novel paradigm for in vitro neuronal model systems.[198] A wireless, biodegradable 3D piezoelectric electrospinning nanofiber scaffold was designed for spinal cord injury repair, offering a novel direction for using radio-driven electrospinning nanomaterials.[227] However, achieving uniform fiber diameters and consistent morphologies is difficult with electrospinning, and unstable topographical cues may adversely affect spinal cord injury repair.[228] Additionally, synthetic polymer fibers have limitations, including poor biocompatibility, inadequate cell adhesion, and low cell affinity, which impedes cell infiltration and migration.[229] Furthermore, the cytotoxicity and sterilization challenges of some electrospinning nanofibers limit their clinical translation.

5.3. Advancing Scaffold Design: The Promise of 3D Bioprinting in SCI Repair

Spinal cord tissue has complex 3D structures with layered organization and functional partitioning. 3D printing offers a promising approach for constructing topographical cues, leveraging its unique ability to create intricate biomimetic geometries with high precision and customization. It can create anatomically accurate structures with spatial distributions of NSCs to repair SCI. Many researchers have attempted to integrate various topographical cues using 3D printing for SCI repair.[230] The microscale continuous projection printing (μCPP) technique was used to fabricate complex central nervous system (CNS) structures for applications in spinal cord regenerative medicine.[231] Liu simulated spinal cord structures using functional chitosan, hyaluronic acid derivatives, and Matrigel to print spinal cord-like structures, promoting axonal regeneration and spinal cord injury repair.[23] Li developed a time-programmed linear hierarchical structure scaffold with linear topographical cues to promote neural stem cell migration and differentiation, enhancing motor function recovery in rats.[232] However, 3D printing tissue engineering still faces challenges in the types and quantities of materials used, the construction of high-resolution topographical cues, and the creation of multi-responsive topographical cues.[233] Current spinal cord bioprinting research targets a limited range of cell types and scaffold models, focusing on neural stem cell differentiation and 3D scaffold construction without fully depicting the topographical cues needed for spinal cord injury repair.[224] The safety, efficiency, cost, and scalability of 3D printing also limit its application.

5.4. Precision Engineering: Utilizing Laser Techniques for Topographical Cues

Laser ablation systems are essential for constructing topographical cues by focusing high-quality beams on tiny spots to create periodic relief patterns, including lines, grooves, gratings, micropillars, and microcavities.[234] Laser ablation offers a more straightforward manufacturing process compared to traditional photolithography, enabling the creation of more complex patterns. Benefits of laser ablation include avoiding contamination from direct contact and achieving high aspect ratios in the designs. In contrast, conventional photolithography methods such as UV lithography, extreme ultraviolet lithography (EUVL), X-ray lithography (XRL), and direct laser writing (DLW) are often used for pattern creation. Laser ablation is a widely used method for creating micro/nano-structured substrates to regulate stem cell fate, with controllable periodic pattern arrays like lines, grooves, gratings, micropillars, and microcavities.[235,236] However, laser ablation requires photomask-assisted pattern formation, which is inefficient and limited to small-scale, simple micro/nano-structure fabrication. The structures formed are typically 2D, limiting their broad in vivo applications.[237]

5.5. Advanced Patterning Methods: Creating Complex Topographies for Neural Regeneration

Photolithography has become a dependable technique for rapidly producing complex patterned substrates, making it ideal for large-scale applications such as biosensors. Its compatibility with existing high-throughput photolithography infrastructure allows for efficient scaling and integration into various manufacturing processes.[238] Photolithography can also fabricate intricate 3D structures that are challenging to achieve with conventional patterning methods. This technique involves bond breaking or formation during the photolithography process. By utilizing various photochemical reactions, it is possible to attach biochemical signals such as peptides to biomimetic materials, thereby influencing cellular behavior as part of the extracellular matrix.[239,240] A maskless photopatterning technique was developed, utilizing the

photocatalyzed thiol-yne "click" reaction to produce both binary and gradient patterns on thiolated surfaces. This method is notable for its capability to produce custom gradients, wide-ranging applicability, low defect rate, and rapid prototyping advantages, all with no mask.[241] Photopatterning is also applicable to hydrogels. For example, a collagen-functionalized hydrogel scaffold capable of sustained release of basic fibroblast growth factor (bFGF) was developed, creating a supportive microenvironment for directional neuronal regeneration and bridging the gap between spinal cord stumps, ultimately promoting motor function recovery in rat models.[242]

Laser Interference Lithography (LIL) utilizes the interference of two coherent laser beams to form standing wave patterns, which are then used to fabricate periodic micro/nanostructure arrays. This technique achieves large-scale (centimeter-level) patterning with high uniformity without the need for photomasks.[243] Flexible substrates can be used with LIL to create guided 3D micro/nano-structured materials,[244] and the periodic pattern of gradient lines also provides a powerful tool for screening the optimal parameters of topographical cues,[245] offering potential for clinical translation.

Two-photon polymerization (2PP) utilizes near-infrared (NIR) light for two-photon absorption, enabling high-resolution topographical cue fabrication with controlled, precise patterns.[246] This rapid prototyping technique can produce clear, high-resolution topographical cues, with higher precision at the micro- and nano-scale compared to other methods.[247,248] A variety of natural and synthetic photosensitive materials, including gelatin, zirconia sol-gels, aliphatic polyesters, acrylate-based polymers, and organically modified ceramics, are suitable for two-photon polymerization (2PP).[249] However, the widespread adoption of this technology is hindered by its high equipment costs and the need for specialized expertise.

Advanced micro- and nano-fabrication technologies can further provide versatile approaches for designing topographical cues that closely replicate the native spinal cord microenvironment, thereby effectively guiding and supporting neural stem cell (NSC) behavior. Each approach presents unique strengths: freeze-drying allows tunable porosity, electrospinning mimics ECM nanostructures, 3D printing enables anatomical precision, and laser-based or photolithographic patterning achieves high-resolution spatial control. However, their clinical translation hinges on overcoming several hurdles. Biosafety remains a primary concern, especially regarding residual solvents, crosslinkers, or synthetic polymers with poor biocompatibility. Scalability and reproducibility are also essential, as techniques like 2PP and photolithography often require specialized, high-cost equipment, limiting widespread adoption. In vivo therapeutic efficacy varies across platforms and needs further validation through long-term preclinical studies.

Encouragingly, several studies have shown promising outcomes in animal models. For instance, Liu et al.[23] demonstrated functional recovery and enhanced axonal regeneration using a 3D-printed spinal cord-like scaffold composed of chitosan and hyaluronic acid derivatives. Similarly, Li et al.[232] reported that a time-programmed scaffold with aligned topographies significantly promoted NSC migration and differentiation, improving motor outcomes in rats. These studies underscore the translational potential of topography-guided strategies, yet systematic comparisons and large-animal validations are still lacking. Future research should prioritize the development of standardized fabrication protocols, large-animal studies, and scalable, GMP-compliant manufacturing processes. Integrating multidisciplinary advances in material science, neurobiology, and bioengineering will be essential to translating topographical scaffold technologies from bench to bedside for effective spinal cord injury repair.

6. Translating Research to Practice: In Vivo Applications of Topographical Cues

Spinal cord injuries (SCI) disrupt the integrity of neural circuits, necessitating the development of advanced materials that can support axonal regeneration and tissue repair. Building on the in vitro evidence discussed in Sections 3–5, where nanotopography significantly influenced neural cell behavior, we now explore how these findings translate into scaffold-based therapies for SCI. Unlike conventional scaffolds with flat or non-structured surfaces, topography-engineered scaffolds incorporate aligned fibers, grooved microchannels, or nanoscale features that mimic the native ECM, offering enhanced guidance for axon regrowth, improved stem cell differentiation, and regulated immune responses in vivo. Accordingly, a compelling strategy for neural tissue repair entails the physical bridging of the injury locus coupled with the creation of a permissive microenvironment that actively stimulates endogenous regenerative processes.[250] Specifically, the alignment of fibers, pore size, and the 3D structure of scaffolds have been shown to affect cell infiltration, axonal growth, and neurogenesis.[251] These findings serve as the foundation for selecting specific topographical cues for in vivo applications, ensuring that experimental results are translated into practical designs that align with clinical objectives. While biomaterial implantation has traditionally aimed to minimize immune responses, recent advances underscore the importance of controlled immune activation as a regenerative strategy. Rather than evading immune surveillance, topographically engineered scaffolds are now designed to modulate the phenotypes of macrophages and neutrophils, promoting anti-inflammatory and pro-regenerative responses. For example, aligned microgrooves, specific nanofiber diameters, and optimized surface roughness have been shown to enhance M2 macrophage polarization and suppress detrimental inflammation. This immunomodulatory approach shifts the paradigm from immune avoidance to immune guidance, highlighting the dual role of immune cells as both responders to injury and facilitators of SCI repair. Nerve guidance conduits (NGCs) and nanofibers are typical examples of this approach.

6.1. Nerve Guidance Conduits: Enhancing Axonal Regeneration Across Injury Sites

Compared to smooth-walled conduits, NGCs embedded with aligned microchannels or nanofibers better recapitulate spinal cord architecture, facilitating oriented axonal extension and reducing disorganized scar formation. Section 3 highlighted the importance of anisotropic topographies in guiding cell behavior,

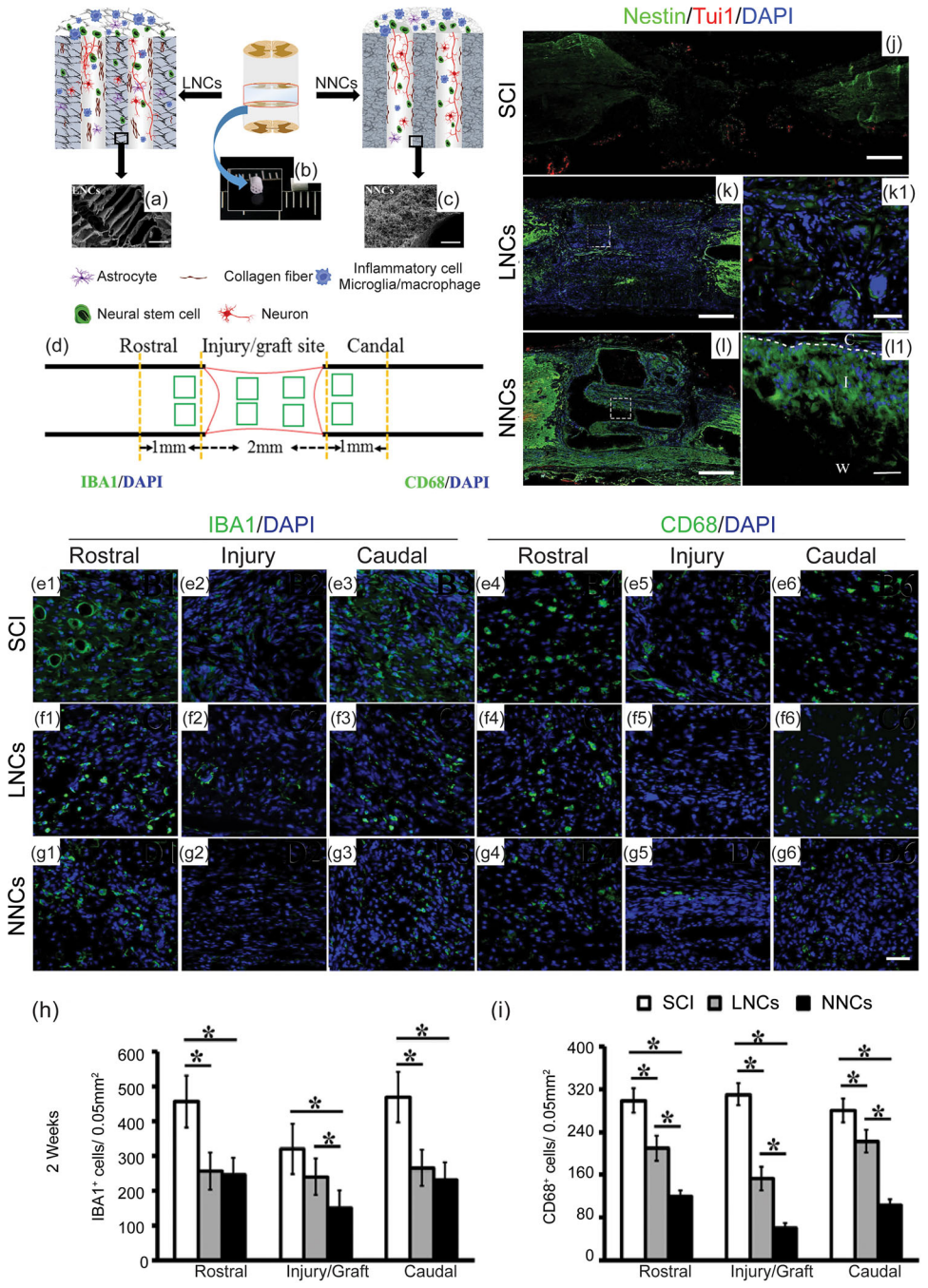

Figure 10. Nerve guidance conduits enhancing axonal regeneration across injury sites. Multi-channel nerve conduits (LNCs and NNCs) for SCI: a–c) Schematics of porous (LNCs) and nano-fibrous (NNCs) channels implanted in SCI models, showing reduced astrocyte/collagen scarring and macrophage/microglia infiltration. Enhanced NSC migration, differentiation, and axonal growth were observed. d–i) Immunofluorescence images show Iba1+ (microglia) and CD68+ (phagocytic macrophage) cells at the injury site in SCI, LNCs, and NNCs groups. j–l) Nestin+ and Tuj1+ cells in each group at 8 weeks post-implantation, showing NSC activity in LNC/NNC channels (n = 6, $*p < 0.05$). Adapted with permission.[200] Copyright 2019, Elsevier.

and these principles are directly applied in the design of NGCs. Recent research indicates that incorporating numerous micro-conduits into a larger conduit enhances nerve migration and axonal growth.[252] The presence of multiple conduits promotes longitudinal axon growth more effectively than a single large conduit, which is essential for bridging the injury gap.[253,254] For example, highly porous, biodegradable multi-conduit scaffolds containing Schwann cells (SCs) have been observed to support nerve regeneration 1-month post-implantation.[255] Organized axon regeneration was achieved only in multi-conduit

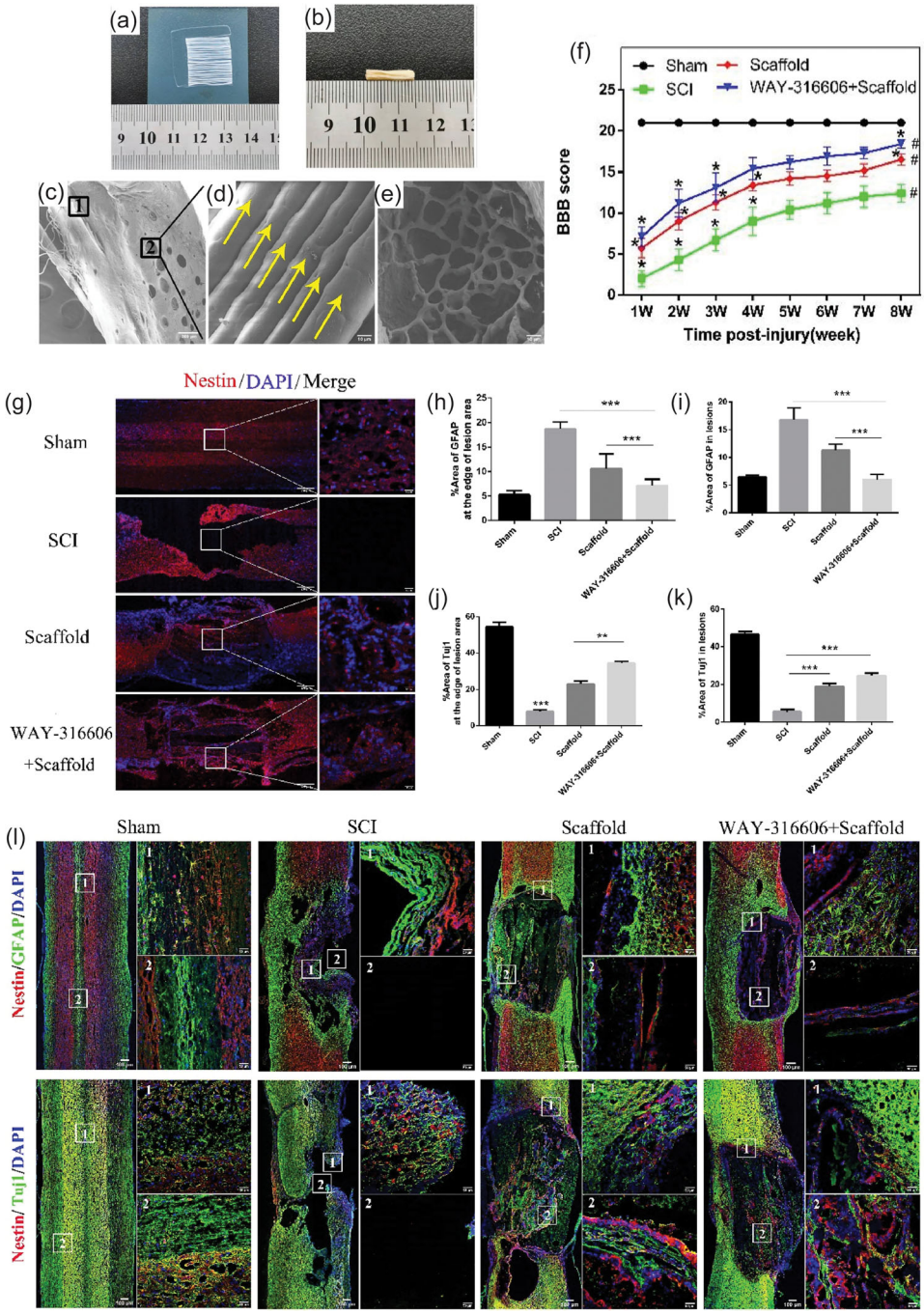

Figure 11. Oriented nanofiber scaffolds promote neural repair. a) Oriented PCL fibers in a 3D-printed hydrogel scaffold; b) composite hydrogel scaffold with directional fibers c–e) SEM images with oriented fibers (yellow arrows). f) BBB score plot showing motor function recovery. g–l) Immunofluorescence of NSC differentiation and migration in lesion areas; Nestin+ and GFAP+ cells indicate NSC and glial activity, with significant NSC migration at lesion sites ($*p < 0.05$, $**p < 0.01$). Adapted with permission.[250] Copyright 2019, Elsevier.

agarose scaffolds; injected cell suspensions did not show such organized growth.[256] Another study demonstrated that smaller diameter multi-conduit scaffolds (450 µm) outperformed larger diameter scaffolds (660 µm) in promoting axon regeneration and reducing scar reaction in a rodent SCI model, suggesting an optimal parameter range for contact-guidance functionality.[254]

Multi-conduit systems can also maintain the linear and bundled structure of the spinal cord, increase SC adhesion and activation, and facilitate the release of neurotrophic factors like nerve growth factor (NGF).[202,257,258] For instance, conduits with an average conduit diameter of 125µm embedded with brain-derived neurotrophic factor (BDNF) supported organized axonal regeneration.[199] These findings highlight the critical role of

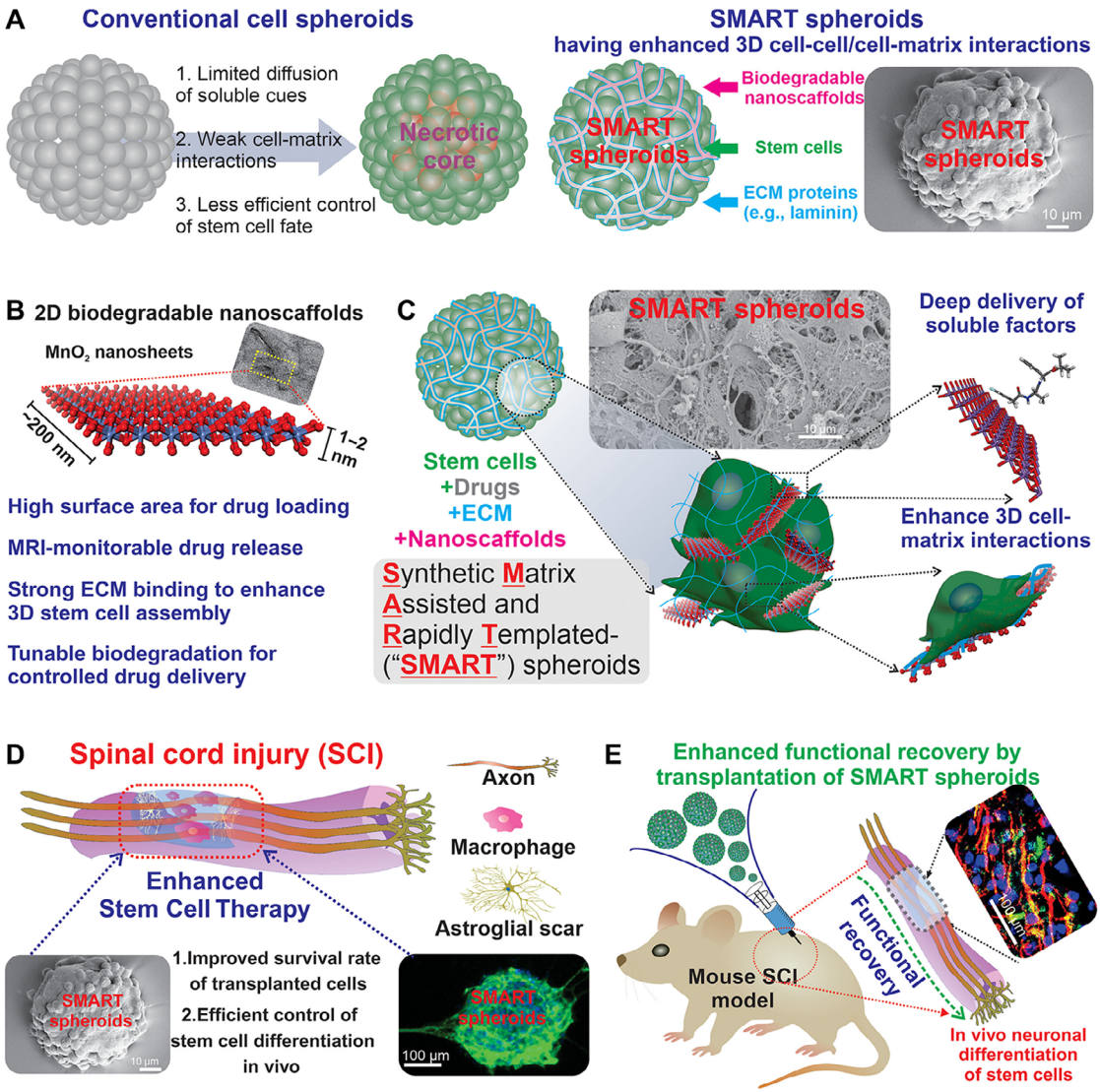

Figure 12. Assembly of smart spheroids for advanced cell therapy. A) To more accurately replicate the natural architecture of 3D tissues and amplify the therapeutic potential of stem cells, we integrate advanced biodegradable nanomaterials. These materials serve a dual purpose: acting as a bonding agent while providing structural support and functioning as a drug delivery system. B) Manganese dioxide nanosheets are selected as the optimal component for our hybrid system due to their exceptional physical, chemical, and biological properties. C) 2D manganese dioxide nanosheets are coated with extracellular matrix (ECM) proteins and therapeutic drugs, then combined with cells. This assembly is facilitated by the unique physicochemical properties of the nanomaterials, enabling the formation of SMART spheroids. D and E) As a proof of concept, we delivered SMART spheroids in an in vivo spinal cord injury (SCI) model. The results demonstrated that the SMART assembly significantly improved stem cell survival at both 1-week and 1-month intervals. Additionally, it enhanced the differentiation efficiency of the implanted cells into neurons, reduced glial scar formation, and increased neuroprotection. These outcomes collectively contributed to improved motor function recovery. Adapted with permission.[272] Copyright 2021, American Association for the Advancement of Science.

topographical cues in axonal regeneration within injured spinal cords when combined with cellular or molecular therapies. Sun utilized 3D printing to create multi-conduit scaffolds mimicking spinal cord structures. They found that nanofiber nerve conduits with high porosity could promote NSC differentiation into neurons and synapse formation, even without key neurotrophic factors, reinforcing the importance of contact-guidance conduits in neural regeneration[200,259] (**Figure 10**). These designs leverage the established understanding (please see Section 3 for details) that neuronal cells exhibit distinct responses to diverse topographical features. A critical next step involves comprehensive research to pinpoint and refine the optimal topographical cues and their defining parameters for guiding neuronal behavior.

6.2. Nanofiber Scaffolds: A Versatile Approach to Promote Neural Repair

Traditional electrospun scaffolds with random fiber orientation lack the guidance capacity needed for SCI repair. In contrast, as

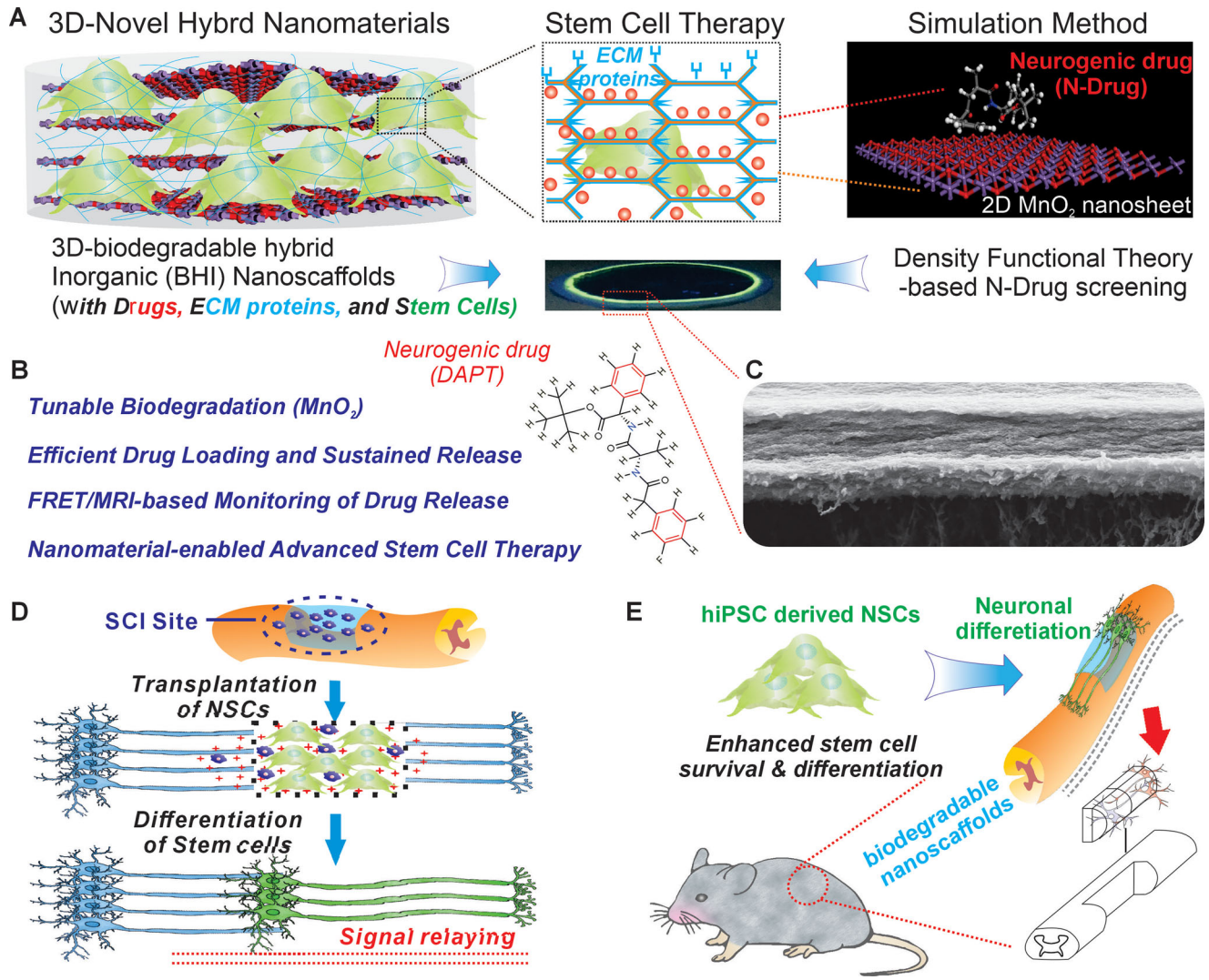

Figure 13. Nanoscaffolds for spinal cord repair and neural regeneration. A) 3D nanoscaffolds self-assembled from 2D nanomaterials with tailored nanotopography for drug loading, ECM protein embedding, and stem cell delivery. Images on the right show the nanostructure and topography of the nanomaterials for specific interactions with cells. B) The advantages of 3D nanoscaffolds for stem cell transplantation and treatment of spinal cord injury. C) SEM images showing the nanotopographies of the self-assembled nanoscaffolds. Scale bar: 500 nm. D,E) Schematic diagrams showing the process of nanoscaffold-mediated transplantation of NSCs and the mechanism for promoting spinal cord regeneration after injury. Adapted with permission.[270] Copyright 2018, Nature Pub. Group.

Section 3 pointed out, aligned nanofiber scaffolds direct neurite outgrowth along the rostrocaudal axis, enhance NSC migration, and promote synapse formation. Electrospinning creates fibers with a high surface area-to-volume ratio and significant porosity. Several studies have investigated the efficacy of electrospinning fibers in SCI repair.[204,260,261] Colello et al. created cylinder-shaped scaffolds via air gap electrospinning, which matched the shape of the spinal cord and promoted SCI repair. They found that aligned fibers were more conducive to cellular infiltration compared to randomly oriented fibers, indicating that aligned electrospinning scaffolds provide directional guidance cues and nutritional support, enhancing axonal regeneration post-SCI.[262] Comparable findings were reported by Zhao et al., demonstrating that the aligned PCL microfibers facilitated neurite outgrowth along the longitudinal axis[250] (**Figure 11**). Hurtado et al. implanted films and random and aligned microfibers into 3 mm thoracic SCI gaps in rats and observed organized tissue composed of regenerating axons and aligned astrocytes four weeks post-implantation. Aligned fibers were more effective in promoting long-distance rostrocaudal axonal regeneration.[263] Conversely, in an acute SC, Liu et al. observed substantial cellular infiltration in electrospinning nanofibers, regardless of fiber orientation.[264] This discrepancy implies that fiber diameter is a crucial topographical cue in SCI repair, alongside alignment, with potential optimal ranges. Although the exact parameter range is still undetermined, Chen et al. produced fibers ranging from ≈400 nm to 1.5 µm, mimicking spinal cord fibers. In comparison, Li created 3D nanofiber sponges with diameters around 400 nm, both achieving promising results in SCI repair.[204,260] Furthermore, Ley analyzed the response of neutrophils on

polymer electrospun scaffolds and found that, compared to larger diameter fibers (≈1.9 µm), smaller diameter fibers (≈0.3 µm) led to more significant neutrophil aggregation and activation, resulting in a stronger NETotic response.[265] Self-assembled nanofibers (SAPs), composed of amphiphilic peptides that form cylindrical structures (6–8 nm diameter) with bioactive surfaces, can trigger specific cellular responses.[201,266] Vicki et al. demonstrated that injection of self-assembling nanofibers into a mouse model of SCI *causes* axon elongation and reduces glial scar formation.[267] These insights are translated into the design of nanofiber scaffolds with varying diameters to optimize the inflammatory response and enhance tissue repair.

Nanofibers also show promise in modulating the microenvironment. Bartnet's research indicates that changes in material topographical cues have a much greater impact on the adhesion, migration, and phenotype of primary human macrophages compared to surface chemical modifications. 3D nanoscaffolds can effectively reduce the release of pro-inflammatory cytokines.[203] Kaneko found that electrospinning nanofiber conduit walls reduced macrophage activity and pro-inflammatory cytokine secretion, limiting macrophage infiltration and improving the regenerative microenvironment post-SCI.[268,269] Saino investigated the effect of electrospinning fiber diameters on macrophage activation and secretion, showing that nanofiber PLLA scaffolds minimized inflammatory responses more effectively than film or microfiber scaffolds, highlighting fiber diameter's critical role in influencing macrophage behavior and pro-inflammatory molecule secretion.[170]

6.3. Nanoscaffolds: Integrating Multiple Cues for Enhanced Regeneration

Unlike conventional hydrogel or polymer scaffolds, nanoscaffolds with defined 2D or 3D nanotopography support the assembly of stem cells into regenerative spheroids and enhance host tissue integration by directing neural differentiation and axonal alignment in vivo. Constructed from nanomaterials of various dimensionalities (0D–3D), these scaffolds present tunable topographical, mechanical, and chemical cues within a unified platform. In contrast to electrospun nanofibers that predominantly facilitate 2D interactions, 3D nanoscaffolds enable volumetric cell encapsulation, thereby improving delivery, viability, and regenerative efficacy in spinal cord injury repair. For instance, our recent work developed a series of 3D biodegradable inorganic hybrid (BHI) nanoscaffolds designed to synergistically combine drug delivery and stem cell transplantation for SCI treatment. In contrast to organic or polymeric nanomaterials, inorganic nanomaterials offer unique advantages: their crystal growth can be precisely controlled to synthesize 0D, 1D, 2D, and 3D nanomaterials with defined sizes and geometries. These materials not only enable programmable, sustained drug release but also provide size- and shape-dependent topographical cues to cells. The first-generation 3D-BHI nanoscaffolds employ laminin-functionalized 2D manganese dioxide nanosheets to co-assemble with human-induced pluripotent stem cell-derived neural stem cells (hiPSC-NSCs) while integrating a monitorable, controlled-release system for the Notch inhibitor DAPT or methylprednisolone (MP).[270,271] This comprehensive system successfully promoted the survival and neuronal differentiation of hiPSC-NSCs both in vitro and in vivo in a murine hemisection SCI model (**Figure 12**). This approach directly builds upon the cellular-level knowledge from Section 3, where specific surface features were shown to influence stem cell neurogenesis and axonal growth. The 3D nature of these scaffolds further enhances their ability to replicate the complex architecture of the spinal cord, providing a more realistic environment for cell growth and tissue repair. However, the molecular mechanisms underlying how these topographical cues facilitate functional improvement remain unclear.

The second generation of the 3D BHI nanoscaffolds further utilized the topographical cues mediated by 2D nanomaterials to assemble hiPSC-NSCs into injectable 3D stem cell spheroids.[272] This advancement is particularly significant, as regulating 3D nanotopographical cues within cell-encapsulating nanoscaffolds has long posed a major challenge. Furthermore, compared to the first-generation 3D-BHI nanoscaffolds, the second-generation iteration was engineered in an injectable format, avoiding invasive surgery and reducing secondary damage to spinal tissue. Subsequently, third-generation 3D-BHI nanoscaffolds were developed as injectable stem cell spheroids, fabricated via the assembly of fibronectin-functionalized 1D manganese dioxide nanotubes co-assembled with mesenchymal stem cells (MSCs).[273] Moreover, 2D manganese dioxide nanosheets were incorporated into shear-thinning peptide hydrogels to enable controlled therapeutic regeneration of non-neural tissues, such as intervertebral disc degeneration.[274] The ongoing evolution of 3D-BHI nanoscaffolds underscores the critical role of nanotopographical design in 3D injectable systems for spinal cord regeneration, particularly following injury SCI (**Figure 13**).[270]

In conclusion, topographical cues offered by materials like nanofibers, conduits, and nanoscaffolds demonstrate significant effectiveness in regulating cell behavior, improving the local microenvironment, directing axonal growth, and facilitating neural regeneration. These properties position them as highly promising candidates for advancing spinal cord injury (SCI) repair.

7. Navigating Challenges: Future Directions in Topography-Based SCI Therapies

Neural regeneration and circuit reconstruction are essential for functional recovery after spinal cord injury (SCI). Topographical cues have emerged as critical modulators of neural stem cell (NSC) fate by influencing cell adhesion, alignment, neurite extension, differentiation pathways, and immune responses, thereby contributing to a more favorable regenerative microenvironment. However, the molecular and genetic mechanisms underpinning these cell-topography interactions remain insufficiently understood. Unraveling these mechanisms could pave the way for designing next-generation biomaterials capable of more precisely orchestrating topographical cues.

Preclinical studies demonstrate that micro- and nano-scale topographies can effectively guide axonal regrowth and cellular organization within SCI models. Incorporating such topographical cues into scaffolds offers considerable potential for advancing in vitro and in vivo regeneration strategies.[275–277] Yet, bridging

Table 4. An overview of current clinical trials registered on https://clinicaltrials.gov/ and some research progress. However, many challenges remain before these approaches can be translated into mature clinical applications.

Material	Topographical cues	Combined cues	Participation Criteria	Methodology	Enrollment	Outcomes	Sponsor	ClinicalTrials.gov identifier or refs
Neuro-Spinal Scaffold™ (NSS)	glucose porogens of ≈180–430 µm particle size, ≈300 µm, highly porous structure of sufficient size[282,283]	N/A	Complete acute spinal cord injury, T2-T12 Level, Recent injury (< 7 days)	Phase I/II, Randomized, controlled, single-blind, multicenter, two Arm research	20	No Results Posted	InVivo Therapeutics, USA	NCT03762655
NeuroRegen Scaffold™ (NRS)	≈200 µm multiple longitudinally arranged collagen fibers, tiny channels along the aligned fibers[284,285]	bone marrow mononuclear cells (BMMCs) or mesenchymal stem cells (MSCs)	Complete chronic spinal cord injury, cervical and thoracic level (C5-T12)	Phase I/II, Single Group Assignment	30	NRS shows preliminary safety and efficacy for chronic spinal cord injury. 62.5% of the patients had an expanded sensory level, and 3 with neck injuries had increased finger flexibility. 87.5% had a significant expansion of the MEP response area, 2 patients recovered defecation sensation, and 4 had increased sitting stability and trunk balance, but without ASIA improvement.	Chinese Academy of Sciences, China	NCT02352077[285]
Functional Scaffold	No Results Posted	Epidural Electrical Stimulation	Complete acute and chronic spinal cord injury, C4-T12/L1 level	Phase I/II, Non-Randomized	9	No Results Posted	Chinese Academy of Sciences, China	NCT03966794
NeuroRegen Scaffold™ (NRS)	≈200 µm multiple longitudinally arranged collagen fibers, tiny channels along the aligned fibers[284,285]	Mesenchymal Stem Cells or NSCs	Complete chronic spinal cord injury, cervical and thoracic level (C5-T12)	Phase I/II; double blind; randomized	30	No Results Posted	Chinese Academy of Sciences, China	NCT02688049
Functional Neural Regeneration Collagen Scaffold	multiple longitudinally arranged collagen fibers, tiny channels along the aligned fibers[284,286]	Autologous Bone Marrow Mononuclear Cells	Complete acute spinal cord injury, C4-T12 Level, Recent injury (< 21 days)	Phase I, Single Group Assignment	20	No adverse symptoms associated with functional scaffold. Partial shallow sensory and autonomic nervous functional improved in some patients without motor function recovery.	Chinese Academy of Sciences, China	NCT02510365[287]

(*Continued*)

Table 4. (Continued)

Material	Topographical cues	Combined cues	Participation Criteria	Methodology	Enrollment	Outcomes	Sponsor	ClinicalTrials.gov identifier or refs
NeuroRegen Scaffold™ (NRS)	Multiple longitudinally arranged collagen fibers, tiny channels along the aligned fibers[284,286]	Bone Marrow Mononuclear Cells	Complete chronic spinal cord injury at the thoracic level	Phase I/II; double blind; randomized	22	No Results Posted	Chinese Academy of Sciences, China	NCT02688062
Neuro-Spinal Scaffold™ (NSS)	glucose porogens of ≈180–430 µm particle size, ≈300 µm, highly porous structure of sufficient size[282,283]	N/A	Complete acute traumatic spinal cord injury, T2-T12 Level, Recent injury (< 7 days)	Phase I/II, Single Group Assignment	19	NSS appeared to be a safe and probable benefit. Seven of 16 evaluable patients (44%) had an improvement of ≥1 AIS grade at 6 months to AIS B (n = 5) or AIS C (n = 2). Three patients with AIS B at 6 months had further neurological improvement to AIS C by 12 (n = 2) and 24 (n = 1) months,	InVivo Therapeutics, USA	NCT02138110[288]
RMx Biomatrix Scaffold	No Results Posted	autologous NSCs	Complete and incomplete chronic spinal cord injury, AISA = A OR B, Injury duration 1 month to 5 years	Phase I/, Non-Randomized	30	No Results Posted	Federal Research Clinical Center of Federal Medical & Biological Agency, Russia	NCT02326662
Collagen scaffold	No Results Posted	Autologous Bulbar Olfactory Ensheathing Cells[289]	Complete spinal cord injury Single level, C5-T10	Phase I/II, Single Group Assignment	2	No Results Posted	Nicholls Spinal Injury Foundation, Poland	NCT03933072
Functional Self-assembling Peptide Nanofiber Hydrogels	based on the short peptide RADA16, peptide dimensions are ≈6 nm long depending on end capping, 1.3 nm wide, and 0.8 nm thick, Anisotropic continuous network structure[290]	Stromal Vascular Fraction,	Complete chronic spinal cord injury at the thoracic level (T1-T12)	Not Applicable, Single Group Assignment	15	No Results Posted	Kunming Tongren Hospital, China	NCT05967325

the gap between bench and bedside requires integrative design principles grounded in clinical realities. Notably, existing FDA-approved devices for peripheral nerve repair, such as NeuroMatrix, AxoGuard, Neurolac, and SaluTunnel, share key features, including aligned or tubular architectures for physical guidance, biocompatibility, and support for cellular infiltration and ECM remodeling. Despite their clinical success in peripheral nerve repair, these strategies have shown limited efficacy in spinal cord applications, largely due to the spinal cord's complex architecture, absence of spontaneous regeneration, and heightened inflammatory sensitivity.

To address these challenges, future SCI biomaterial design must integrate topographical cues with biochemical, mechanical, and cellular components to better mimic native spinal cord architecture. This "cocktail-like" approach should unify mechanical support, directional guidance, nutrient exchange, and immune modulation to enhance therapeutic outcomes.[278–281] Translational strategies should also incorporate scalable fabrication techniques, minimally invasive delivery systems, and designs that promote vascularization. Furthermore, aligning preclinical assessments with clinically relevant outcomes, such as motor and sensory recovery and electrophysiological performance, will improve predictive accuracy.

Table 4 provides an overview of current clinical trials registered on ClinicalTrials.gov, highlighting both ongoing efforts and remaining gaps. Compared with current clinical strategies, typically involving neuroprotective agents, cell transplantation, or general scaffold systems, topography-engineered materials offer unique advantages in spatially guiding axonal growth and modulating immune responses. However, topographical sophistication such as anisotropic nanostructures and hierarchical designs remains largely absent from clinical trials. Bridging this gap between fundamental discoveries and scalable translational platforms remains a key objective for the field.

The integration of topographical cues with biochemical, cellular, and physical stimuli further enhances regenerative potential. Scaffold systems incorporating ECM components, neurotrophic factors, or therapeutic cells have shown promise in promoting neural differentiation and tissue remodeling.[25,58,291–293] Additionally, electromagnetic stimulation, an established physical approach, can modify scaffold microenvironments to boost neuronal differentiation and mitigate glial scarring.[294,297] Moreover, magnetically responsive self-assembling peptide hydrogels offer tunable topographical cues that support axon growth and reduce inflammation, although clinical translation remains a challenge[298,300]

Recent advances in nanotechnology have enabled bioactive nanotopographical systems to exhibit stimuli-responsive behavior. These systems can be engineered to respond to endogenous signals (e.g., pH, ROS, enzymes) or exogenous stimuli (e.g., NIR light, ultrasound, magnetic fields) to dynamically control material properties and biological responses.[301–308] Intelligent nanomaterials—including synthetic polymers, biomaterials, and metal-based systems—have demonstrated utility in precision diagnostics[309,313] and targeted drug delivery,[314–318] and these functionalities are closely tied to their topographical design. Given the spinal cord's inherently aligned structure, integrating such intelligent materials with directional cues presents a promising strategy for SCI repair.

One of the key hurdles in clinical translation is the multifactorial complexity of SCI pathology. Effective topographical strategies must address both shared and cell-type-specific behaviors among NSCs, neurons, glia, and immune cells. A comprehensive understanding of both the universal ('common') and cell-specific ('individual') responses to these cues is essential for tailoring scaffolds to direct repair processes across different cell types. Moreover, combining topography with stem cells, ECM-mimicking materials, and cytokine delivery may synergistically enhance cellular integration and endogenous repair mechanisms. Despite these advancements, the path toward clinical translation is obstructed by several key challenges. For instance, reproducibility and scalability of fabrication methods remain a significant concern, as topographical cues must be precisely manufactured to ensure consistency across large-scale clinical applications. Additionally, achieving effective vascularization and minimizing immune rejection in spinal cord scaffolds are critical barriers that need to be addressed. Furthermore, the lack of spontaneous regeneration in the central nervous system, along with the complexity of the spinal cord's neural architecture, adds to the difficulty of achieving functional recovery.

To overcome these barriers, multimodal approaches that incorporate topographical cues into multifunctional platforms will be essential. "Cocktail" therapies that integrate topography with stem cells, biochemical factors, and physical stimulation are showing promise. For instance, co-delivery of topographical scaffolds with electromagnetic stimulation has been shown to enhance axonal regeneration while dampening inflammation in animal models. Likewise, biodegradable scaffolds incorporating aligned nanostructures and NSC transplantation have demonstrated improved cellular infiltration and tissue integration.[299,301,304]

Ultimately, successful clinical translation will require iterative biomaterial optimization, rigorous testing in large animal models, and development of scalable, clinically compliant manufacturing methods. Through this integrative and multidisciplinary approach, patient-specific strategies that emulate the spinal cord's native architecture may finally realize the goal of functional SCI repair.

In conclusion, advancing our understanding of how topographical cues influence cellular behavior, along with the development of intelligent, multifactorial, and integrative approaches, holds great promise for transforming the clinical landscape of SCI treatment. These strategies offer an exciting path toward clinically translatable therapies that can significantly improve patient outcomes and quality of life.

Acknowledgements

L.Y. acknowledges the partial financial support from the National Key Research and Development Program of China (2024YFA1108200), the National Natural Science Foundation of China (32301106), the Fundamental Research Funds for the Central Universities (22120240435) and Peak Disciplines (Type IV) of Institutions of Higher Learning in Shanghai. L. C. acknowledges the partial financial support from the National Key Research and Development Program of China (2024YFA1108200), the Key Program of the National Natural Science Foundation of China (82330062). K.-B.L. acknowledges the partial financial support from the New Jersey Commission on Spinal Cord (CSCR17IRG010, CSCR16ERG019, CSCR24IRG005),

NIH R01 (1R01NS130836-01A1), NIH RM1 (RM1 NS133003-01), NIH R21 (R21 NS132556-01), and Alzheimer's Association (AARG-NTF-21-847862).

Conflict of Interest

The authors declare no conflict of interest.

Keywords

biomimetic scaffolds, biophysical cues, mechanotransduction, micro- and nanoscale topography, neural regeneration, regenerative medicine, spinal cord injury (SCI), stem cell therapy, tissue engineering, topographical cues

Received: April 3, 2025
Revised: May 13, 2025
Published online:

[1] Center, N. S. C. I. S., *Traumatic spinal cord injury facts and figures at a glance*, University of Alabama at Birmingham, Birmingham, AL **2022**.
[2] J. W. McDonald, C. Sadowsky, *Lancet* **2002**, *359*, 417.
[3] X. Hu, W. Xu, Y. Ren, Z. Wang, X. He, R. Huang, B. Ma, J. Zhao, R. Zhu, L. Cheng, *Signal Transduction Targeted Ther.* **2023**, *8*, 245.
[4] A. Anjum, M. D. Yazid, M. Fauzi Daud, J. Idris, A. M. H. Ng, A. Selvi Naicker, O. H.@. R. Ismail, R. K. Athi Kumar, Y. Lokanathan, *Int. J. Mol. Sci.* **2020**, *21*, 7533.
[5] C. Li, Z. Wu, L. Zhou, J. Shao, X. Hu, W. Xu, Y. Ren, X. Zhu, W. Ge, K. Zhang, J. Liu, R. Huang, J. Yu, D. Luo, X. Yang, W. Zhu, R. Zhu, C. Zheng, Y. E. Sun, L. Cheng, *Signal Transduct. Target. Ther.* **2022**, *7*, 65.
[6] J. A. G. Crispo, L. K. Kuramoto, J. J. Cragg, *Lancet Neurol.* **2023**, *22*, 976.
[7] M. Karsy, G. Hawryluk, *Curr. Neurol. Neurosci. Rep.* **2019**, *19*, 65.
[8] E. Widerstrom-Noga, *Drugs* **2023**, *83*, 1001.
[9] P. Jendelova, *Int. J. Mol. Sci.* **2018**, *19*, 3200.
[10] Y. Du, Y. Huo, Q. Yang, Z. Han, L. Hou, B. Cui, K. Fan, Y. Qiu, Z. Chen, W. Huang, J. Lu, L. Cheng, W. Cai, L. Kang, *Exploration (Beijing)* **2023**, *3*, 20220041.
[11] G. Gao, J. Li, Y. Ma, M. Xie, J. Luo, K. Wang, C. Peng, H. Yang, T. Chen, G. Zhang, J. Ouyang, H. Lin, Z. Ji, *Exploration (Beijing)* **2025**, https://doi.org/10.1002/EXP.70012.
[12] K. Fouad, P. G. Popovich, M. A. Kopp, J. M. Schwab, *Nat. Rev. Neurol.* **2021**, *17*, 53.
[13] J. H. Badhiwala, J. R. Wilson, J. S. Harrop, A. R. Vaccaro, B. Aarabi, F. H. Geisler, M. G. Fehlings, *JAMA Surg.* **2022**, *157*, 1024.
[14] F. Yuan, W. Peng, Y. Yang, J. Xu, Y. Liu, Y. Xie, T. Huang, C. Shi, Y. Ding, C. Li, T. Qin, S. Xie, F. Zhu, H. Lu, J. Huang, J. Hu, *J. Neuroinflammation* **2023**, *20*, 156.
[15] Z. Liu, Y. Yang, L. He, M. Pang, C. Luo, B. Liu, L. Rong, *Neurology* **2019**, *93*, 841.
[16] C. S. Ahuja, S. Nori, L. Tetreault, J. Wilson, B. Kwon, J. Harrop, D. Choi, M. G. Fehlings, *Neurosurgery* **2017**, *80*, S9.
[17] C. Y. Adegeest, P. V. Ter Wengel, W. C. Peul, *Curr. Opin. Crit. Care* **2023**, *29*, 659.
[18] M. D. Sunshine, V. E. Bindi, B. L. Nguyen, V. Doerr, F. P. Boeno, V. Chandran, A. J. Smuder, D. D. Fuller, *J Neuroinflammation* **2023**, *20*, 303.
[19] A. J. Smuder, S. M. Turner, C. M. Schuster, A. B. Morton, J. M. Hinkley, D. D. Fuller, *Int. J. Mol. Sci.* **2020**, *21*, 7219.
[20] M. P. Côté, M. Murray, M. A. Lemay, *J. Neurotrauma* **2017**, *34*, 1841.
[21] H. Lorach, A. Galvez, V. Spagnolo, F. Martel, S. Karakas, N. Intering, M. Vat, O. Faivre, C. Harte, S. Komi, J. Ravier, T. Collin, L. Coquoz, I. Sakr, E. Baaklini, S. D. Hernandez-Charpak, G. Dumont, R. Buschman, N. Buse, T. Denison, I. van Nes, L. Asboth, A. Watrin, L. Struber, F. Sauter-Starace, L. Langar, V. Auboiroux, S. Carda, S. Chabardes, T. Aksenova, et al., *Nature* **2023**, *618*, 126.
[22] G. Courtine, M. V. Sofroniew, *Nat. Med.* **2019**, *25*, 898.
[23] X. Liu, M. Hao, Z. Chen, T. Zhang, J. Huang, J. Dai, Z. Zhang, *Biomaterials* **2021**, *272*, 120771.
[24] K. Liu, X. Dong, Y. Wang, X. Wu, H. Dai, *Carbohydr. Polym.* **2022**, *298*, 120047.
[25] H. Shen, B. Xu, C. Yang, W. Xue, Z. You, X. Wu, D. Ma, D. Shao, K. Leong, J. Dai, *Biomaterials* **2022**, *280*, 121279.
[26] S. Wang, J. Li, Z. Zhou, S. Zhou, Z. Hu, *Molecules* **2018**, *24*, 75.
[27] X. Cun, L. Hosta-Rigau, *Nanomaterials* **2020**, *10*, 2070.
[28] C. Simitzi, K. Karali, A. Ranella, E. Stratakis, *ChemPhysChem* **2018**, *19*, 1143.
[29] Z. Zhang, R. Xu, Y. Yang, C. Liang, X. Yu, Y. Liu, T. Wang, Y. Yu, F. Deng, *J. Nanobiotechnol.* **2021**, *19*, 78.
[30] A. A. K. Moe, M. Suryana, G. Marcy, S. K. Lim, S. Ankam, J. Z. W. Goh, J. Jin, B. K. K. Teo, J. B. K. Law, H. Y. Low, E. L. K. Goh, M. P. Sheetz, E. K. F. Yim, *Small* **2012**, *8*, 3050.
[31] Y. Xu, W. Cui, Y. Zhang, P. Zhou, Y. Gu, X. Shen, B. Li, L. Chen, *Adv. Healthcare Mater.* **2017**, *6*, 1601457.
[32] J. M. H. Liu, J. Zhang, X. Zhang, K. A. Hlavaty, C. F. Ricci, J. N. Leonard, L. D. Shea, R. M. Gower, *Biomaterials* **2016**, *80*, 11.
[33] S. Liu, *Mat. Biolo. Appli.* **2018**, *83*, 130.
[34] A. Aydeger, N. Aysit, G. Baydas, C. Cakici, U. C. Erim, M. D. Arpa, I. Ozcicek, *Biomater. Adv.* **2023**, *152*, 213472.
[35] W. Xue, W. Shi, Y. Kong, M. Kuss, B. Duan, *Bioact. Mater.* **2021**, *6*, 4141.
[36] H. Zhao, *Small* **2024**, *20*, 2311456.
[37] S. Chen, C. Wu, T. Zhou, K. Wu, N. Xin, X. Liu, Z. Qiao, D. Wei, J. Sun, H. Luo, L. Zhou, H. Fan, *Carbohydr. Polym.* **2022**, *278*, 118961.
[38] B. Kaplan, U. Merdler, A. A. Szklanny, I. Redenski, S. Guo, Z. Bar-Mucha, N. Michael, S. Levenberg, *Biomaterials* **2020**, *251*, 120062.
[39] M. Liu, D. Wang, S. Gu, B. Tian, J. Liang, Q. Suo, Z. Zhang, G. Yang, Y. Zhou, S. Li, *Acta Biomater.* **2021**, *124*, 130.
[40] M. Stanners, M. O'Riordan, E. Theodosiou, J. R. G. Souppez, A. Gardner, *Spine J.* **2024**, *24*, 1302.
[41] R. D. Bartlett, D. Eleftheriadou, R. Evans, D. Choi, J. B. Phillips, *Biomaterials* **2020**, *258*, 120303.
[42] J. Kolb, V. Tsata, N. John, K. Kim, C. Möckel, G. Rosso, V. Kurbel, A. Parmar, G. Sharma, K. Karandasheva, S. Abuhattum, O. Lyraki, T. Beck, P. Müller, R. Schller, R. Frischknecht, A. Wehner, N. Krombholz, B. Steigenberger, D. Beis, A. Takeoka, I. Blümcke, S. Möllmert, K. Singh, J. Guck, K. Kobow, D. Wehner, *Nat. Commun.* **2023**, *14*, 6814.
[43] D. J. Hellenbrand, C. M. Quinn, Z. J. Piper, C. N. Morehouse, J. A. Fixel, A. S. Hanna, *J. Neuroinflammation* **2021**, *18*, 284.
[44] M. B. Orr, J. C. Gensel, *Neurotherapeutics* **2018**, *15*, 541.
[45] T. Clifford, Z. Finkel, B. Rodriguez, A. Joseph, L. Cai, *Cells* **2023**, *12*, 853.
[46] G. Huang, Y. Liu, X. Zhu, L. He, T. Chen, *Exploration* **2025**, https://doi.org/10.1002/EXP.20240415.
[47] T. Wang, Z. Song, X. Zhao, Y. Wu, L. Wu, A. Haghparast, H. Wu, *Exploration (Beijing)* **2023**, *3*, 20220133.
[48] L. Y. Jin, J. Li, K. F. Wang, W. W. Xia, Z. Q. Zhu, C. R. Wang, X. F. Li, H. Y. Liu, *J. Neurotrauma* **2021**, *38*, 1203.
[49] J. Yang, S. Wu, M. He, *Exploration* **2025**, https://doi.org/10.1002/EXP.20240349

[50] Y. Ye, Y. Tian, H. Liu, J. Liu, C. Zhou, C. Xu, T. Zhou, Y. Nie, Y. Wu, L. Qin, Z. Zhou, X. Wei, J. Zhao, Z. Wang, M. Li, T. Tao, L. Sun, *Exploration* **2025**, https://doi.org/10.1002/EXP.70040.
[51] W. Yi, S. Hu, X. Qian, W. Yan, Y. Li, *Exploration* **2025**, *5*, 20240095.
[52] J. Bennett, J. M. Das, P. D. Emmady, *StatPearls*, StatPearls Publishing LLC, Tampa, Florida **2025**.
[53] R. C. Sterner, R. M. Sterner, *Front. Immunol.* **2022**, *13*, 1084101.
[54] T. Tian, S. Zhang, M. Yang, *Protein Cell* **2023**, *14*, 635.
[55] F. Bretheau, A. Castellanos-Molina, D. Bélanger, M. Kusik, B. Mailhot, A. Boisvert, N. Vallières, M. Lessard, M. Gunzer, X. Liu, É. Boilard, N. Quan, S. Lacroix, *Nat. Commun.* **2022**, *13*, 5786.
[56] Y. Li, X. He, R. Kawaguchi, Y. Zhang, Q. Wang, A. Monavarfeshani, Z. Yang, B. Chen, Z. Shi, H. Meng, S. Zhou, J. Zhu, A. Jacobi, V. Swarup, P. G. Popovich, D. H. Geschwind, Z. He, *Nature* **2020**, *587*, 613.
[57] M. A. Skinnider, M. Gautier, A. Y. Y. Teo, C. Kathe, T. H. Hutson, A. Laskaratos, A. de Coucy, N. Regazzi, V. Aureli, N. D. James, B. Schneider, M. V. Sofroniew, Q. Barraud, J. Bloch, M. A. Anderson, J. W. Squair, G. Courtine, *Nature* **2024**, *631*, 150.
[58] C. M. Zipser, J. J. Cragg, J. D. Guest, M. G. Fehlings, C. R. Jutzeler, A. J. Anderson, A. Curt, *Lancet Neurol.* **2022**, *21*, 659.
[59] G. J. Duncan, S. B. Manesh, B. J. Hilton, P. Assinck, J. R. Plemel, W. Tetzlaff, *Glia* **2020**, *68*, 227.
[60] H. Liu, J. Yi, C. Zhang, Y. Li, Q. Wang, S. Wang, S. Dai, Z. Zheng, T. Jiang, P. Gao, A. Xue, Z. Huang, F. Kong, Y. Wang, B. He, X. Guo, Q. Li, J. Chen, G. Yin, S. Zhao, *Glia* **2024**, *72*, 1674.
[61] O. Zveik, A. Rechtman, T. Ganz, A. Vaknin-Dembinsky, *Mol. Neurodegener.* **2024**, *19*, 53.
[62] S. A. Liddelow, K. A. Guttenplan, L. E. Clarke, F. C. Bennett, C. J. Bohlen, L. Schirmer, M. L. Bennett, A. E. Münch, W.-S. Chung, T. C. Peterson, D. K. Wilton, A. Frouin, B. A. Napier, N. Panicker, M. Kumar, M. S. Buckwalter, D. H. Rowitch, V. L. Dawson, T. M. Dawson, B. Stevens, B. A. Barres, *Nature* **2017**, *541*, 481.
[63] J. Hou, H. Bi, Q. Ge, H. Teng, G. Wan, B. Yu, Q. Jiang, X. Gu, *FASEB J.* **2022**, *36*, 22442.
[64] E. G. Cameron, M. Nahmou, A. B. Toth, L. Heo, B. Tanasa, R. Dalal, W. Yan, P. Nallagatla, X. Xia, S. Hay, C. Knasel, T. L. Stiles, C. Douglas, M. Atkins, C. Sun, M. Ashouri, M. Bian, K.-C. Chang, K. Russano, S. Shah, M. B. Woodworth, J. Galvao, R. V. Nair, M. S. Kapiloff, J. L. Goldberg, *Nature* **2024**, *626*, 574.
[65] M. Stenudd, H. Sabelström, J. Frisén, *JAMA Neurol.* **2015**, *72*, 235.
[66] Y. Luo, V. Coskun, A. Liang, J. Yu, L. Cheng, W. Ge, Z. Shi, K. Zhang, C. Li, Y. Cui, H. Lin, D. Luo, J. Wang, C. Lin, Z. Dai, H. Zhu, J. Zhang, J. Liu, H. Liu, J. deVellis, S. Horvath, Y. E. Sun, S. Li, *Cell* **2015**, *161*, 1175.
[67] J. Li, W. Luo, C. Xiao, J. Zhao, C. Xiang, W. Liu, R. Gu, *Theranostics* **2023**, *13*, 3966.
[68] F. H. Brennan, Y. Li, C. Wang, A. Ma, Q. Guo, Y. Li, N. Pukos, W. A. Campbell, K. G. Witcher, Z. Guan, K. A. Kigerl, J. C. E. Hall, J. P. Godbout, A. J. Fischer, D. M. McTigue, Z. He, Q. Ma, P. G. Popovich, *Nat. Commun.* **2022**, *13*, 4096.
[69] Y. Li, Z. Lei, R. M. Ritzel, J. He, H. Li, H. M. C. Choi, M. M. Lipinski, J. Wu, *Theranostics* **2022**, *12*, 5364.
[70] G.-Y. Xu, S. Xu, Y.-X. Zhang, Z.-Y. Yu, F. Zou, X.-S. Ma, X.-L. Xia, W.-J. Zhang, J.-Y. Jiang, J. Song, *Small* **2022**, *18*, 2107838.
[71] Z. Feng, L. Min, L. Liang, B. Chen, H. Chen, Y. Zhou, W. Deng, H. Liu, J. Hou, *Front. Immunol.* **2021**, *12*, 698249.
[72] A. D. Greenhalgh, J. G. Zarruk, L. M. Healy, S. J. Baskar Jesudasan, P. Jhelum, C. K. Salmon, A. Formanek, M. V. Russo, J. P. Antel, D. B. McGavern, B. W. McColl, S. David, *PLoS Biol.* **2018**, *16*, 2005264.
[73] J. Wang, F. Tian, L. Cao, R. Du, J. Tong, X. Ding, Y. Yuan, C. Wang, *Heliyon* **2023**, *9*, 22914.
[74] I. Cockerill, Y. Su, J. H. Lee, D. Berman, M. L. Young, Y. Zheng, D. Zhu, *Nano Lett.* **2020**, *20*, 4594.
[75] A. D. Schoenenberger, H. Tempfer, C. Lehner, J. Egloff, M. Mauracher, A. Bird, J. Widmer, K. Maniura-Weber, S. F. Fucentese, A. Traweger, U. Silvan, J. G. Snedeker, *Biomaterials* **2020**, *249*, 120034.
[76] N. T. Fiore, B. A. Keating, Y. Chen, S. I. Williams, G. Moalem-Taylor, *Cells* **2023**, *12*, 2317.
[77] G. Sun, S. Yang, G. Cao, Q. Wang, J. Hao, Q. Wen, Z. Li, K.-F. So, Z. Liu, S. Zhou, Y. Zhao, H. Yang, L. Zhou, Z. Yin, *J. Exp. Med.* **2018**, *215*, 521.
[78] M. Costigan, A. Moss, A. Latremoliere, C. Johnston, M. Verma-Gandhu, T. A. Herbert, L. Barrett, G. J. Brenner, D. Vardeh, C. J. Woolf, M. Fitzgerald, *J. Neurosci.* **2009**, *29*, 14415.
[79] A. Mehanna, E. Szpotowicz, M. Schachner, I. Jakovcevski, *Exp. Neurol.* **2014**, *261*, 147.
[80] C. Wu, L. Wang, S. Chen, L. Shi, M. Liu, P. Tu, J. Sun, R. Zhao, Y. Zhang, J. Wang, Y. Pan, Y. Ma, Y. Guo, *J. Neuroinflammation* **2023**, *20*, 171.
[81] F. Barnabé-Heider, C. Göritz, H. Sabelström, H. Takebayashi, F. W. Pfrieger, K. Meletis, J. Frisén, *Cell Stem Cell* **2010**, *7*, 470.
[82] E. C. Cope, E. Gould, *Cell Stem Cell* **2019**, *24*, 690.
[83] H. A. Cameron, L. R. Glover, *Annu. Rev. Psychol.* **2015**, *66*, 53.
[84] Z. Yang, A. Zhang, H. Duan, S. Zhang, P. Hao, K. Ye, Y. E. Sun, X. Li, *Proc. Natl. Acad. Sci. USA* **2015**, *112*, 13354.
[85] H. Sabelström, M. Stenudd, P. Réu, D. O. Dias, M. Elfineh, S. Zdunek, P. Damberg, C. Göritz, J. Frisén, *Science* **2013**, *342*, 637.
[86] Y. Ren, Y. Ao, T. M. O'Shea, J. E. Burda, A. M. Bernstein, A. J. Brumm, N. Muthusamy, H. T. Ghashghaei, S. T. Carmichael, L. Cheng, M. V. Sofroniew, *Sci. Rep.* **2017**, *7*, 41122.
[87] G. Bonvento, J. P. Bolaños, *Cell Metab.* **2021**, *33*, 1546.
[88] J. E. Burda, T. M. O'Shea, Y. Ao, K. B. Suresh, S. Wang, A. M. Bernstein, A. Chandra, S. Deverasetty, R. Kawaguchi, J. H. Kim, S. McCallum, A. Rogers, S. Wahane, M. V. Sofroniew, *Nature* **2022**, *606*, 557.
[89] G. Yu, Y. Zhang, B. Ning, *Front. Cell Neurosci.* **2021**, *15*, 792764.
[90] S. P. Yun, T.-I. Kam, N. Panicker, S. Kim, Y. Oh, J.-S. Park, S.-H. Kwon, Y. J. Park, S. S. Karuppagounder, H. Park, S. Kim, N. Oh, N. A. Kim, S. Lee, S. Brahmachari, X. Mao, J. H. Lee, M. Kumar, D. An, S.-U. Kang, Y. Lee, K. C. Lee, D. H. Na, D. Kim, S. H. Lee, V. V. Roschke, S. A. Liddelow, Z. Mari, B. A. Barres, V. L. Dawson, et al., *Nat. Med.* **2018**, *24*, 931.
[91] Q. Zhao, Y. Zhu, Y. Ren, S. Yin, L. Yu, R. Huang, S. Song, X. Hu, R. Zhu, L. Cheng, N. Xie, *Front. Cell Neurosci.* **2022**, *16*, 1049562.
[92] X. Zhou, G. Li, D. Wu, H. Liang, W. Zhang, L. Zeng, Q. Zhu, P. Lai, Z. Wen, C. Yang, Y. Pan, *Exploration (Beijing)* **2023**, *3*, 20220090.
[93] Y. Zou, B. Gao, J. Lu, K. Zhang, M. Zhai, Z. Yuan, M. Aschner, J. Chen, W. Luo, L. Wang, J. Zhang, *Exploration (Beijing)* **2024**, *4*, 20230154.
[94] L. Zhou, C.-Y. Shao, Y.-J. Xie, N. Wang, S.-M. Xu, B.-Y. Luo, Z.-Y. Wu, Y. H. Ke, M. Qiu, Y. Shen, *eLife* **2020**, *9*, 52056.
[95] Z.-F. Yao, Y. Wang, Y.-H. Lin, Y. Wu, A.-Y. Zhu, R. Wang, L. Shen, J. Xi, Q. Qi, Z.-Q. Jiang, H.-Z. Lü, J.-G. Hu, *Front. Cell Neurosci.* **2017**, *11*, 79.
[96] B. Nagarajan, A. Harder, A. Japp, F. Häberlein, E. Mingardo, H. Kleinert, Ö. Yilmaz, A. Zoons, B. Rau, A. Christ, U. Kubitscheck, B. Eiberger, R. Sandhoff, M. Eckhardt, D. Hartmann, B. Odermatt, *Glia* **2020**, *68*, 509.
[97] Z. Belhadj, Y. Qie, R. P. Carney, Y. Li, G. Nie, *BMEMat* **2023**, *1*, 1201.
[98] C. Buckley, R. Ibrahim, F. Giordano, N. Xu, B. Sems, H. Wang, *BMEMat* **2024**, 12118 .
[99] Y. Su, X. Wang, Y. Yang, L. Chen, W. Xia, K. K. Hoi, H. Li, Q. Wang, G. Yu, X. Chen, S. Wang, Y. Wang, L. Xiao, A. Verkhratsky, S. P. J. Fancy, C. Yi, J. Niu, *Neuron* **2023**, *111*, 190.
[100] H. Fan, H.-B. Tang, L.-Q. Shan, S.-C. Liu, D.-G. Huang, X. Chen, Z. Chen, M. Yang, X.-H. Yin, H. Yang, D.-J. Hao, *J. Neuroinflammation* **2019**, *16*, 206.

[101] Z. Liu, X. Yao, W. Jiang, W. Li, S. Zhu, C. Liao, L. Zou, R. Ding, J. Chen, *J. Neuroinflammation* **2020**, *17*, 90.
[102] H. Fan, H.-B. Tang, Z. Chen, H.-Q. Wang, L. Zhang, Y. Jiang, T. Li, C.-F. Yang, X.-Y. Wang, X. Li, S.-X. Wu, G.-L. Zhang, *J. Neuroinflammation* **2020**, *17*, 295.
[103] A. D. Greenhalgh, S. David, *Journal Neurosci.* **2014**, *34*, 6316.
[104] Y.-J. Chen, H. Zhu, N. Zhang, L. Shen, R. Wang, J.-S. Zhou, J.-G. Hu, H.-Z. Lü, *J. Neurosci. Res.* **2015**, *93*, 1526.
[105] A. Kroner, A. D. Greenhalgh, J. G. Zarruk, R. Passos dos Santos, M. Gaestel, S. David, *Neuron* **2014**, *83*, 1098.
[106] X. Wang, K. Cao, X. Sun, Y. Chen, Z. Duan, L. Sun, L. Guo, P. Bai, D. Sun, J. Fan, X. He, W. Young, Y. Ren, *Glia* **2015**, *63*, 635.
[107] J. Guo, X. Tang, P. Deng, H. Hui, B. Chen, J. An, G. Zhang, K. Shi, J. Wang, Y. He, D. Hao, H. Yang, *Cell Commun. Signal.* **2024**, *22*, 162.
[108] J. Ren, B. Zhu, G. Gu, W. Zhang, J. Li, H. Wang, M. Wang, X. Song, Z. Wei, S. Feng, *Cell Death Dis.* **2023**, *14*, 70.
[109] Y. Xia, R. Yang, H. Wang, Y. Hou, Y. Li, J. Zhu, F. Xu, C. Fu, *J. Tissue Eng.* **2022**, *13*, 20417314221143059.
[110] V. Neirinckx, C. Coste, R. Franzen, A. Gothot, B. Rogister, S. Wislet, *J. Neuroinflammation* **2014**, *11*, 150.
[111] C. Gattlen, C. Clarke, N. Piller, G. Kirschmann, M. Pertin, I. Decosterd, R.-D. Gosselin, M. Suter, *Int. J. Mol. Sci.* **2016**, *17*, 352.
[112] J. Kumar, A. Varela-Ramirez, M. Narayan, *BMEMat* **2024**, *2*, 1207.
[113] H. Liu, *BMEMat* **2024**, *2*, 1204.
[114] J.-G. Hu, L.-L. Shi, Y.-J. Chen, X.-M. Xie, N. Zhang, A.-Y. Zhu, Z.-S. Jiang, Y.-F. Feng, C. Zhang, J. Xi, H.-Z. Lü, *Exp. Neurol.* **2016**, *277*, 190.
[115] V. Bellver-Landete, F. Bretheau, B. Mailhot, N. Vallières, M. Lessard, M.-E. Janelle, N. Vernoux, M.-È. Tremblay, T. Fuehrmann, M. S. Shoichet, S. Lacroix, *Nat. Commun.* **2019**, *10*, 518.
[116] S. Yoshizaki, T. Tamaru, M. Hara, K. Kijima, M. Tanaka, D.-J. Konno, Y. Matsumoto, Y. Nakashima, S. Okada, *J. Neuroinflammation* **2021**, *18*, 12.
[117] Y. Wei, Z. Wang, Z. Qin, Q. Wan, Y. Li, F. R. Tay, C. Wang, T. Zhang, L. Niu, *BMEMat* **2024**, 12127
[118] R. A. Fernandes, K. A. Ganzinger, J. C. Tzou, P. Jönsson, S. F. Lee, M. Palayret, A. M. Santos, A. R. Carr, A. Ponjavic, V. T. Chang, C. Macleod, B. C. Lagerholm, A. E. Lindsay, O. Dushek, A. Tilevik, S. J. Davis, D. Klenerman, *Proc. Natl. Acad. Sci. USA* **2019**, *116*, 14002.
[119] M. A. Govendir, D. Kempe, S. Sianati, J. Cremasco, J. K. Mazalo, F. Colakoglu, M. Golo, K. Poole, M. Biro, *Dev. Cell* **2022**, *57*, 2237.
[120] D. Saltukoglu, B. Özdemir, M. Holtmannspötter, R. Reski, J. Piehler, R. Kurre, M. Reth, *EMBO J.* **2023**, *42*, 112030.
[121] P. Weiss, *J. Exp. Zool.* **1934**, *68*, 39.
[122] M. Marcus, K. Baranes, M. Park, I. S. Choi, K. Kang, O. Shefi, *Adv. Healthcare Mater.* **2017**, *6*, 1700267.
[123] E. C. Spivey, Z. Z. Khaing, J. B. Shear, C. E. Schmidt, *Biomaterials* **2012**, *33*, 4264.
[124] Z. Zhang, Y. Lv, J. Harati, J. Song, P. Du, P. Ou, J. Liang, H. Wang, P.-Y. Wang, *J. Funct. Biomater.* **2023**, *14*, 238.
[125] A. M. McCormick, M. V. S. N. Maddipatla, S. Shi, E. A. Chamsaz, H. Yokoyama, A. Joy, N. D. Leipzig, *ACS Appl. Mater. Interfaces* **2014**, *6*, 1965.
[126] S. Xie, *BMEMat* **2023**, *1*, 1203.
[127] C. Simitzi, A. Ranella, E. Stratakis, *Acta Biomater.* **2017**, *51*, 21.
[128] L. Qi, N. Li, R. Huang, Q. Song, L. Wang, Q. Zhang, R. Su, T. Kong, M. Tang, G. Cheng, *PLoS One* **2013**, *8*, 59022.
[129] N. Gomez, Y. Lu, S. Chen, C. E. Schmidt, *Biomaterials* **2007**, *28*, 271.
[130] J. F. Walsh, M. E. Manwaring, P. A. Tresco, *Tissue Eng.* **2005**, *11*, 1085.
[131] T. Hirono, K. Torimitsu, A. Kawana, J. Fukuda, *Brain Res.* **1988**, *446*, 189.
[132] P. Clark, P. Connolly, A. S. Curtis, J. A. Dow, C. D. Wilkinson, *Development* **1990**, *108*, 635.
[133] N. Li, A. Folch, *Exp. Cell Res.* **2005**, *311*, 307.
[134] M. J. Mahoney, R. R. Chen, J. Tan, W. M. Saltzman, *Biomaterials* **2005**, *26*, 771.
[135] K. H. Song, J. Lee, H. R. Jung, H. Park, J. Doh, *Sci. Rep.* **2017**, *7*, 11533.
[136] A. Ferrari, M. Cecchini, A. Dhawan, S. Micera, I. Tonazzini, R. Stabile, D. Pisignano, F. Beltram, *Nano Lett.* **2011**, *11*, 505.
[137] A. Ferrari, M. Cecchini, M. Serresi, P. Faraci, D. Pisignano, F. Beltram, *Biomaterials* **2010**, *31*, 4682.
[138] F. Johansson, P. Carlberg, N. Danielsen, L. Montelius, M. Kanje, *Biomaterials* **2006**, *27*, 1251.
[139] L. Yao, S. Wang, W. Cui, R. Sherlock, C. O'Connell, G. Damodaran, A. Gorman, A. Windebank, A. Pandit, *Acta Biomater.* **2009**, *5*, 580.
[140] A. Béduer, C. Vieu, F. Arnauduc, J.-C. Sol, I. Loubinoux, L. Vaysse, *Biomaterials* **2012**, *33*, 504.
[141] K. Yang, E. Park, J. S. Lee, I.-S. Kim, K. Hong, K. I. Park, S.-W. Cho, H. S. Yang, *Macromol. Biosci.* **2015**, *15*, 1348.
[142] S. Ankam, M. Suryana, L. Y. Chan, A. A. K. Moe, B. K. K. Teo, J. B. K. Law, M. P. Sheetz, H. Y. Low, E. K. F. Yim, *Acta Biomater.* **2013**, *9*, 4535.
[143] S. Chen, J. A. Jones, Y. Xu, H.-Y. Low, J. M. Anderson, K. W. Leong, *Biomaterials* **2010**, *31*, 3479.
[144] X. Zheng, L. Xin, Y. Luo, H. Yang, X. Ye, Z. Mao, S. Zhang, L. Ma, C. Gao, *ACS Appl. Mater. Interfaces* **2019**, *11*, 43689.
[145] M. Al-Jumaa, M. B. Hallett, S. Dewitt, *Biochim. Biophys. Acta Mol. Cell Res.* **2020**, *1867*, 118832.
[146] V. Sergunova, V. Inozemtsev, N. Vorobjeva, E. Kozlova, E. Sherstyukova, S. Lyapunova, A. Chernysh, *Cells* **2023**, *12*, 2199.
[147] P. C. Wilkinson, J. M. Shields, W. S. Haston, *Exp. Cell Res.* **1982**, *140*, 55.
[148] X. Sun, M. K. Driscoll, C. Guven, S. Das, C. A. Parent, J. T. Fourkas, W. Losert, *Proc. Natl. Acad. Sci. USA* **2015**, *112*, 12557.
[149] B. Sung, D. H. Kim, M. H. Kim, D. Vigolo, *Adv. Biol.* **2022**, *6*, 2101312.
[150] B. A. Wheatley, I. Rey-Suarez, M. J. Hourwitz, S. Kerr, H. Shroff, J. T. Fourkas, A. Upadhyaya, *Mol. Biol. Cell* **2022**, *33*, ar88.
[151] C. M. Ketchum, X. Sun, A. Suberi, J. T. Fourkas, W. Song, A. Upadhyaya, *Mol. Biol. Cell* **2018**, *29*, 1732.
[152] J. S. Chua, C.-P. Chng, A. A. K. Moe, J. Y. Tann, E. L. K. Goh, K.-H. Chiam, E. K. F. Yim, *Biomaterials* **2014**, *35*, 7750.
[153] S. H. Lim, X. Y. Liu, H. Song, K. J. Yarema, H. Q. Mao, *Biomaterials* **2010**, *31*, 9031.
[154] J. M. Corey, D. Y. Lin, K. B. Mycek, Q. Chen, S. Samuel, E. L. Feldman, D. C. Martin, *J. Biomed. Mater. Res., Part A* **2007**, *83*, 636.
[155] J. Xie, S. M. Willerth, X. Li, M. R. Macewan, A. Rader, S. E. Sakiyama-Elbert, Y. Xia, *Biomaterials* **2009**, *30*, 354.
[156] S. Shah, P. T. Yin, T. M. Uehara, S.-T. Dean Chueng, L. Yang, K.-B. Lee, *Adv. Mater.* **2014**, *26*, 3673.
[157] G. T. Christopherson, H. Song, H. Q. Mao, *Biomaterials* **2009**, *30*, 556.
[158] Y. Zou, J. Qin, Z. Huang, G. Yin, X. Pu, D. He, *ACS Appl. Mater. Interfaces* **2016**, *8*, 12576.
[159] Y. Jia, W. Yang, K. Zhang, S. Qiu, J. Xu, C. Wang, Y. Chai, *Acta Biomater.* **2019**, *83*, 291.
[160] F. Yang, R. Murugan, S. Wang, S. Ramakrishna, *Biomaterials* **2005**, *26*, 2603.
[161] C. Czeisler, A. Short, T. Nelson, P. Gygli, C. Ortiz, F. P. Catacutan, B. Stocker, J. Cronin, J. Lannutti, J. Winter, J. J. Otero, *J. Comp. Neurol.* **2016**, *524*, 3485.
[162] H. B. Wang, M. E. Mullins, J. M. Cregg, C. W. McCarthy, R. J. Gilbert, *Acta Biomater.* **2010**, *6*, 2970.
[163] Y. Yuan, P. Zhang, Y. Yang, X. Wang, X. Gu, *Biomaterials* **2004**, *25*, 4273.
[164] X. Wen, P. A. Tresco, *J. Biomed. Mater. Res., Part A* **2006**, *76*, 626.
[165] N. Rangappa, A. Romero, K. D. Nelson, R. C. Eberhart, G. M. Smith, *J. Biomed. Mater. Res.* **2000**, *51*, 625.

[166] Y. T. Kim, V. K. Haftel, S. Kumar, R. V. Bellamkonda, *Biomaterials* **2008**, *29*, 3117.
[167] Y. Xu, X. Wang, Z. Wang, Q. Chen, D. Zhang, N. Dong, J. Wang, *BMEMat* **2025**, 70005.
[168] A. Ko, C. Liao, *BMEMat* **2023**, *1*, 1203.
[169] E. Schnell, K. Klinkhammer, S. Balzer, G. Brook, D. Klee, P. Dalton, J. Mey, *Biomaterials* **2007**, *28*, 3012.
[170] E. Saino, M. L. Focarete, C. Gualandi, E. Emanuele, A. I. Cornaglia, M. Imbriani, L. Visai, *Biomacromolecules* **2011**, *12*, 1900.
[171] M. A. Bucaro, Y. Vasquez, B. D. Hatton, J. Aizenberg, *ACS Nano* **2012**, *6*, 6222.
[172] J. N. Hanson, M. J. Motala, M. L. Heien, M. Gillette, J. Sweedler, R. G. Nuzzo, *Lab Chip* **2009**, *9*, 122.
[173] A. Tsuruma, M. Tanaka, S. Yamamoto, M. Shimomura, *Colloids Surf. A* **2008**, *313*, 53.
[174] E. Martínez, E. Engel, J. A. Planell, J. Samitier, *Ann. Anat.* **2009**, *191*, 126.
[175] F. Haq, V. Anandan, C. Keith, G. Zhang, *Int. J. Nanomed.* **2007**, *2*, 107.
[176] N. M. Dowell-Mesfin, M.-A. Abdul-Karim, A. M. P. Turner, S. Schanz, H. G. Craighead, B. Roysam, J. N. Turner, W. Shain, *J. Neural Eng.* **2004**, *1*, 78.
[177] N. R. Blumenthal, O. Hermanson, B. Heimrich, V. P. Shastri, *Proc. Natl. Acad. Sci. USA* **2014**, *111*, 16124.
[178] Y. I. Cho, J. S. Choi, S. Y. Jeong, H. S. Yoo, *Acta Biomater.* **2010**, *6*, 4725.
[179] L. A. Cyster, K. G. Parker, T. L. Parker, D. M. Grant, *Biomaterials* **2004**, *25*, 97.
[180] S. P. Khan, G. G. Auner, G. M. Newaz, *Nanomedicine* **2005**, *1*, 125.
[181] G. Lamour, N. Journiac, S. Souès, S. Bonneau, P. Nassoy, A. Hamraoui, *Colloids Surf., B* **2009**, *72*, 208.
[182] X. Mou, S. Wang, W. Guo, S. Ji, J. Qiu, D. Li, X. Zhang, J. Zhou, W. Tang, C. Wang, H. Liu, *Nanoscale* **2016**, *8*, 13186.
[183] K. Yang, H. Jung, H.-R. Lee, J. S. Lee, S. R. Kim, K. Y. Song, E. Cheong, J. Bang, S. G. Im, S.-W. Cho, *ACS Nano* **2014**, *8*, 7809.
[184] S. B. Yu, J. Baek, M. Choi, Y. Oh, H. R. Lee, S. J. Yu, E. Lee, J.-W. Sohn, S. G. Im, S. Jon, *ACS Nano* **2016**, *10*, 9909.
[185] A. Solanki, S. Shah, P. T. Yin, K. B. Lee, *Sci. Rep.* **2013**, *3*, 1553.
[186] K. M. Hotchkiss, G. B. Reddy, S. L. Hyzy, Z. Schwartz, B. D. Boyan, R. Olivares-Navarrete, *Acta Biomater.* **2016**, *31*, 425.
[187] K. M. Hotchkiss, N. B. Ayad, S. L. Hyzy, B. D. Boyan, R. Olivares-Navarrete, *Clin. Oral Implants Res.* **2017**, *28*, 414.
[188] K. M. Hotchkiss, K. T. Sowers, R. Olivares-Navarrete, *Dent. Mater.* **2019**, *35*, 176.
[189] Y. Zhang, X. Cheng, J. A. Jansen, F. Yang, J. van den Beucken, *Mater. Biol. Appl.* **2019**, *95*, 143.
[190] J. Wang, F. Meng, W. Song, J. Jin, Q. Ma, D. Fei, L. Fang, L. Chen, Q. Wang, Y. Zhang, *Int. J. Nanomed.* **2018**, *13*, 4029.
[191] R. Ion, A. B. Stoian, C. Dumitriu, S. Grigorescu, A. Mazare, A. Cimpean, I. Demetrescu, P. Schmuki, *Acta Biomater.* **2015**, *24*, 370.
[192] M. Chen, Y. Zhang, P. Zhou, X. Liu, H. Zhao, X. Zhou, Q. Gu, B. Li, X. Zhu, Q. Shi, *Bioact. Mater.* **2020**, *5*, 880.
[193] M. Li, X. Guo, W. Qi, Z. Wu, J. D. de Bruijn, Y. Xiao, C. Bao, H. Yuan, *J. Mater. Chem. B* **2020**, *8*, 1863.
[194] A. Ruiz, L. Buzanska, D. Gilliland, H. Rauscher, L. Sirghi, T. Sobanski, M. Zychowicz, L. Ceriotti, F. Bretagnol, S. Coecke, P. Colpo, F. Rossi, *Biomaterials* **2008**, *29*, 4766.
[195] L. Buzanska, A. Ruiz, M. Zychowicz, H. Rauscher, L. Ceriotti, F. Rossi, P. Colpo, K. Domanska-Janik, S. Coecke, *Acta Neurobiol. Exp.* **2009**, *69*, 24.
[196] C. R. Almeida, T. Serra, M. I. Oliveira, J. A. Planell, M. A. Barbosa, M. Navarro, *Acta Biomater.* **2014**, *10*, 613.
[197] X. Li, Z. Chen, H. Zhang, Y. Zhuang, H. Shen, Y. Chen, Y. Zhao, B. Chen, Z. Xiao, J. Dai, *Polymers* **2019**, *11*, 341.
[198] Z. Li, Y. Qi, Z. Li, S. Chen, H. Geng, J. Han, J. Wang, Z. Wang, S. Lei, B. Huang, G. Li, X. Li, S. Wu, S. Ni, *Biomaterials* **2023**, *298*, 122146.
[199] S. Stokols, M. H. Tuszynski, *Biomaterials* **2006**, *27*, 443.
[200] X. Sun, Y. Bai, H. Zhai, S. Liu, C. Zhang, Y. Xu, J. Zou, T. Wang, S. Chen, Q. Zhu, X. Liu, H. Mao, D. Quan, *Acta Biomater.* **2019**, *86*, 194.
[201] J. Li, Y. Zhao, P. Zhou, X. Hu, D. Wang, S. M. King, S. E. Rogers, J. Wang, J. R. Lu, H. Xu, *Small* **2020**, *16*, 2003945.
[202] T. T. Yu, M. S. Shoichet, *Biomaterials* **2005**, *26*, 1507.
[203] M. Bartneck, K.-H. Heffels, Y. Pan, M. Bovi, G. Zwadlo-Klarwasser, J. Groll, *Biomaterials* **2012**, *33*, 4136.
[204] Z. Li, Y. Qi, L. Sun, Z. Li, S. Chen, Y. Zhang, Y. Ma, J. Han, Z. Wang, Y. Zhang, H. Geng, B. Huang, J. Wang, G. Li, X. Li, S. Wu, S. Ni, *Theranostics* **2023**, *13*, 4762.
[205] A. Reversat, F. Gaertner, J. Merrin, J. Stopp, S. Tasciyan, J. Aguilera, I. de Vries, R. Hauschild, M. Hons, M. Piel, A. Callan-Jones, R. Voituriez, M. Sixt, *Nature* **2020**, *582*, 582.
[206] M. J. Dalby, N. Gadegaard, R. O. Oreffo, *Nat. Mater.* **2014**, *13*, 558.
[207] B. Geiger, J. P. Spatz, A. D. Bershadsky, *Nat. Rev. Mol. Cell Biol.* **2009**, *10*, 21.
[208] C. Grandy, F. Port, J. Pfeil, M. A. G. Oliva, M. Vassalli, K.-E. Gottschalk, *Biomater. Adv.* **2023**, *145*, 213277.
[209] P. Kanchanawong, D. A. Calderwood, *Nat. Rev. Mol. Cell Biol.* **2023**, *24*, 142.
[210] Y.-C. Chen, D.-C. Lee, T.-Y. Tsai, C.-Y. Hsiao, J.-W. Liu, C.-Y. Kao, H.-K. Lin, H.-C. Chen, T. J. Palathinkal, W.-F. Pong, N.-H. Tai, I.-N. Lin, I.-M. Chiu, *Biomaterials* **2010**, *31*, 5575.
[211] L. S. Campos, *BioEssays* **2005**, *27*, 698.
[212] Z. Álvarez, A. N. Kolberg-Edelbrock, I. R. Sasselli, J. A. Ortega, R. Qiu, Z. Syrgiannis, P. A. Mirau, F. Chen, S. M. Chin, S. Weigand, E. Kiskinis, S. I. Stupp, *Science* **2021**, *374*, 848.
[213] X.-Y. Xu, X.-T. Li, S.-W. Peng, J.-F. Xiao, C. Liu, G. Fang, K. C. Chen, G.-Q. Chen, *Biomaterials* **2010**, *31*, 3967.
[214] J. Li, Y. Zhang, Z. Lou, M. Li, L. Cui, Z. Yang, L. Zhang, Y. Zhang, N. Gu, F. Yang, *Small* **2022**, *18*, 2201123.
[215] L. Yang, K. M. Jurczak, L. Ge, P. van Rijn, *Adv. Healthcare Mater.* **2020**, *9*, 2000117.
[216] X. Zheng, L. Chen, J. Tan, J. Miao, X. Liu, T. Yang, Z. Ding, *Regener. Biomater.* **2022**, *9*, rbac075.
[217] Y. Guo, Y. Ao, C. Ye, R. Xia, J. Mi, Z. Shan, M. Shi, L. Xie, Z. Chen, *Nano Res.* **2023**, *6*, 9715.
[218] Y. Yang, Y. Lin, Z. Zhang, R. Xu, X. Yu, F. Deng, *Biomater. Sci.* **2021**, *9*, 3334.
[219] C. Xie, S. Liu, Q. Zhang, H. Ma, S. Yang, Z.-X. Guo, T. Qiu, X. Tuo, *ACS Nano* **2021**, *15*, 10000.
[220] H. Joukhdar, A. Seifert, T. Jüngst, J. Groll, M. S. Lord, J. Rnjak-Kovacina, *Adv. Mater.* **2021**, *33*, 2100091.
[221] F. Diaz, N. Forsyth, A. R. Boccaccini, *Adv. Healthcare Mater.* **2023**, *12*, 2203205.
[222] Y. Yang, J. Zhang, S. Wu, Y. Deng, S. Wang, L. Xie, X. Li, L. Yang, *Biomaterials* **2024**, *308*, 122558.
[223] J. Fan, J. Yang, *J. Biomater. Sci., Polym. Ed.* **2017**, *28*, 569.
[224] Y. Sun, C. Yang, X. Zhu, J.-J. Wang, X.-Y. Liu, X.-P. Yang, X.-W. An, J. Liang, H.-J. Dong, W. Jiang, C. Chen, Z.-G. Wang, H.-T. Sun, Y. Tu, S. Zhang, F. Chen, X.-H. Li, *J. Biomed. Mater. Res., Part A* **2019**, *107*, 1898.
[225] X.-H. Li, X. Zhu, X.-Y. Liu, H.-H. Xu, W. Jiang, J.-J. Wang, F. Chen, S. Zhang, R.-X. Li, X.-Y. Chen, Y. Tu, *J. Mater. Sci. Mater. Med.* **2021**, *32*, 31.
[226] M. C. Amores de Sousa, C. A. V. Rodrigues, I. A. F. Ferreira, M. M. Diogo, R. J. Linhardt, J. M. S. Cabral, F. C. Ferreira, *Front. Bioeng. Biotechnol.* **2020**, *8*, 580135.
[227] P. Chen, C. Xu, P. Wu, K. Liu, F. Chen, Y. Chen, H. Dai, Z. Luo, *ACS Nano* **2022**, *16*, 16513.

[228] N. J. Schaub, C. D. Johnson, B. Cooper, R. J. Gilbert, *J. Neurotrauma* **2016**, *33*, 1405.
[229] Y. Cheng, Y. Zhang, H. Wu, *Front. Bioeng. Biotechnol.* **2021**, *9*, 807533.
[230] T. Y. Yuan, J. Zhang, T. Yu, J. P. Wu, Q. Y. Liu, *Front. Bioeng. Biotechnol.* **2022**, *10*, 847344.
[231] J. Koffler, W. Zhu, X. Qu, O. Platoshyn, J. N. Dulin, J. Brock, L. Graham, P. Lu, J. Sakamoto, M. Marsala, S. Chen, M. H. Tuszynski, *Nat. Med.* **2019**, *25*, 263.
[232] Y. Li, S. Cheng, H. Wen, L. Xiao, Z. Deng, J. Huang, Z. Zhang, *Acta Biomater.* **2023**, *168*, 400.
[233] A. Zarepour, S. Hooshmand, A. Gökmen, A. Zarrabi, E. Mostafavi, *Cells* **2021**, *10*, 3189.
[234] M. Handrea-Dragan, I. Botiz, *Polymers* **2021**, *13*, 445.
[235] C. N. LaFratta, J. T. Fourkas, T. Baldacchini, R. A. Farrer, *Angew. Chem. Int. ed.* **2007**, *46*, 6238.
[236] R. Sheth, E. R. Balesh, Y. S. Zhang, J. A. Hirsch, A. Khademhosseini, R. Oklu, *J. Vasc. Interventional Radiol.* **2016**, *27*, 859.
[237] X. Ding, K. Liu, Z. L. Shi, *Mass Spectrom Rev.* **2021**, *40*, 566.
[238] S. Y. Park, S. Lee, J. Yang, M. S. Kang, *Adv. Mater.* **2023**, *35*, 2300546.
[239] G. Delaittre, A. S. Goldmann, J. O. Mueller, C. Barner-Kowollik, *Angew. Chem., Int. Ed.* **2015**, *54*, 11388.
[240] Y. Zheng, S. Zhang, J. B. Tok, Z. Bao, *J. Am. Chem. Soc.* **2022**, *144*, 4699.
[241] M. Mitmoen, O. Kedem, *ACS Appl. Mater. Interfaces* **2022**, *14*, 32696.
[242] Z. Guo, S. Kofink, H. Chen, J. Liang, D. W. Grijpma, A. A. Poot, *Biomed. Mater.* **2019**, *14*, 034101.
[243] F. Yu, P. Li, H. Shen, S. Mathur, C.-M. Lehr, U. Bakowsky, F. Mücklich, *Biomaterials* **2005**, *26*, 2307.
[244] S. N. Yang, X. Q. Liu, J. X. Zheng, Y. M. Lu, B. R. Gao, *Nanomaterials* **2020**, *10*, 1313.
[245] L. Yang, B. M. Conley, C. Rathnam, H.-Y. Cho, T. Pongkulapa, B. Conklin, K.-B. Lee, *ACS Nano* **2022**, *16*, 5577.
[246] S. O'Halloran, A. Pandit, A. Heise, A. Kellett, *Adv. Sci.* **2023**, *10*, 2204072.
[247] M. Carlotti, V. Mattoli, *Small* **2019**, *15*, 1902687.
[248] K. Liu, H. Ding, S. Li, Y. Niu, Y. Zeng, J. Zhang, X. Du, Z. Gu, *Nat. Commun.* **2022**, *13*, 4563.
[249] *Nat. Nanotechnol.* **2024**, *19*, 11.
[250] X. Zhao, X. Lu, K. Li, S. Song, Z. Luo, C. Zheng, C. Yang, X. Wang, L. Wang, Y. Tang, C. Wang, J. Liu, *Bioact. Mater.* **2023**, *24*, 331.
[251] P. M. Jenkins, M. R. Laughter, D. J. Lee, Y. M. Lee, C. R. Freed, D. Park, *Nanoscale Res. Lett.* **2015**, *10*, 972.
[252] D. Y. Wong, J.-C. Leveque, H. Brumblay, P. H. Krebsbach, S. J. Hollister, F. LaMarca, *J. Neurotrauma* **2008**, *25*, 1027.
[253] W. A. Abbas, M. E. Ibrahim, M. El-Naggar, W. A. Abass, I. H. Abdullah, B. I. Awad, N. K. Allam, *ACS Biomater. Sci. Eng.* **2020**, *6*, 6490.
[254] A. J. Krych, G. E. Rooney, B. Chen, T. C. Schermerhorn, S. Ameenuddin, L. Gross, M. J. Moore, B. L. Currier, R. J. Spinner, J. A. Friedman, M. J. Yaszemski, A. J. Windebank, *Acta Biomater.* **2009**, *5*, 2551.
[255] M. J. Moore, J. A. Friedman, E. B. Lewellyn, S. M. Mantila, A. J. Krych, S. Ameenuddin, A. M. Knight, L. Lu, B. L. Currier, R. J. Spinner, R. W. Marsh, A. J. Windebank, M. J. Yaszemski, *Biomaterials* **2006**, *27*, 419.
[256] S. Stokols, J. Sakamoto, C. Breckon, T. Holt, J. Weiss, M. H. Tuszynski, *Tissue Eng.* **2006**, *12*, 2777.
[257] M. D. Bender, J. M. Bennett, R. L. Waddell, J. S. Doctor, K. G. Marra, *Biomaterials* **2004**, *25*, 1269.
[258] S. Stokols, M. H. Tuszynski, *Biomaterials* **2004**, *25*, 5839.
[259] C. Zeng, P. Sheng, G. Xie, J. Zhu, P. Dong, D. Quan, *J. Controlled Release* **2011**, *152*, 234.
[260] Z. Chen, Z. Sun, Y. Fan, M. Yin, C. Jin, B. Guo, Y. Yin, R. Quan, S. Zhao, S. Han, X. Cheng, W. Liu, B. Chen, Z. Xiao, J. Dai, Y. Zhao, *ACS Nano* **2023**, *17*, 25591.
[261] Y. Sun, J. Wu, L. Zhou, W. Wang, H. Wang, S. Sun, Y. Xu, L. Zhang, X. Jiang, G. Zhu, K. Xi, Y. Gu, L. Chen, *Front. Bioeng. Biotechnol.* **2024**, *12*, 1415527.
[262] R. J. Colello, W. N. Chow, J. W. Bigbee, C. Lin, D. Dalton, D. Brown, B. S. Jha, B. E. Mathern, K. D. Lee, D. G. Simpson, *J. Tissue Eng. Regener. Med.* **2016**, *10*, 656.
[263] A. Hurtado, J. M. Cregg, H. B. Wang, D. F. Wendell, M. Oudega, R. J. Gilbert, J. W. McDonald, *Biomaterials* **2011**, *32*, 6068.
[264] T. Liu, J. D. Houle, J. Xu, B. P. Chan, S. Y. Chew, *Tissue Eng. Part A* **2012**, *18*, 1057.
[265] K. Ley, *J. Immunol.* **2017**, *199*, 2191.
[266] A. C. Farsheed, C. Zevallos-Delgado, L. T. Yu, S. Saeidifard, J. W. R. Swain, J. T. Makhoul, A. J. Thomas, C. C. Cole, E. Garcia Huitron, K. J. Grande-Allen, M. Singh, K. V. Larin, J. D. Hartgerink, *ACS Nano* **2024**, *18*, 12477.
[267] V. M. Tysseling-Mattiace, V. Sahni, K. L. Niece, D. Birch, C. Czeisler, M. G. Fehlings, S. I. Stupp, J. A. Kessler, *J. Neurosci.* **2008**, *28*, 3814.
[268] A. Kaneko, A. Matsushita, Y. Sankai, *Biomed. Mater.* **2015**, *10*, 015008.
[269] P. Saadai, Y. S. Nout, J. Encinas, A. Wang, T. L. Downing, M. S. Beattie, J. C. Bresnahan, S. Li, D. L. Farmer, *J. Pediatr. Surgery* **2011**, *46*, 2279.
[270] L. Yang, S.-T. D. Chueng, Y. Li, M. Patel, C. Rathnam, G. Dey, L. Wang, L. Cai, K.-B. Lee, *Nat. Commun.* **2018**, *9*, 3147.
[271] L. Yang, B. M. Conley, S. R. Cerqueira, T. Pongkulapa, S. Wang, J. K. Lee, K. B. Lee, *Adv. Mater.* **2020**, *32*, 2002578.
[272] C. Rathnam, L. Yang, S. Castro-Pedrido, J. Luo, K.-B. Lee, *Sci. Adv.* **2021**, *7*, abj2281.
[273] S. Wang, L. Yang, B. Cai, F. Liu, Y. Hou, H. Zheng, F. Cheng, H. Zhang, L. Wang, X. Wang, Q. Lv, L. Kong, K.-B. Lee, Q. Zhang, *Natl. Sci. Rev.* **2022**, *9*, nwac037.
[274] B. M. Conley, L. Yang, B. Bhujel, J. Luo, I. Han, K.-B. Lee, *ACS Nano* **2023**, *17*, 3750.
[275] K. R. Jessen, R. Mirsky, *J. Physiol.* **2016**, *594*, 3521.
[276] R. Guo, S. Zhang, M. Xiao, F. Qian, Z. He, D. Li, X. Zhang, H. Li, X. Yang, M. Wang, R. Chai, M. Tang, *Biomaterials* **2016**, *106*, 193.
[277] I. Tonazzini, E. Jacchetti, S. Meucci, F. Beltram, M. Cecchini, *Adv. Healthcare Mater.* **2015**, *4*, 1849.
[278] C. Wang, Y. Jia, W. Yang, C. Zhang, K. Zhang, Y. Chai, *J. Biomed. Mater. Res., Part A* **2018**, *106*, 2070.
[279] R. Li, D. Li, C. Wu, L. Ye, Y. Wu, Y. Yuan, S. Yang, L. Xie, Y. Mao, T. Jiang, Y. Li, J. Wang, H. Zhang, X. Li, J. Xiao, *Theranostics* **2020**, *10*, 1649.
[280] Z. Fang, X. Ge, X. Chen, Y. Xu, W.-E. Yuan, Y. Ouyang, *J. Nanobiotechnol.* **2020**, *18*, 46.
[281] K. J. Zuo, T. Gordon, K. M. Chan, G. H. Borschel, *Exp. Neurol.* **2020**, *332*, 113397.
[282] J. D. Guest, S. W. Moore, A. A. Aimetti, A. B. Kutikov, A. J. Santamaria, C. P. Hofstetter, A. E. Ropper, N. Theodore, T. R. Ulich, R. T. Layer, *Biomaterials* **2018**, *185*, 284.
[283] J. R. Slotkin, C. D. Pritchard, B. Luque, J. Ye, R. T. Layer, M. S. Lawrence, T. M. O'Shea, R. R. Roy, H. Zhong, I. Vollenweider, V. R. Edgerton, G. Courtine, E. J. Woodard, R. Langer, *Biomaterials* **2017**, *123*, 63.
[284] H. Lin, B. Chen, B. Wang, Y. Zhao, W. Sun, J. Dai, *J. Biomed. Mater. Res., Part A* **2006**, *79*, 591.
[285] Y. Zhao, F. Tang, Z. Xiao, G. Han, N. Wang, N. Yin, B. Chen, X. Jiang, C. Yun, W. Han, C. Zhao, S. Cheng, S. Zhang, J. Dai, *Cell Transplant.* **2017**, *26*, 891.

[286] Z. Xiao, F. Tang, J. Tang, H. Yang, Y. Zhao, B. Chen, S. Han, N. Wang, X. Li, S. Cheng, G. Han, C. Zhao, X. Yang, Y. Chen, Q. Shi, S. Hou, S. Zhang, J. Dai, *Sci. China Life Sci.* **2016**, *59*, 647.
[287] W. Chen, Y. Zhang, S. Yang, J. Sun, H. Qiu, X. Hu, X. Niu, Z. Xiao, Y. Zhao, Y. Zhou, J. Dai, T. Chu, *Cell Transplant.* **2020**, *29*, 096368972095063.
[288] K. D. Kim, K. S. Lee, D. Coric, J. S. Harrop, N. Theodore, R. M. Toselli, *Neurosurgery* **2022**, *90*, 668.
[289] P. Tabakow, G. Raisman, W. Fortuna, M. Czyz, J. Huber, D. Li, P. Szewczyk, S. Okurowski, R. Miedzybrodzki, B. Czapiga, B. Salomon, A. Halon, Y. Li, J. Lipiec, A. Kulczyk, W. Jarmundowicz, *Cell Transplant.* **2014**, *23*, 1631.
[290] F. Gelain, Z. Luo, M. Rioult, S. Zhang, *NPJ Regener. Med.* **2021**, *6*, 9.
[291] W. He, H. Wang, X. Zhang, T. Mao, Y. Lu, Y. Gu, D. Ju, L. Qi, Q. Wang, C. Dong, *J. Biomater. Sci. Polym. Ed.* **2022**, *33*, 2124.
[292] G. Li, B. Zhang, J. Sun, L. Shi, M. Huang, L. Huang, Z. Lin, Q. Lin, B. Lai, Y. Ma, B. Jiang, Y. Ding, H. Zhang, M. Li, P. Zhu, Y. Wang, X. Zeng, Y. Zeng, *Bioact. Mater.* **2021**, *6*, 3766.
[293] D. Liu, *Adv. Healthcare Mater.* **2023**, *12*, 2300123.
[294] H. J. Kim, J. S. Lee, J. M. Park, S. Lee, S. J. Hong, J. S. Park, K.-H. Park, *ACS Appl. Mater. Interfaces* **2020**, *12*, 30750.
[295] J. B. Senger, K. N. Rabey, M. J. Morhart, K. M. Chan, C. A. Webber, *Ann. Neurol.* **2020**, *88*, 363.
[296] H. Liu, Y. Feng, S. Che, L. Guan, X. Yang, Y. Zhao, L. Fang, A. V. Zvyagin, Q. Lin, *Biomacromolecules* **2023**, *24*, 86.
[297] C. Wu, S. Chen, T. Zhou, K. Wu, Z. Qiao, Y. Zhang, N. Xin, X. Liu, D. Wei, J. Sun, H. Luo, L. Zhou, H. Fan, *ACS Appl. Mater. Interfaces* **2021**, *13*, 52346.
[298] K. A. Tran, Y. Jin, J. Bouyer, B. J. DeOre, L. Suprewicz, A. Figel, H. Walens, I. Fischer, P. A. Galie, *Biomater. Sci.* **2022**, *10*, 2237.
[299] Š. Kubinová, *Neurochem. Res.* **2020**, *45*, 171.
[300] Y. S. Choi, Y.-Y. Hsueh, J. Koo, Q. Yang, R. Avila, B. Hu, Z. Xie, G. Lee, Z. Ning, C. Liu, Y. Xu, Y. J. Lee, W. Zhao, J. Fang, Y. Deng, S. M. Lee, A. Vázquez-Guardado, I. Stepien, Y. Yan, J. W. Song, C. Haney, Y. S. Oh, W. Liu, H.-J. Yoon, A. Banks, M. R. MacEwan, G. A. Ameer, W. Z. Ray, Y. Huang, T. Xie, et al., *Nat. Commun.* **2020**, *11*, 5990.
[301] D. Liu, F. Yang, F. Xiong, N. Gu, *Theranostics* **2016**, *6*, 1306.
[302] M. Luo, T. Fan, Y. Zhou, H. Zhang, L. Mei, *Adv. Funct. Mater.* **2019**, *29*, 1808306.
[303] M. Qiu, W. X. Ren, T. Jeong, M. Won, G. Y. Park, D. K. Sang, L.-P. Liu, H. Zhang, J. S. Kim, *Chem. Soc. Rev.* **2018**, *47*, 5588.
[304] W. Tao, N. Kong, X. Ji, Y. Zhang, A. Sharma, J. Ouyang, B. Qi, J. Wang, N. Xie, C. Kang, H. Zhang, O. C. Farokhzad, J. S. Kim, *Chem. Soc. Rev.* **2019**, *48*, 2891.
[305] J. Shao, H. Xie, H. Huang, Z. Li, Z. Sun, Y. Xu, Q. Xiao, X.-F. Yu, Y. Zhao, H. Zhang, H. Wang, P. K. Chu, *Nat. Commun.* **2016**, *7*, 12967.
[306] T. Xue, W. Liang, Y. Li, Y. Sun, Y. Xiang, Y. Zhang, Z. Dai, Y. Duo, L. Wu, K. Qi, B. N. Shivananju, L. Zhang, X. Cui, H. Zhang, Q. Bao, *Nat. Commun.* **2019**, *10*, 28.
[307] M. Qiu, D. Wang, W. Liang, L. Liu, Y. Zhang, X. Chen, D. K. Sang, C. Xing, Z. Li, B. Dong, F. Xing, D. Fan, S. Bao, H. Zhang, Y. Cao, *Proc. Natl. Acad. Sci. USA* **2018**, *115*, 501.
[308] Z. Sun, Y. Zhao, Z. Li, H. Cui, Y. Zhou, W. Li, W. Tao, H. Zhang, H. Wang, P. K. Chu, X. F. Yu, *Small* **2017**, *13*, 1602896.
[309] Z. Xie, S. Chen, Y. Duo, Y. Zhu, T. Fan, Q. Zou, M. Qu, Z. Lin, J. Zhao, Y. Li, L. Liu, S. Bao, H. Chen, D. Fan, H. Zhang, *ACS Appl. Mater. Interfaces* **2019**, *11*, 22129.
[310] B. Zhang, T. Fan, N. Xie, G. Nie, H. Zhang, *Adv. Sci.* **2019**, *6*, 1901787.
[311] H. Ding, X. Shu, Y. Jin, T. Fan, H. Zhang, *Nanoscale* **2019**, *11*, 5839.
[312] Y. Wang, G. Wei, X. Zhang, F. Xu, X. Xiong, S. Zhou, *Adv. Mater.* **2017**, *29*, 1605357.
[313] P. E. Saw, H. Yao, C. Lin, W. Tao, O. C. Farokhzad, X. Xu, *Nano Lett.* **2019**, *19*, 5967.
[314] C. Xing, S. Chen, M. Qiu, X. Liang, Q. Liu, Q. Zou, Z. Li, Z. Xie, D. Wang, B. Dong, L. Liu, D. Fan, H. Zhang, *Adv. Healthcare Mater.* **2018**, *7*, 1701510.
[315] W. Tao, X. Zhu, X. Yu, X. Zeng, Q. Xiao, X. Zhang, X. Ji, X. Wang, J. Shi, H. Zhang, L. Mei, *Adv. Mater.* **2017**, *29*, 1603276.
[316] X. Ji, N. Kong, J. Wang, W. Li, Y. Xiao, S. T. Gan, Y. Zhang, Y. Li, X. Song, Q. Xiong, S. Shi, Z. Li, W. Tao, H. Zhang, L. Mei, J. Shi, *Adv. Mater.* **2018**, *30*, 1803031.
[317] Z. Sun, H. Xie, S. Tang, X.-F. Yu, Z. Guo, J. Shao, H. Zhang, H. Huang, H. Wang, P. K. Chu, *Angew. Chem., Int. Ed.* **2015**, *54*, 11526.
[318] X. Tang, W. Liang, J. Zhao, Z. Li, M. Qiu, T. Fan, C. S. Luo, Y. Zhou, Y. Li, Z. Guo, D. Fan, H. Zhang, *Small* **2017**, *13*, 1702739.
[319] C. Leclech, M. Renner, C. Villard, C. Métin, *Biomaterials* **2019**, *214*, 119194.

Wei Xu is an attending spinal surgeon at Tongji Hospital, lecturer at Tongji University, and researcher at the Key Laboratory of Spine and Spinal Cord Injury and Repair, Ministry of Education. He received his M.D. from Tongji University and is currently conducting postdoctoral research in Prof. Ki-Bum Lee's lab at Rutgers University. His research focuses on the application of novel bio-nanomaterials for spinal cord injury and intervertebral disc degeneration. His work has been published in *Signal Transduction and Targeted Therapy, Advanced Science, ACS Nano, and Journal of Materials Chemistry B.*, etc.

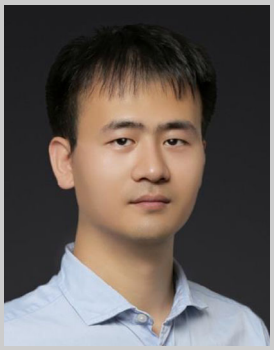

Letao Yang is currently a professor at the affiliated Tongji Hospital and School of Life Science and Technologies, and a PI at the Key Laboratory of Spine and Spinal Cord Injury and Repair, Ministry of Education at Tongji University. He received his bachelor's and doctoral degrees from Nankai and Rutgers University, followed by postdoctoral training at Columbia. He then joined Tongji University as a faculty. His research interests have been focused on nanotechnology and stem cell engineering. His work has been published in *Advanced Materials*, *Nature Communications*, *Science Advances*, *Gastroenterology*, *Advanced Functional Materials*, *ACS Nano*, *Nano Letters*, *Biomaterials*, etc.

Liming Cheng, M.D., is a tenured professor at Tongji University and a leading spinal surgeon and scientist in China. He serves as Vice Dean of the Faculty of Medicine and Life Sciences, Director of the Ministry of Education Key Laboratory for Spinal Cord Injury Repair, and Head of Orthopedics at Tongji Hospital. His research focuses on biomechanical and biological approaches to spine and spinal cord injury repair. Prof. Cheng has published over 200 papers, including in *Cell, Nature Medicine, Advanced Materials, Advanced Science, Signal Transduction and Targeted Therapy*, etc., and received numerous national awards for his pioneering work in clinical translation and innovative treatment strategies.

Ki-Bum Lee is a distinguished professor of Chemistry and Chemical Biology at Rutgers University, where he has been a faculty since 2008. He received his Ph.D. in Chemistry from Northwestern University and completed his postdoctoral training at The Scripps Research Institute, respectively. The primary research interest of his group is to develop and integrate nanotechnologies and chemical biology to modulate signaling pathways in stem cells and cancer cells toward specific cell lineages or behaviors. Prof. Lee's work has been published in *Science*, *Nature Chemical Biology*, *Nature Communications*, *Advanced Materials*, *Advanced Functional Materials*, *ACS Nano*, and many others.